

WRC RESEARCH REPORT NO. 102

A STUDY OF THE TREATMENT OF  
LAKE MICHIGAN WATER USING DIRECT FILTRATION

Raymond D. Letterman

Department of Environmental Engineering  
Illinois Institute of Technology  
Chicago, Illinois

F I N A L   R E P O R T

Project No. A-062-ILL

The work upon which this publication is based was supported  
by funds provided by the U.S. Department of the Interior  
as authorized under the Water Resources Research  
Act of 1964, P.L. 88-379.  
Agreement No. 14-31-0001-5013

UNIVERSITY OF ILLINOIS  
WATER RESOURCES CENTER  
2535 Hydrosystems Laboratory  
Urbana, Illinois 61801

June, 1975

## ABSTRACT

A STUDY OF THE TREATMENT OF  
LAKE MICHIGAN WATER USING DIRECT FILTRATION

The direct filtration process can be an effective and economical alternative to the conventional sequence of operations used for water clarification. In most cases the process has been used to treat water with a consistently low turbidity. Its effectiveness in other cases, e.g., treating water from Lake Michigan, will require a thorough understanding of process behavior and control techniques. Pilot plant studies were performed using a constant-rate dual-media filter preceded by a pretreatment reactor in which a cationic polyelectrolyte coagulant was added. For each filter design and set of operating conditions there is an optimum distribution of deposit within the filter bed at run termination which maximizes the water production per filter run. It was determined that the pretreatment conditions (the polyelectrolyte concentration and the mixing intensity and duration) can be used to maximize the water production per filter run and maintain an acceptable effluent turbidity. The pretreatment conditions determine the rate of clogging front advancement in the filter bed, which, in conjunction with the terminal headloss, determines the distribution of deposit within the bed at run termination.

Letterman, Raymond D.

A STUDY OF THE TREATMENT OF LAKE MICHIGAN WATER USING DIRECT  
FILTRATION

Final Report to the Office of Water Research and Technology,  
Department of the Interior, June, 1975, Washington, D.C. 110p.

KEYWORDS--water treatment\*/direct filtration\*/flocculation/  
polyelectrolytes

## ACKNOWLEDGMENT

The author gratefully acknowledges the efforts of the graduate students in the Department of Environmental Engineering at Illinois Institute of Technology who conducted the studies which are described in this report. The preliminary filtration study was conducted by Roy D. Tanner. Rami Reddy Sama was in charge of the design and construction of the laboratory pilot plant and along with Edward DiDomenico carried out the laboratory filtration study. Anthony E. Burgarino developed the methodology which was used to determine the optimum specific deposit distributions by dynamic programming. Pranee Kulprapha determined the floc size distributions and densities and Shin-Chang Chay conducted the field studies. Special appreciation is extended to the City of Chicago, Department of Water and Sewers, particularly Mr. N. J. Davoust, Engineer of Water Purification, for providing space and equipment at the Central Water Filtration Plant for the field study.

## TABLE OF CONTENTS

	<u>Page</u>
ABSTRACT . . . . .	i
ACKNOWLEDGMENT . . . . .	ii
LIST OF FIGURES . . . . .	iv
LIST OF TABLES . . . . .	vii
I INTRODUCTION	
A. Objectives . . . . .	1
B. Background . . . . .	2
II EXPERIMENTAL APPARATUS AND PROCEDURES	
A. Laboratory Filtration Studies . . . . .	8
B. Preliminary Filtration Studies . . . . .	16
C. Floc Size Distribution and Density Determinations . . . . .	18
III RESULTS AND DISCUSSION	
A. Preliminary Filtration Studies . . . . .	21
B. General Results . . . . .	33
C. Optimum Specific Deposit Distribution Concept . . . . .	43
D. Pretreatment Studies . . . . .	62
E. Field Study . . . . .	77
IV SUMMARY AND CONCLUSIONS . . . . .	88
V RESEARCH APPLICATIONS . . . . .	93
VI APPENDICES	
A. List of Experimental Conditions . . . . .	94
B. List of Symbols and Abbreviations . . . . .	98
VII REFERENCES . . . . .	100
VIII LIST OF PUBLICATIONS . . . . .	102

## LIST OF FIGURES

<u>Figure</u>		<u>Page</u>
1	Schematic Diagram of the Experimental Apparatus . . . . .	9
2	Geometric Sketch of the Prefiltration Mixing Reactor and Impellers . . . . .	11
3	G value versus Impeller Rotational Speed . . . . .	13
4	Schematic Diagram of the Filter Assembly . . . . .	14
5	Filter Media Size Distributions . . . . .	15
6	Effluent Turbidity versus Time for Polymers A and D . . . . .	22
7	Effluent Turbidity and Zeta Potential as a Function of Polymer Concentration . . . . .	25
8	Effect of Influent Turbidity on Particle Zeta Potential for a Given Polymer Concentration . . . . .	28
9	Effect of Polymer Concentration on the Headloss versus Time Relationship for Polymer D . . . . .	29
10	Effect of Polymer Type on Headloss versus Time Relationship for a Zero Particle Zeta Potential . . . . .	31
11	Headloss at 6.5 Hours as a Function of Influent Turbidity - 5 mg/l Polymer A . . . . .	32
12	Effluent Turbidity versus Volume of Water Filtered With and Without Turbidity Breakthrough . . . . .	35
13	Effluent Turbidity at 337 gal/ft <sup>2</sup> and Particle Zeta Potential versus Polymer Concentration . . . . .	37
14	Overall Headloss versus Volume of Water Filtered . . . . .	39
15	Headloss versus Volume of Water Filtered for Each Layer of the Filter Bed, G = 700 sec <sup>-1</sup> . . . . .	41
16	Headloss versus Volume of Water Filtered for Each Layer of the Filter Bed, G = 25 sec <sup>-1</sup> . . . . .	42

<u>Figure</u>		<u>Page</u>
17	Graphs of Mohanka's (20) and Sakthivadivel's (20) Equations . . . . .	47
18	Terminal Headloss and Specific Deposit Distributions . . . . .	51
19	Specific Deposit Parameter versus Volume of Water Filtered for Four Filter Runs . . . . .	52
20	Specific Deposit Parameter versus Water Production per Filter Run, $\Delta H = 30''$ . . . . .	54
21	Specific Deposit Parameter versus Water Production per Filter Run, $\Delta H = 86''$ . . . . .	55
22	Maximum Water Production per Filter Run versus Filtration Rate . . . . .	57
23	Observed Water Production per Filter Run versus Filtration Rate, $G = 25 \text{ sec}$ $PC = 1.5 \text{ mg/l}$ and $\bar{T} = 4 \text{ min.}$ . . . . .	60
24	Percent of Maximum Water Production per Filter Run versus $G$ value . . . . .	63
25	Percent of Maximum Water Production versus Polymer Concentration . . . . .	65
26	Percent of Maximum Water Production per Filter Run versus Mean Detention Time . . . . .	67
27	Floc Size Distributions . . . . .	70
28	Relationship Between Floc Size and Density . . . . .	71
29	Terminal Headloss and Specific Deposit Distributions . . . . .	73
30	Terminal Headloss and Specific Deposit Distributions . . . . .	74
31	Statistical Distribution of Lake Michigan Water Turbidity . . . . .	79
32	Statistical Distribution of Lake Michigan Water Plankton Densities . . . . .	80
33	Effluent Turbidity and Overall Headloss versus Volume of Water Filtered - Field Study . . . . .	82

<u>Figure</u>		<u>Page</u>
34	Effluent Turbidity and Overall Headloss versus Volume of Water Filtered - Field Study . . . . .	84
35	Effluent Turbidity and Overall Headloss versus Volume of Water Filtered - Field Study . . . . .	86

## LIST OF TABLES

<u>Table</u>		<u>Page</u>
1	Effect of Coagulant Type and Filter Media on Length of Filter Run, Reference 7. . . . .	6
2	Effluent Turbidity at 6.5 Hours for Several Influent Turbidity Levels - 5 mg/l Polymer A. . . . .	23
3	Effective and Optimum Polymer Concentrations and Corresponding Particle Zeta Potentials. . . . .	26
4	Polymer Concentrations Required to Achieve a Zero Zeta Potential for High and Low Influent Turbidities. . . . .	26
5	Calculated Optimum Terminal Headloss Distributions. . . . .	49
6	Coefficients Used to Calculate Layer by Layer Clean Bed Headloss. . . . .	58
7	Effect of Pretreatment and Filter Operating Conditions on the Rate of Clogging Front Advancement. . . . .	76



## I. INTRODUCTION

A. Objectives: The overall objective of this project was to evaluate, using a 1 gpm pilot plant, the effectiveness of the direct filtration process in treating water of the quality generally obtained from Lake Michigan. The specific objectives of the project included the following:

(a) Determine the feasibility of using a cationic polyelectrolyte as the sole coagulant in the direct filtration process.

(b) Evaluate the use of controlled pretreatment conditions such as the coagulant concentration and the prefiltration mixing intensity and duration to maximize the filtered water produced per filter run and maintain an acceptable effluent turbidity.

(c) Determine the effect of the filter operating conditions including the terminal headloss, filtration rate and media grain size distribution on the pretreatment conditions required to maximize water production and maintain an acceptable effluent turbidity.

(d) Derive and verify experimentally mathematical relationships which describe the direct filtration system and which could be used to optimize the system design (including the pretreatment step) and determine optimum operational strategies during future studies.

(e) Conduct a statistical analysis of 1085 daily average values of water quality parameters which are pertinent to the feasibility of treating Lake Michigan water using direct filtration.

(f) Test the relationships and observations from (a) through (d) using water obtained directly from Lake Michigan.

B. Background: The direct filtration process is a variation of the conventional water treatment system in which the raw water is treated with a coagulant during a period of agitation and then applied directly to the filter without prior clarification by sedimentation. The absence of sedimentation or large conventional flocculation tanks can decrease the size of the treatment plant, decrease capital costs and eliminate the problem of dealing with two sources of sludge. Direct filtration is especially effective when the raw water turbidity is low. The conventional flocculation-sedimentation sequence is relatively ineffective and therefore unessential in this situation.

Recent literature contains several articles which deal with proposed or existing direct filtration facilities. In the Province of Ontario (1,2) there are four direct filtration plants. The original of these four resulted from the conversion of an existing plant on Lake Ontario at Toronto to direct filtration in 1964. In the United States the city of Springfield, Massachusetts has constructed a 60 mgd direct filtration addition to its existing facility (3). A 200 mgd direct filtration plant has been constructed in Nevada to treat water from Lake Mead (4). An 840 mgd high-rate direct filtration plant will be constructed near Sydney, Australia (5).

Construction costs have been shown to be reduced significantly by the use of the direct filtration scheme. Savings in dollars per mgd design capacity for direct filtration over the

conventional flocculation-sedimentation-filtration sequence range from 15,000 for the new plant in Sydney (5) to 42,000 and 72,000 for the plant additions in Springfield (3) and Toronto (1). Camp (6) has claimed that if the direct filtration process were applied in all new plant construction in the U.S. where annual water treatment plant construction expenditures amount to \$300 million, approximately \$60 million would be saved annually.

The use of cationic polyelectrolytes as primary coagulants and bi-media (also called dual media) and multi-media filters has been shown to be an effective combination in the direct filtration process (7,8). Cationic polyelectrolytes are high molecular weight, long chain organic polymers with positive (cationic) ionizable groups. When introduced to a suspension of negatively charged particles, e.g., clay particles, bacteria, etc., the polymer chains rapidly absorb on the particles. If a typical, commercially available, cationic polyelectrolyte is used, the positive charges on the polymer tend to neutralize the stabilizing negative charges on the particles in the suspension. At the same time the partially adsorbed polymer chains may extend into the solution and become adsorbed on other particles. This is known as interparticle bridging. Both factors, charge neutralization and interparticle bridging, play significant roles in the flocculation process.

The mechanisms by which polyelectrolytes may enhance the removal of particles in water filtration have been discussed

in detail by Habibian (9) and Wnek (10). Interparticle bridging, according to Habibian (9), is a controlling mechanism. The bridging which is significant in this case is between the filtered particle and the media grains in the filter bed. Habibian also notes that there is an "optimum dosage" of cationic polyelectrolyte applied to the filter influent. Removal of particles in the filter bed decreases when dosages less than or greater than the optimum dose are used.

Cationic polyelectrolytes have been shown to permit greater fluctuations in the filtration rate without danger of turbidity breakthrough and, in general, to permit the use of higher filtration rates, e.g., 10 gpm/ft<sup>2</sup> (7). Filtration cycle output in one study (8) was decreased only slightly by higher filtration rates when polyelectrolytes were used. Polymer coagulants have been shown to permit the use of larger filter media grains (8). This was found to decrease the rate of headloss build-up, yet enabled the maintenance of an acceptable effluent quality.

Adin and Rebhun (8) have observed that filtration using cationic polyelectrolytes as the sole coagulant is characterized by the formation of a relatively narrow "working layer" within the filter bed. The working layer was observed to move down through the bed at a rate which was a function of the polyelectrolyte concentration and the media grain size. Above the working layer the filter was essentially "saturated" with deposit and below it the filter was relatively clean. When alum was used the working layer was broad and poorly defined and tended to move down through the bed rapidly.

Polymer coagulants in comparison with hydrolyzing salt coagulants result in less weight and volume of backwash sludge which must be handled and disposed of. Sludge disposal is a critical problem in water treatment practice. When the coagulant used is aluminum hydroxide, more than 50 percent of the sludge by weight may be the hydroxide precipitate (11).

Dual media filters, consisting typically of a layer of anthracite coal on top of a layer of sand, are advantageous in the direct filtration process. The larger grain coal layer filters and stores particles with less headloss per unit of deposit compared to a stratified single media bed which tends, in many cases, to form a compressible layer of deposit on top of the media. Craft (12) has reported that single media sand filter beds are inadequate for direct filtration using filtration rates of from 5 to 7 gpm/ft<sup>2</sup>. While the purpose of the coarse anthracite layer, in a dual media filter, is primarily for deposit storage, the lower, smaller grain size, sand layer is essential for the achievement of a low (<0.3 FTU) effluent turbidity.

Shea, et al. (7), conducted experiments using four different pilot plant filter beds and aluminum sulfate and a cationic polyelectrolyte as sole coagulants. A conventional sand filter and three dual media beds, one with a fine and two with coarse anthracite layers were studied. As shown in Table 1, the longest filter runs were obtained when the cationic polyelectrolyte and the coarse anthracite layer were used. The deeper coarse anthracite layer gave the longest filter run,

Table 1. Effect of Coagulant Type and Filter Media on Length of Filter Run (7).

Media	6.0 mg/l Suspended Solids		24.10 mg/l Suspended Solids			
	<u>Dose</u> mg/l	<u>Longest</u> Run, hr.	<u>Dose</u> mg/l	<u>Longest</u> Run, hr.		
SAND	with Alum		with Cat-floc			
E.S.=0.45 mm	20	7.0	0.5	10.0	1.0	2.5
U.C.=1.55						
Sand depth=22"						
FINE DUAL MEDIA	with Alum		with Cat-floc			
E.S.=0.98mm	10	6.5	0.74	14.0	1.0	10.0
U.C.=1.35						
Coal depth=16"						
COARSE DUAL MEDIA	with Alum		with Cat-floc			
E.S.=2.5mm	10	3.5	1.0	33.0	4.0	11.0
U.C.=1.32						
Coal depth=16"						
COARSE DUAL MEDIA	with Alum		with Cat-floc			
E.S.=2.5mm	10	4.5	1.0	43.0	4.0	14.5
U.C.=1.32						
Coal depth=23"						

43.0 hrs. This corresponds to a water production per filter run of 7740 gal/ft<sup>2</sup>. A terminal headloss of 72 inches of water and a filtration rate of 3 gpm/ft<sup>2</sup> were used during the study. Shea, et al. (7), also observed the filter run length was inversely proportional to the influent suspended solids concentration when the deposit was distributed within the filter bed at run termination.

Hutchison and Foley (1) in reporting on full scale and pilot plant experience with direct filtration in Canada noted that the short filter runs which occurred during periods when diatom densities increased above 1000/ml could be avoided by the use of dual media filters in which the anthracite layer had an effective size of 1.5 mm. However, it was noted that these filters required increased operator skill during low diatom density periods in order to avoid turbidity breakthrough. In the absence of diatoms overall filter performance was best when the dual media filters contained 1.0-1.1 mm effective size anthracite.

In summary, the literature contains a significant amount of information on the direct filtration process. Its economic advantages are apparent. The advantages of dual media filters and cationic polyelectrolyte coagulants have been made apparent by several studies. However, there is very little, if any, information in the literature on the use of a short duration prefiltration mixing step to aid in maximizing water production, and maintaining an acceptable effluent turbidity. There are apparently no mathematical relationships which can be used in lieu of pilot plant studies for process design and optimization.

## II. EXPERIMENTAL APPARATUS AND PROCEDURE

A. Laboratory Filtration Studies: A constant rate direct filtration pilot plant system was used in this study. The apparatus consisted of four major sections; an influent raw water preparation and feed system, a polymer feed system, a prefiltration mixing reactor, and an anthracite-sand dual-media filter with a flow rate control assembly. A schematic diagram of the entire system is shown in Figure 1.

The raw water suspension used throughout this study consisted of 44 mg/l bentonite clay<sup>#</sup> and 22 mg/l of kaolin clay<sup>\*</sup> in Chicago tap water. The turbidity of this suspension was 32 FTU (Formazin Turbidity Units). This mixture was chosen after a jar test study was conducted to find a mixture of clays which resembled natural suspensions from Lake Michigan in terms of its response to coagulation with cationic polymers. A mixture with a turbidity of 32 FTU was selected because a statistical analysis of offshore intake water turbidities (at Chicago's Central Water Filtration Plant) showed that a turbidity of 32 FTU is exceeded only about one percent of the time. The water temperature throughout this study was  $18^{\circ}\text{C} \pm 4^{\circ}\text{C}$ . The 250 gal. raw water suspensions were mixed using filtered compressed air. The average characteristics of the Chicago tap water used during the laboratory phase of the study were: alkalinity - 108 mg/l as  $\text{CaCO}_3$ ; residual chlorine - 0.7 mg/l; hardness - 137 mg/l as  $\text{CaCO}_3$ ; turbidity - 0.15 JTU and pH - 8.3.

The cationic polyelectrolyte used throughout the laboratory filtration study, Cat-floc T<sup>##</sup>, was pumped to the "tee" fitting

<sup>#</sup>Fisher Scientific Company, Fair Lawn, N.J.

<sup>\*</sup>J.T. Baker Chemical Company, Philipsburg, N.J.

<sup>##</sup>Calgon Corporation, Pittsburgh, Pa.



- P - Pump
- R - Rotometer
- D - Drains
- B - Backwash Discharge
- PMR - Prefiltration Mixing Reactor

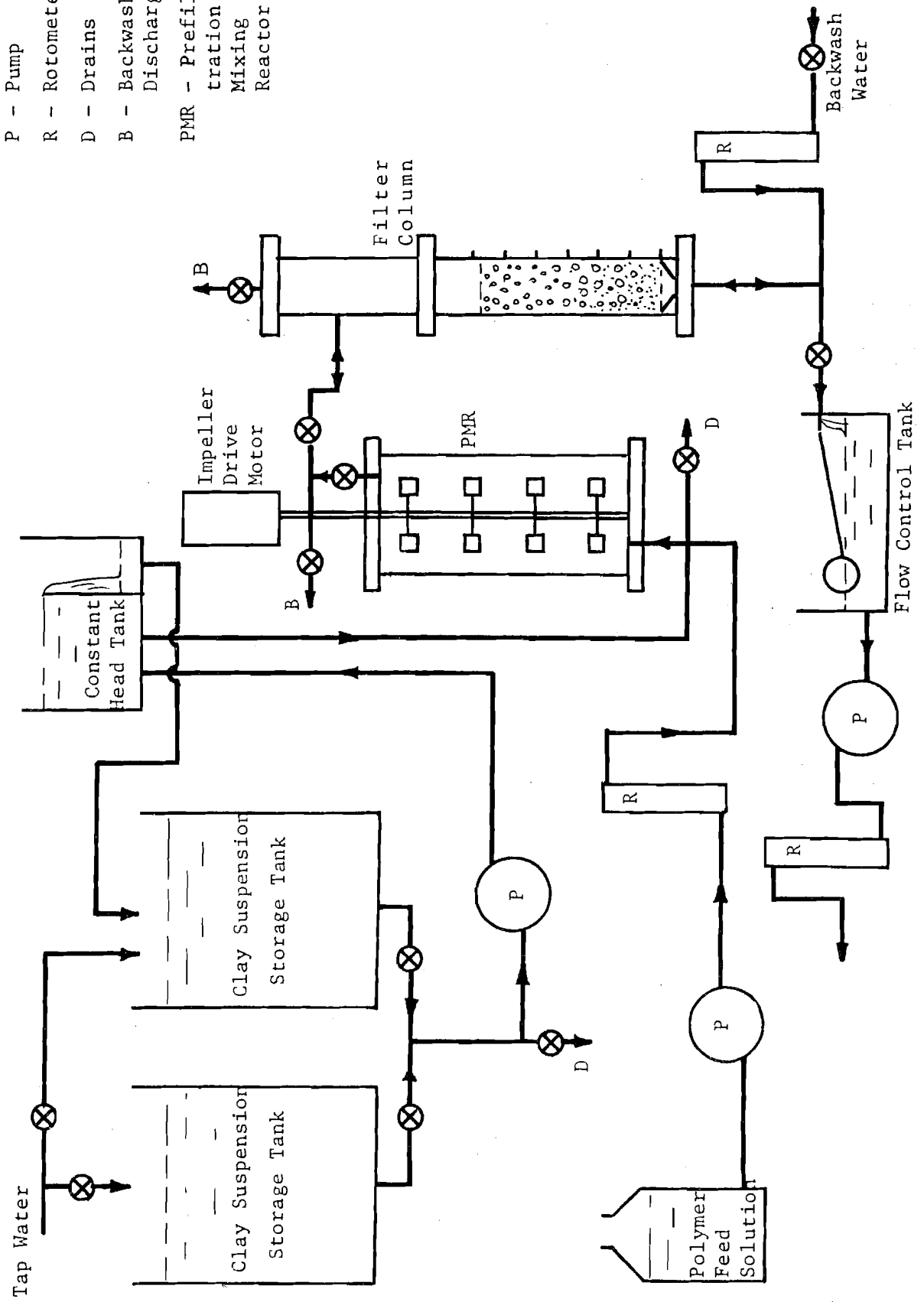


Figure 1. Schematic Diagram of the Experimental Apparatus

just below the prefiltration mixing reactor using a peristaltic action pump. The polymer feed solution was prepared each day using polymer concentrations in the range 0.02 to 0.5 gm/l. The feed solution concentration used depended on the PMR flow-rate and the polymer concentration desired in the suspension. At the tee the feed solution mixed with the influent suspension which flowed by gravity to this point from the constant head tank. The top of the weir in the constant head tank was located 90 inches above the bottom of the media compartment in the filter column. The range of polymer concentrations used was from 0.5 to 10.0 mg/l.

The 8.5 liter prefiltration mixing reactor was used to provide a short period of flocculation for the polymer-treated suspension. A diagram of the reactor is shown in Figure 2. The fully-baffled reactor contained 4 turbine-type impellers which were mounted on a single shaft. The rotational speed of the impellers could be varied over a broad range using an electronic controller connected to the drive motor. The mixing intensity within the reactor (as the rms velocity gradient or G value) was determined using net torque and shaft rotational speed measurements and the equation

$$G \text{ value} = \left[ \frac{2\pi gNT}{60V\mu} \right]^{\frac{1}{2}},$$

where T is the measured net torque on the impeller shaft (measured using a calibrated Servodyne motor controller), N is the shaft rotational speed, V is the volume of fluid in the reactor, g is the acceleration of gravity and  $\mu$  is the absolute viscosity. The calibration

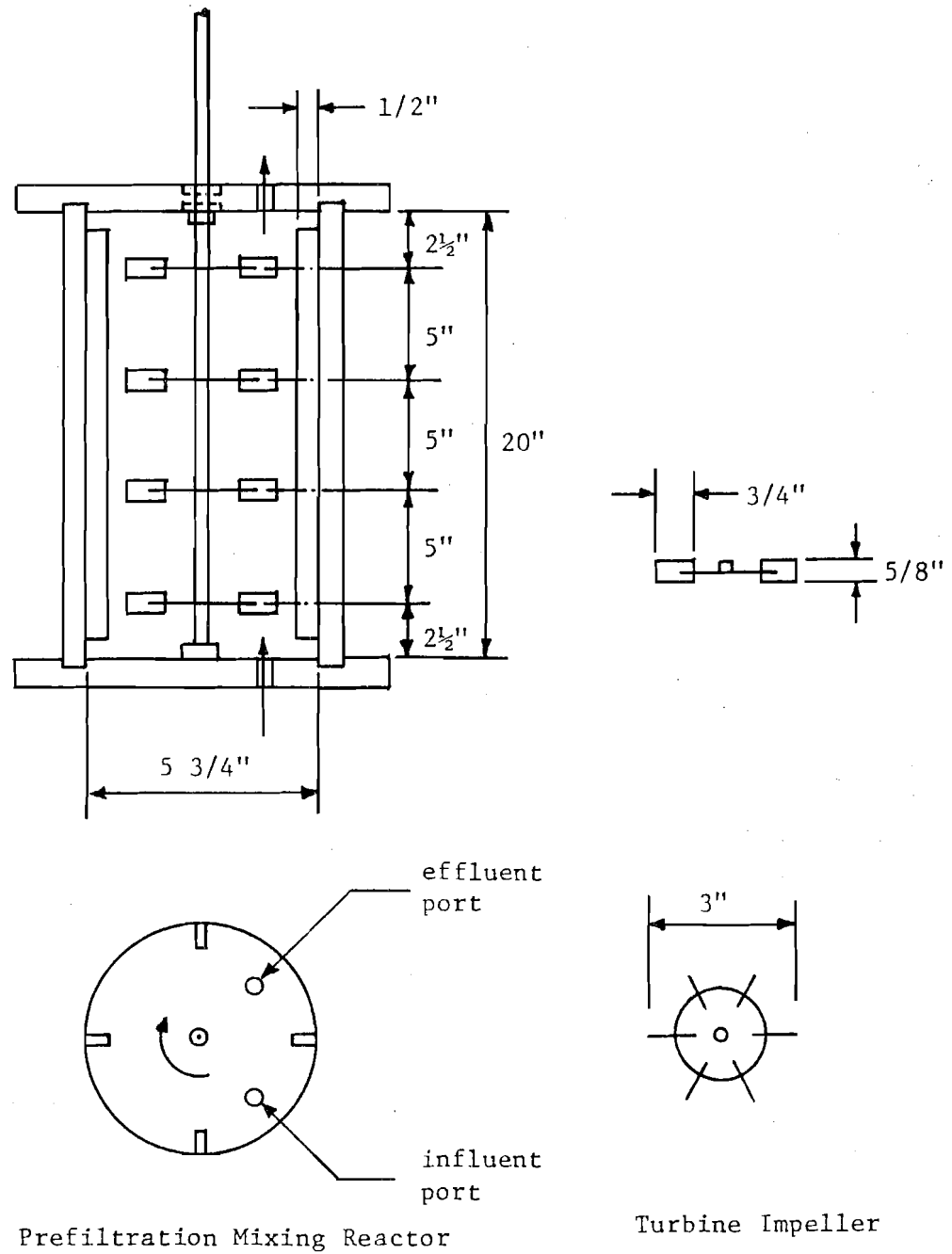


Figure 2. Geometric Sketch of the Prefiltration Mixing Reactor and Impellers

curve obtained, as the G value versus the shaft rotational speed, is shown in Figure 3. The range of G values used during the study was from approximately 0 to  $700 \text{ sec}^{-1}$ . The average detention time in the PMR was controlled by wasting part of the PMR effluent through a rotometer and valve. Average PMR detention times ranging from 2.0 to 9.2 minutes were used during the study.

The plexiglas filter column had a 3-inch inner diameter, and contained 18 inches of anthracite coal over six inches of silica sand. Manometer taps were installed 4 inches apart along the entire column as shown in Figure 4. The flow rate through the filter bed was controlled by pumping at a constant rate from an effluent collection tank equipped with a float valve. The filtration rates used in the study ranged from 2.5 to  $7.5 \text{ gpm/ft}^2$ .

During the laboratory filtration study three different filter beds were used. Each had a different anthracite media size distribution. The anthracite effective sizes of filter beds numbered 1, 2 and 3 were, respectively, 0.94 mm, 1.20 mm and 1.71 mm. The uniformity coefficients were 1.65, 1.60 and 1.16, respectively. The total anthracite weight in each bed was approximately 1750 grams. The sand media size distribution was the same in each filter bed, and had an effective size of 0.45 mm and a uniformity coefficient of 1.40. The total sand weight in each bed was approximately 1100 grams. Graphs of the media size distributions obtained by sieve analysis are shown in Figure 5. The anthracite in Bed 1 was obtained directly

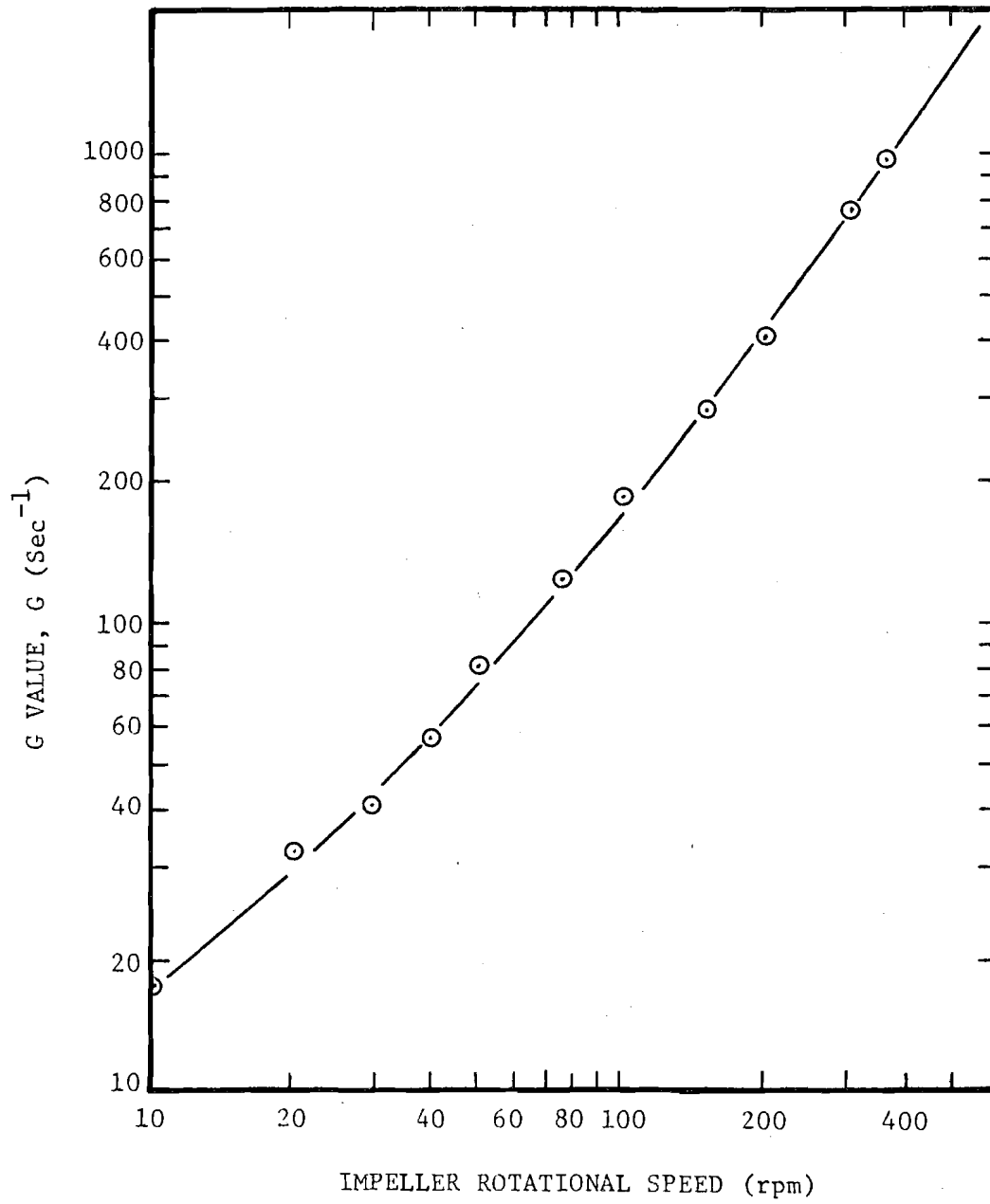


Figure 3. G value versus Impeller Rotational Speed

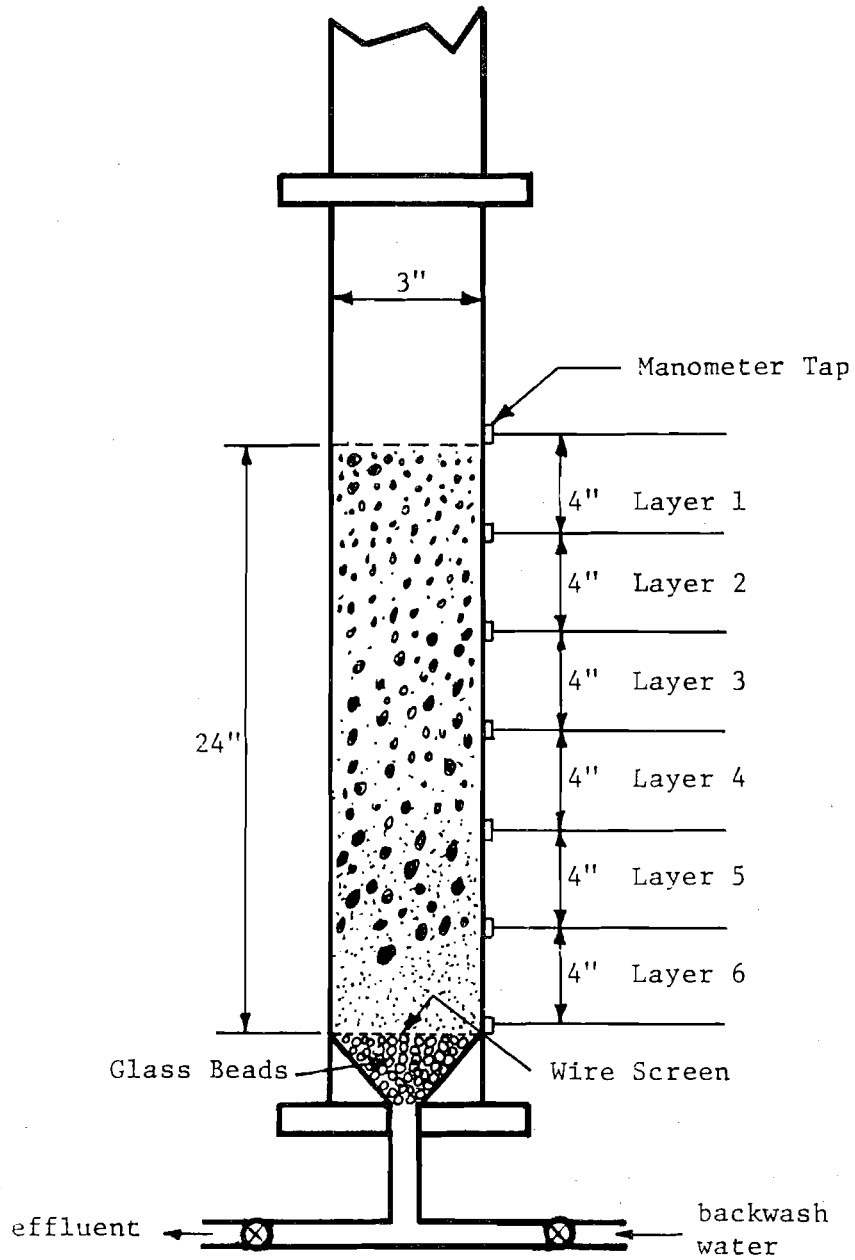


Figure 4. Schematic Diagram of the Filter Assembly

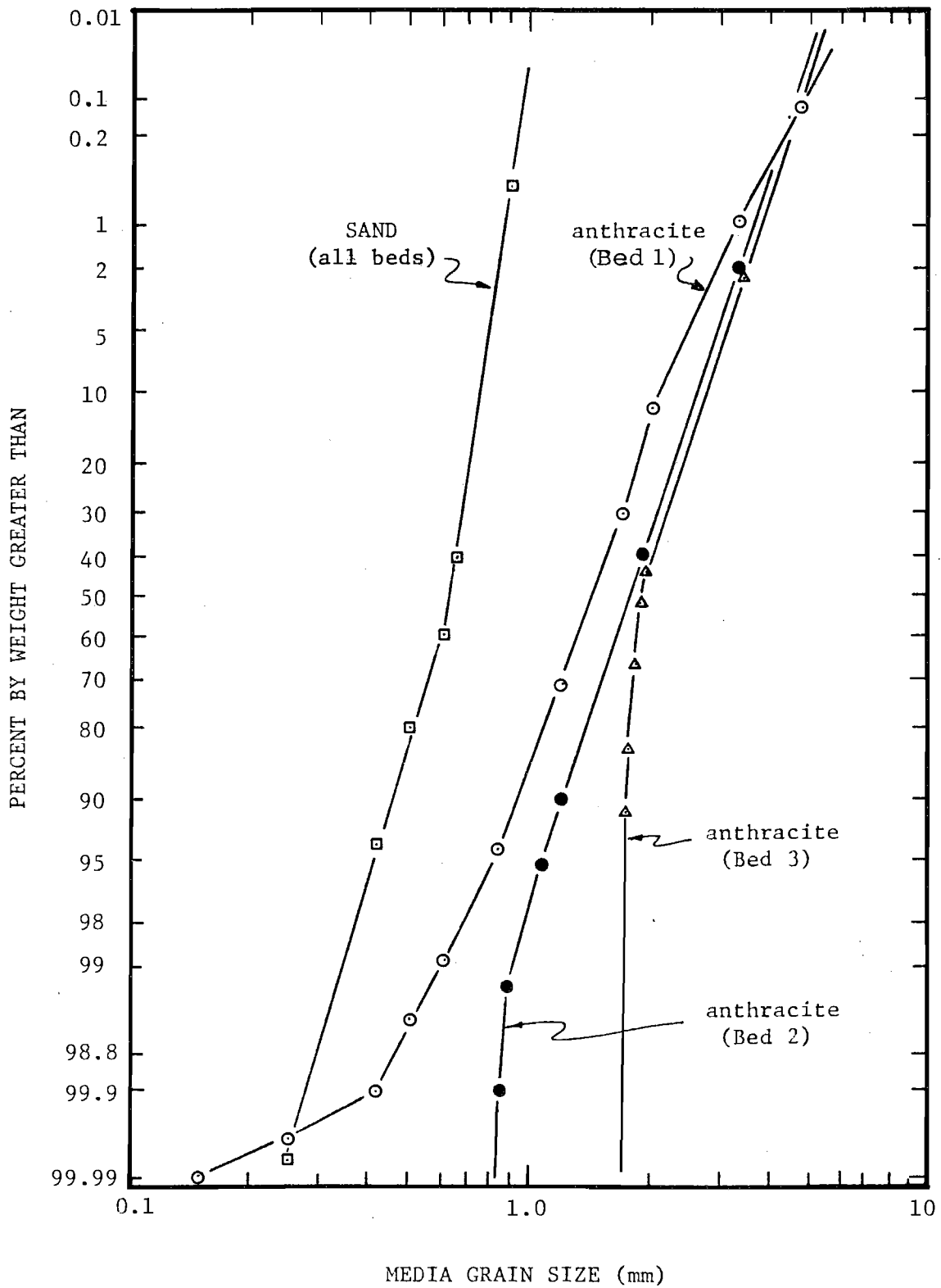


Figure 5. Filter Media Size Distributions

from a well-mixed bag of Philterkol No. 1. The coal was backwashed before the first experiment to remove dust and fines. The sieve analysis was made after the filtration experiments had been completed.

The preparation of the filter bed for a filter run involved backwashing at a 30 to 40 percent bed expansion until the clean bed headloss was reduced to a constant base level for the specific bed and filtration rate used. After backwashing, the media grains were allowed to settle slowly back down into the column by gradually reducing the backwash flow rate over a period of about 1.5 minutes. The column was then tapped lightly in order to compact the bed to a constant depth of 24 inches. The water required per backwash was approximately  $250 \text{ gal/ft}^2$ , i.e.,  $25 \text{ gpm/ft}^2$  for roughly 10 minutes.

Layer-by-layer headloss and column effluent turbidity were measured and recorded at regular and frequent intervals during each filter run. The effluent turbidity was monitored using a Hach Turbidimeter, model 2100 A and is recorded as FTU, Formazin Turbidity Units. The suspension leaving the mixing reactor was sampled periodically and the zeta potential of the particles was determined using a zeta meter (Zeta Meter, Inc.). The procedure recommended by the manufacturer was used. The ZP measurements were corrected to  $22.5^\circ\text{C}$ . Runs were generally terminated when either the total headloss across the bed reach 86 inches of water or turbidity breakthrough occurred.

B. Preliminary Filtration Studies: A six-month preliminary study was conducted using pilot filters at the Central Water Filtration Plant in Chicago to evaluate a number of cationic



polyelectrolytes for use in the direct filtration process and to determine if and how particle zeta-potential measurements can be used to determine the cationic polyelectrolyte concentration that is necessary for effective operation of the direct filtration process.

The pilot filters used consisted of 2.75 inch I.D. plexiglas columns filled with 26 inches of filter sand with an effective size of 0.67 mm and a uniformity coefficient of 1.4. Each filter was equipped with a pressure gauge for measuring headloss across the entire filter bed and a rotometer and valve on the effluent line for manual flow control. The influent to the filters was raw water from Lake Michigan containing 8 to 13 lb. of chlorine per million gallons. A filtration rate of 2 gpm/ft<sup>2</sup> was used in all experiments. Each filtration experiment was conducted for 6.5 hours.

Four cationic polyelectrolytes (polymers) were used during the preliminary study. Each according to the manufacturers, is resistant to adverse effects from chlorine residuals and is approved for use in drinking water. The polymers studied are:

Cat-Floc T (Polymer A)	-	Calgon Corporation
Nalcolyte 607 (Polymer B)	-	Nalco Chemical Co.
Nalcolyte 8101 (Polymer C)	-	Nalco Chemical Co.
Magnifloc 570-C (Polymer D)	-	Cyanamid Chemical Co.

These polymers were chosen because previous tests conducted using Lake Michigan water and approximately ten polymers indicated that these four were among the more effective polymers for

turbidity removal by flocculation and sedimentation (13). During the study the polymer concentration in the filter influent was varied in the range 1 to 25 mg/l. The polymer feed solution was mixed with the raw water at the elbow through which the raw water flowed as it entered the column. The flow time between the elbow and the top of the filter bed was approximately 15 minutes.

During the study the influent turbidity varied from 0.4 to 35 FTU, however, most of the time the turbidity was less than 10 FTU. Influent and effluent turbidity measurements were made using a Hach turbidimeter, Model 2100 A.

All particle zeta potential determinations were conducted in the laboratory immediately after a filtration run had been completed. Measured volumes of the polymer feed solution were pipetted to aliquots of a raw water sample to give the desired range of polymer concentrations. After the addition of the polymer and two minutes of mixing on a magnetic stirrer a part of the treated aliquot was poured into the electrophoresis cell and the mobility of ten particles was measured. The manual supplied by the zeta meter manufacturer was used to determine particle zeta potentials. All zeta potential values reported are for 22.5°C. A complete description of the apparatus and methodology are included in Tanner's thesis (14).

C. Floc Size Distribution and Density Determinations: A supplementary study was conducted to determine the effect of the prefiltration mixing intensity on the size and density distribution of flocs which were applied to the filter. This type

of information is needed to explain the effect of the pre-treatment step on the filter operation.

The floc size and density distributions were determined using a somewhat unique settling column analysis. The flocs were formed in a 500 ml sample bottle which was inserted in the light path of a  $15^{\circ}$  forward scatter nephelometer manufactured by Monitor Technology, Inc. (Monitek Model 250). The Monitek unit projects a highly collimated light beam through the sample bottle at a depth of 5.5 cm below the liquid surface. After the flocculated suspension was inserted in the instrument the scattered light intensity was measured as a function of time. This data was then used in conjunction with the depth of the light beam to determine a cumulative floc settling velocity distribution. Several separate flocculation experiments were conducted using the same conditions to obtain the relationship between floc size and settling velocity. Individual flocs were captured using a large bore eyedropper and inserted in a small settling column containing suspension supernatant. After the settling velocity was measured the floc was retrieved and its size was measured using a microscope equipped with an ocular micrometer. Approximately one hundred size - settling velocity determinations were made using this method. The density of each floc was determined using the measured size and settling velocity and the Stoke's Law equation. The conditions used during these supplementary experiments were selected to correspond to some of the conditions used in the filtration experiments. These conditions were: flocculation

period - 4 minutes; Cat-Floc T concentration - 1.5 mg/l, G values of 25, 200 and 700  $\text{sec}^{-1}$  and the clay mixture which was used in the laboratory filtration experiments. A complete description of the apparatus and methodology is contained in Kulprapha's thesis (15).

### III. RESULTS AND DISCUSSION

A. Preliminary Filtration Studies: The purpose of the preliminary study was to evaluate a number of cationic polyelectrolytes for use in the direct filtration process and to determine if and how particle zeta potential measurements can be used to determine the cationic polyelectrolyte concentration that is necessary for effective operation of the direct filtration process.

The effluent turbidity was found to be a function of time and the polymer concentration. The type of polymer had an almost negligible effect on effluent turbidity.

Figure 6 illustrates the effect of polymer concentration and length of the filter run on effluent turbidity for polymers A and D. Graphs similar in form were obtained for polymers B and C. Note in Figure 6 (polymer A) that increasing the polymer concentration from 1.9 to 5.0 mg/l decreases the length of time required for the effluent turbidity to reach or start to approach a constant minimum value. This length of time is known as the ripening period. The minimum effluent turbidity reached also decreases as the polymer concentration is increased in this range. When the concentration of polymer A was increased to 12.5 mg/l the effluent turbidity increased with time during the run. This same general behavior was observed when the other polymers were used. These results agree with Habibian's (9) observation that there is (with respect to effluent turbidity) an optimum polymer dose.

Table 2 shows the effluent turbidities measured at 6.5 hours for a range of influent turbidities and a 5.0 mg/l

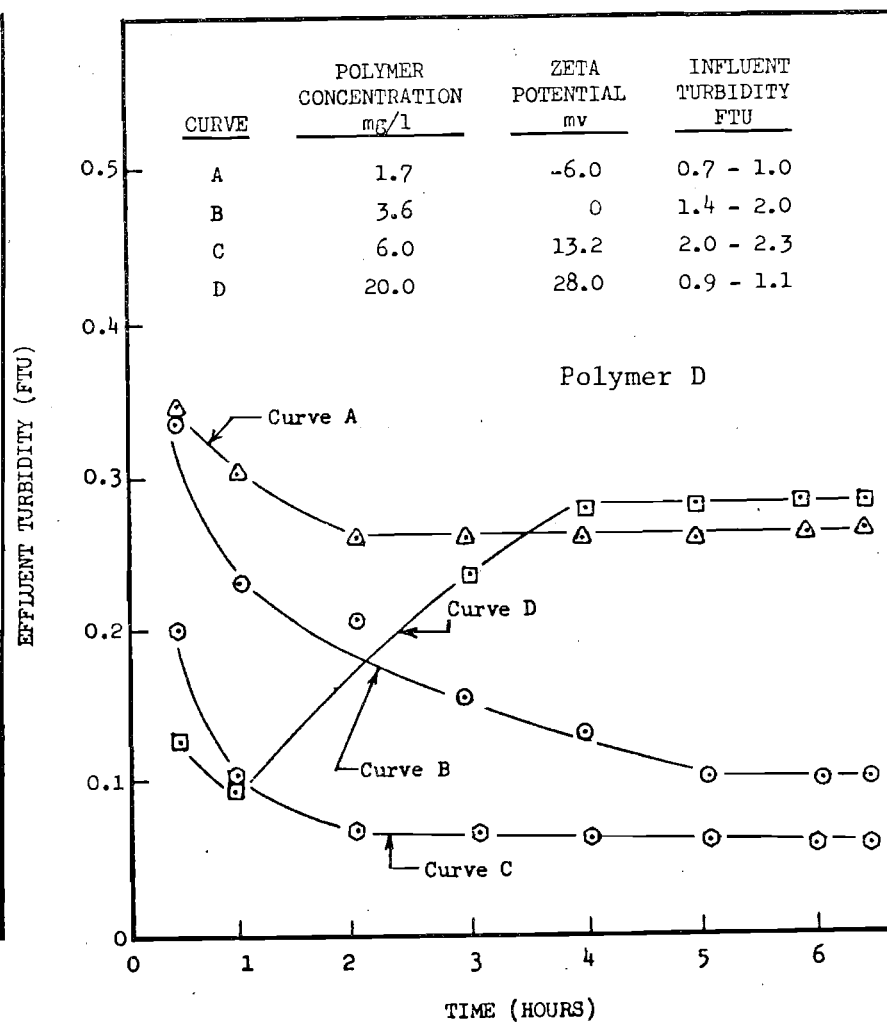
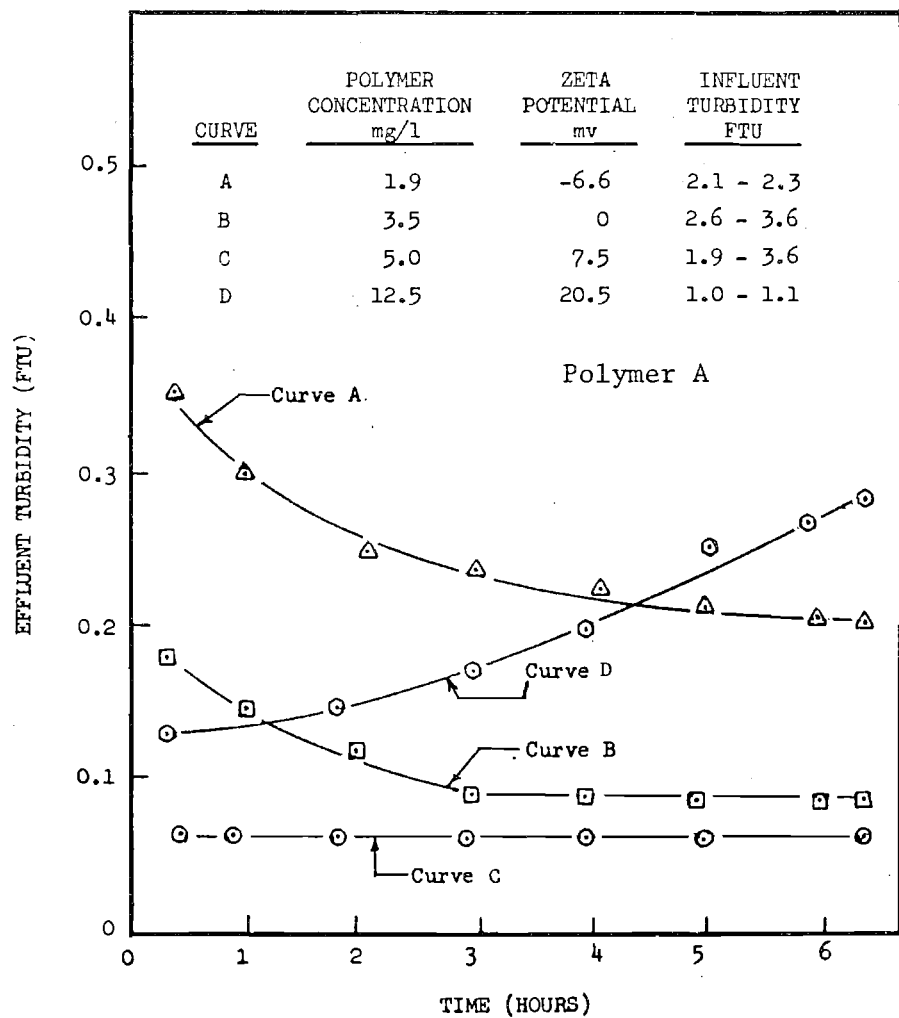


Figure 6. Effluent Turbidity versus Time for Polymers A and D

Table 2. Effluent Turbidity at 6.5 hours for Several Effluent Turbidity Levels, 5 mg/l Polymer A.

---

<u>Maximum influent turbidity during the filter run, FTU</u>	<u>Effluent turbidity at 6.5 hours, FTU</u>
1.3	0.06
2.9	0.07
5.9	0.06
7.2	0.06
8.0	0.06
9.5	0.07
35	0.08*

---

\*Measured at 2.5 hours - run terminated, maximum headloss of 8.6 feet reached.

concentration of polymer A. Note that the effluent in all runs was approximately 0.07 FTU. The run reported for an influent turbidity of 35 FTU was terminated at 2.5 hours due to the excessive headloss which developed, however, the effluent turbidity at this point was continuing to decrease with time.

Figure 7 contains graphs of the effluent turbidity at 6.5 hours of filtration and the particle zeta potential versus the polymer concentration. The influent turbidity during the runs used to obtain the data plotted in these graphs was approximately 2 FTU. Figure 7 was used to determine the optimum dosage and the effective dosage range for each of the four polymers. The optimum dosage is defined as the polymer concentration which minimizes the effluent turbidity at 6.5 hours. As shown in Figure 6 the use of the optimum dosage also minimizes the length of the ripening period. The effective dosage range is defined as the range of polymer concentrations which results in an effluent turbidity at 6.5 hours of filtration of 0.3 FTU or less. Table 3 lists the effective dosage ranges, optimum dosages and corresponding particle zeta potentials for all four polymers and an influent turbidity of approximately 2 FTU. Note that while the effective dosage ranges and optimum dosages are significantly different, the corresponding particle zeta potentials are similar. The effective dosage range corresponds to zeta potentials from -6 to approximately 26 mv and the optimum dosage corresponds to a zeta potential of approximately 13 mv. This correspondence was independent of influent turbidity in the range of 0.5 to 10 FTU.



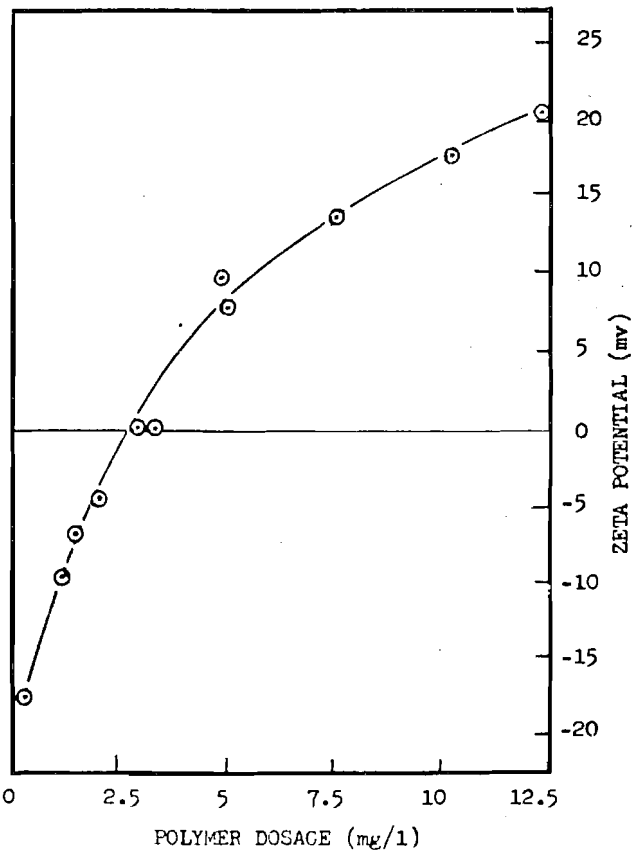
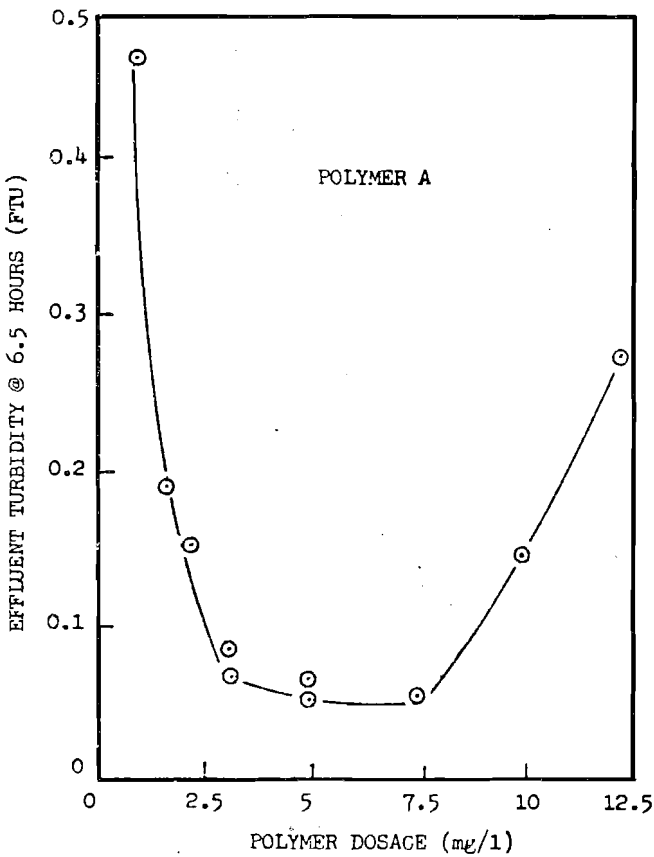
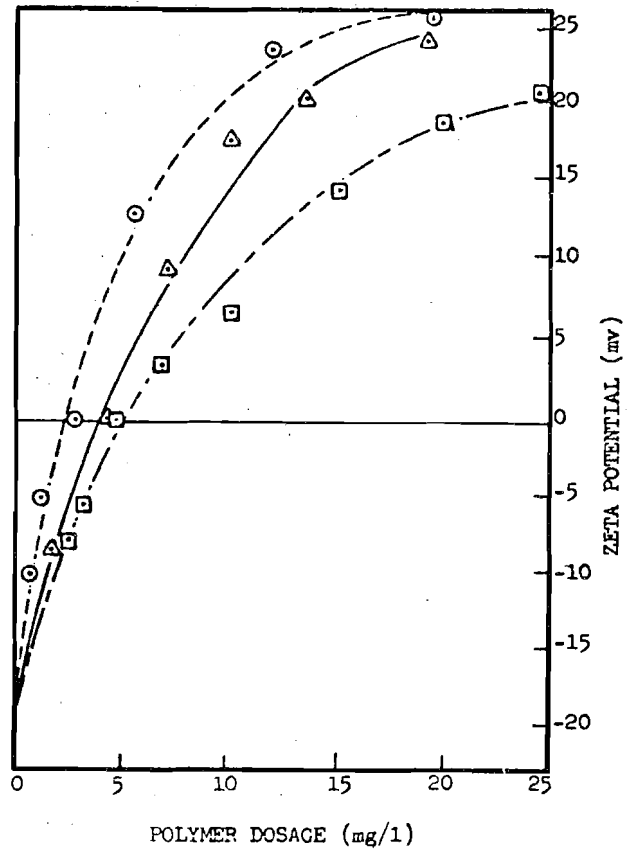
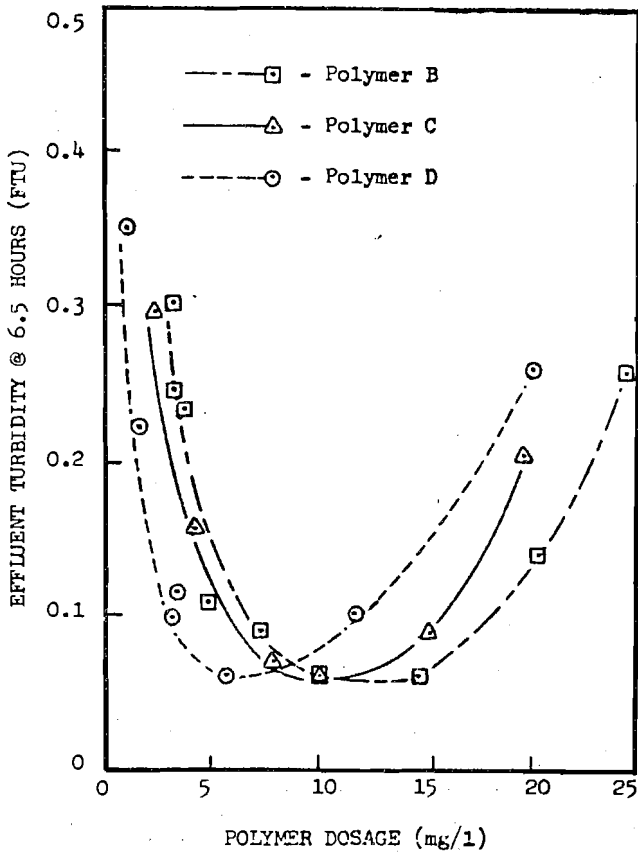


Figure 7. Effluent Turbidity and Zeta Potential as a Function of Polymer Concentration

Table 3. Effective and Optimum Polymer Concentrations and Corresponding Particle Zeta Potentials.

Polymer	Effective Range		Optimum	
	Polymer Conc., mg/l	Zeta Potential mv	Polymer Conc., mg/l	Zeta Potential mv
A	2 to 13	-7 to 21	7	12
B	3 to 25	-7 to 21	12	12
C	2 to 22	-6 to 26	10	14
D	1 to 20	-6 to 26	6	13

Table 4. Polymer Concentrations Required to Achieve a Zero Zeta Potential for High and Low Influent Turbidities.

Polymer	Polymer Concentration at a Zeta Potential of Zero, mg/l	
	Influent turbidity = 1 FTU	Influent turbidity = 35 FTU
A	3.5	5.0
B	5.0	6.0
C	5.0	6.0
D	3.5	4.5

However, the polymer dose required to give a certain particle zeta potential was a function of the influent turbidity.

Figure 8 shows the effect of influent turbidity on the ZP of the particles at a given polymer concentration for polymers A and C. Note that if the polymer concentration is not varied to account for changes in influent turbidity, the zeta potential decreases approximately 3 to 8 mv as the influent turbidity increases from 1 to 35 FTU. This decrease is roughly 25 percent of the 32 mv span of zeta potentials corresponding to the effective dosage range. This suggests that dosage control is not critical with respect to effluent turbidity if a zeta potential near the middle of this effective range, for example, 13 mv, is used as a control point. Table 4 shows the effect of an increase in influent turbidity from 1 to 35 FTU on the polymer dosage required to give a zero particle zeta potential for each of the four polymers studied. Polymer A required the largest increase of 1.5 mg/l.

The rate of headloss build-up across the filter bed during the course of the run was found to be a function of the type and dosage of polymer and the influent turbidity. For a given influent turbidity the polymer dosage which minimized the effluent turbidity maximized the rate of headloss build-up. Figure 9 shows the effect of the polymer concentration (polymer D) on headloss across the filter bed as a function time. The influent turbidity was approximately 1.5 FTU. Note that the three polymer dosages used, 1.7, 3.6 and 6 mg/l resulted, in this case, in particle zeta potentials of -6, 0 and 13 mv

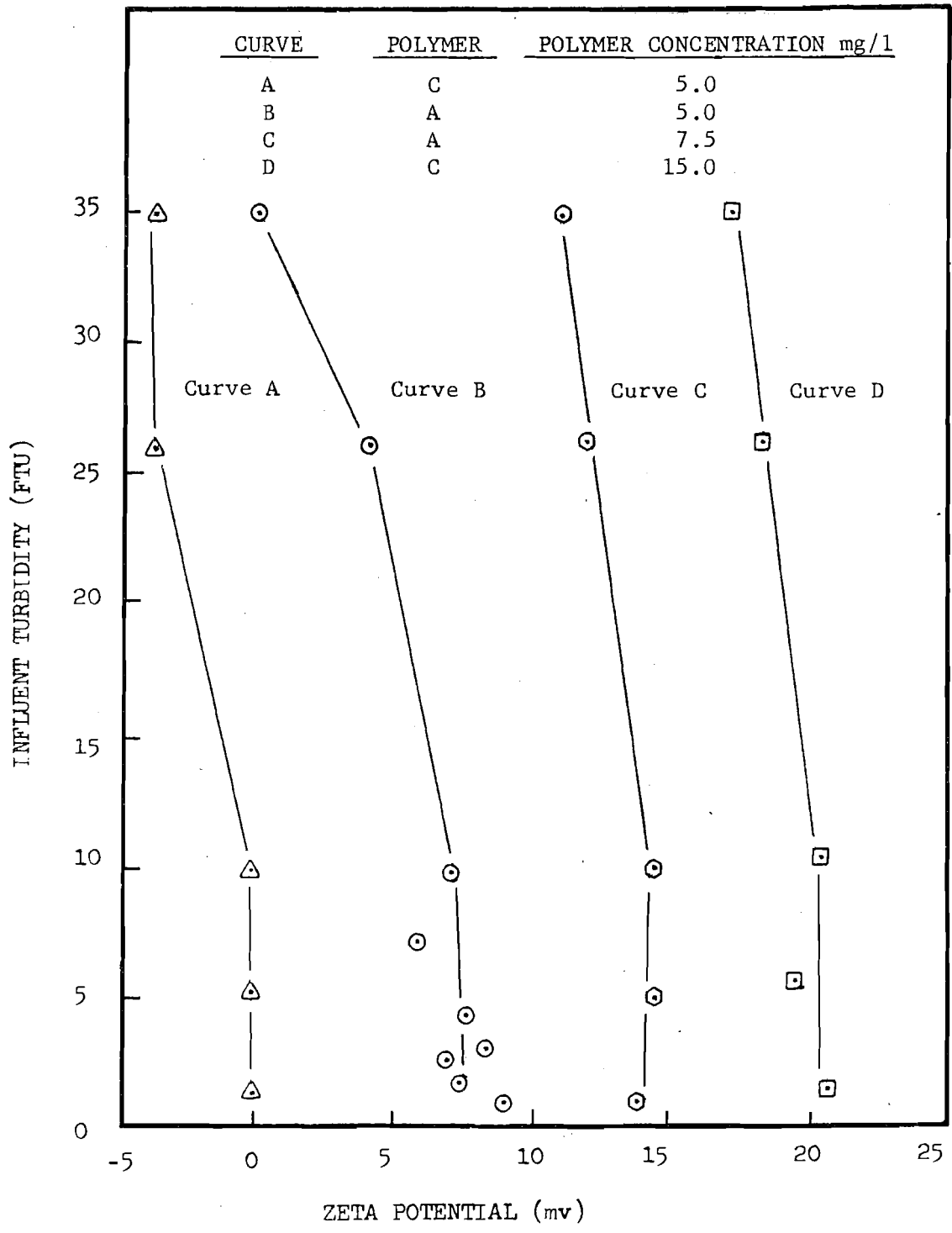


Figure 8. Effect of Influent Turbidity on Particle Zeta Potential for a Given Polymer Concentration

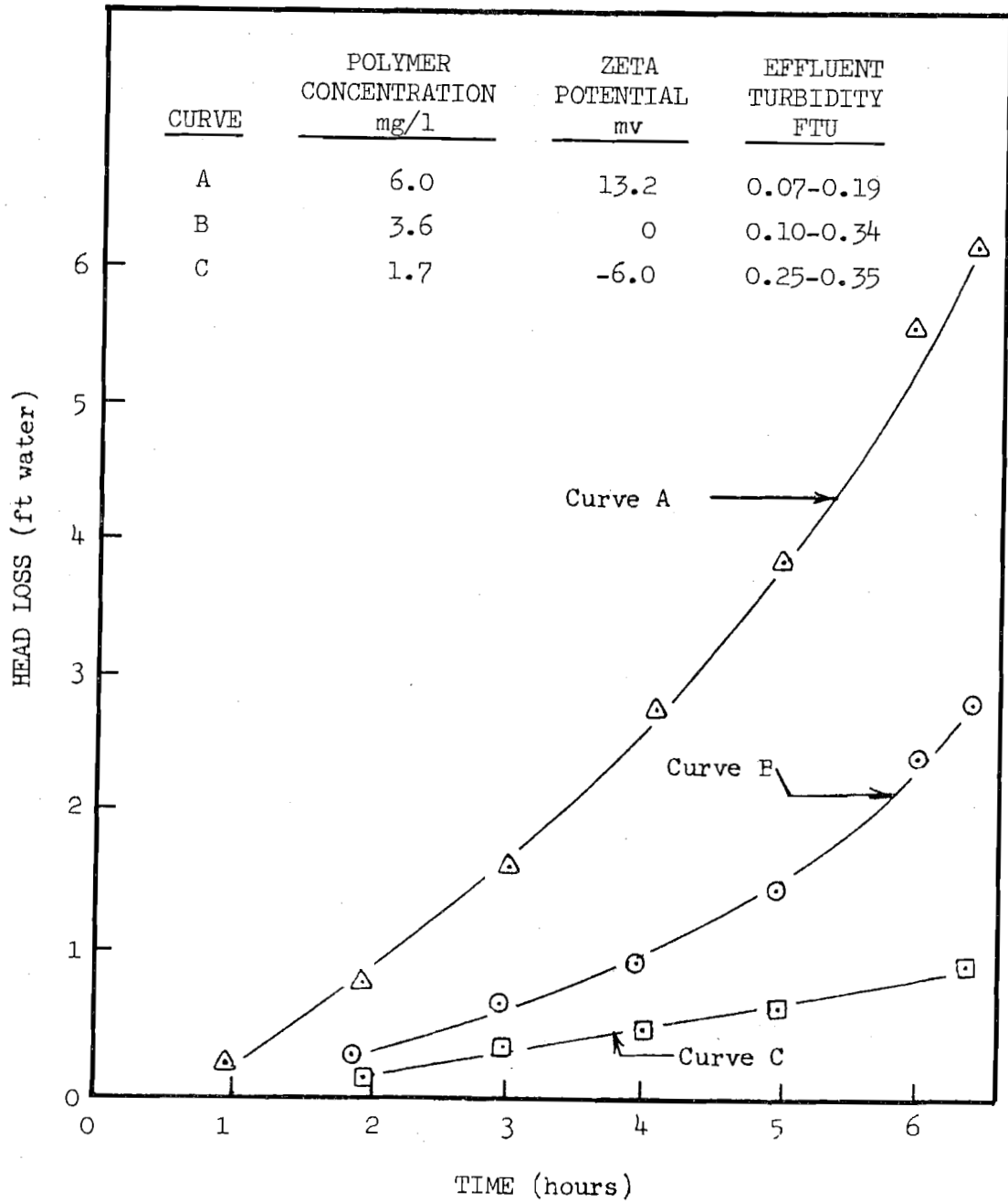


Figure 9. Effect of Polymer Concentration on the Headloss versus Time Relationship for Polymer D

respectively. All three dosages are within the effective range, however, the headloss at 6.5 hours filtration for the dosage closest to the optimum dosage (Curve A) is nearly six times as high as the headloss for a polymer dosage of 1.7 mg/l, Curve C. Similar behavior was observed for the other polymers. Apparently it is advantageous, from the standpoint of minimizing headloss development, to use the lowest possible polymer dosage in the effective range. However, this advantage must be compared with the disadvantages of higher effluent turbidities and longer ripening periods which would also result from such a choice (see Figure 6 ).

Figure 10 shows the effect of polymer type on the rate of headloss build-up. For this graph the influent turbidity was in the range 1.5 to 3.6 FTU. For each polymer type the dosage used resulted in a particle zeta potential of approximately 0 mv. According to Table 4 and Figure 10 the polymers which required the higher concentrations to reach a zero zeta potential also developed the higher headloss. The polymers which resulted in the higher headloss build-up also were the polymers which caused a filter cake to form in and on the upper inches of sand. Polymer A appeared to have the least tendency to form a filter cake. Effluent turbidity was lower for polymer A than for the other three polymers yet the headloss build-up was less for polymer A suggesting that the effect of the nature of the polymer on headloss build-up is greater than the effect of the removal efficiency discussed previously.

Figure 11 illustrates the effect of the influent turbidity on the headloss at 6.5 hours of filtration using a 5 mg/l

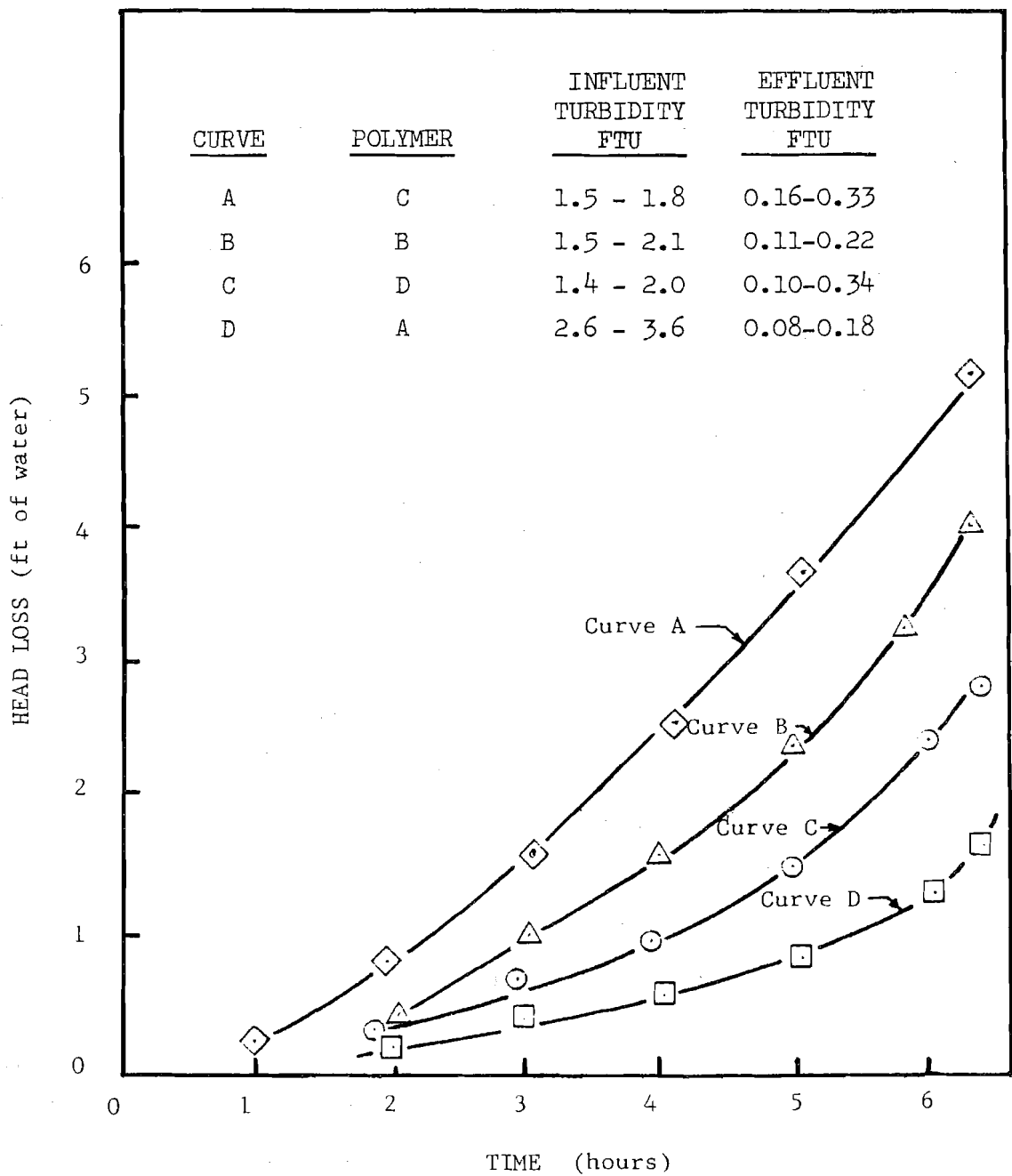


Figure 10. Effect of Polymer Type on Headloss versus Time Relationship for a Zero Particle Zeta Potential.

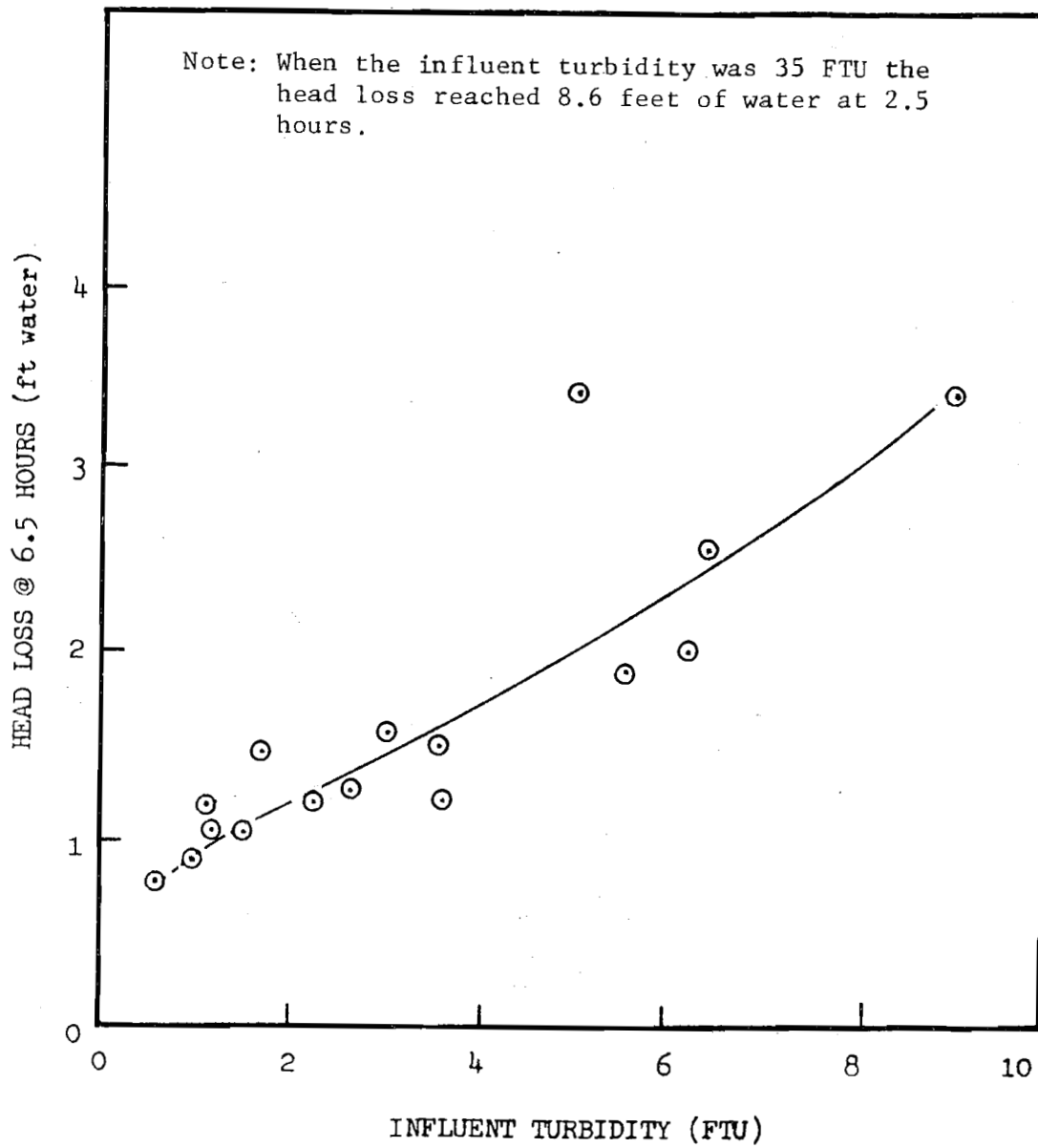


Figure 11. Headloss at 6.5 Hours as a Function of Influent Turbidity  
- 5 mg/l Polymer A



concentration of polymer A. The particle zeta potential was approximately 7 mv for all data points. When the influent turbidity was 35 FTU the headloss reached 8.6 feet in 2.5 hours and the run had to be terminated. This run illustrates the shortcomings of a single media filter for the direct filtration of high turbidity water. Dual or multi-media filters have been shown to be more practicable for high influent turbidities.

Using these preliminary results the major effort of this study was then directed toward determining how a pretreatment step could be used to maximize the performance and efficiency of a dual-media filter, direct filtration system when the sole coagulant was a cationic polyelectrolyte. Cat-Floc T was chosen for study as a result of these preliminary experiments.

B. General Results - Laboratory Filtration Study: During this part of the study 147 experimental filtration runs were conducted using the ranges of pretreatment and filter operating conditions described previously in Section II-A. All experiments were conducted using the cationic polyelectrolyte Cat-Floc T except for several experiments in which Nalco 607 was used. The kaolin/bentonite clay suspension described in Section II-A was used in all experiments. A list of the experimental conditions used for each filtration run is contained in Appendix A. During each experiment effluent turbidity and headloss across four-inch layers of the filter bed were measured as a function of the volume of water filtered per unit area of bed. Each experiment was continued until the overall headloss reached the terminal value (usually 86 inches of water) and/or turbidity breakthrough occurred. To determine the approximate reproducibility of the

experiments one experiment was repeated 14 times during the research period. The pretreatment and filter operating conditions used for these experiments were: polymer concentration,  $PC = 3.0 \text{ mg/l}$ , prefiltration mixing intensity as the  $G$  value,  $G = 25 \text{ sec}^{-1}$ , mean detention time in the prefiltration reactor,  $\bar{T} = 4 \text{ minutes}$ , filtration rate,  $FR = 6 \text{ gpm/ft}^2$ , terminal headloss,  $\Delta H = 30 \text{ inches of water}$  and filter bed 2. The mean value of the water production,  $\overline{WP}_{30}$ , (the subscript denotes the terminal headloss) for the 14 experiments was  $333 \text{ gal/ft}^2$ . The 95 percent confidence interval was  $\pm 13 \text{ gal/ft}^2$  or  $\pm 4$  percent and the range was 305 to  $378 \text{ gal/ft}^2$ . The mean effluent turbidity at  $300 \text{ gal/ft}^2$  was 0.04 FTU and the range was 0.03 to 0.05 FTU.

Figure 12 contains plots of effluent turbidity versus the volume of water filtered per unit area of bed for two sets of pretreatment conditions. In the case of  $G = 700 \text{ sec}^{-1}$ , turbidity breakthrough occurred. This is indicated by the abrupt increase in effluent turbidity at approximately  $1200 \text{ gal/ft}^2$  filtered. In the other case,  $G = 25 \text{ sec}^{-1}$ , the run continued until the terminal headloss of 86 inches was reached. Note that in both cases the effluent turbidity decreased during the ripening period to a value of approximately 0.05 FTU and remained at this level until run termination. This general feature was observed in all experiments. Within a range of polymer concentrations the effluent turbidity was independent of the other pretreatment and the filter operating conditions including the anthracite media grain size distribution. This is apparently the result of the polishing action of the sand

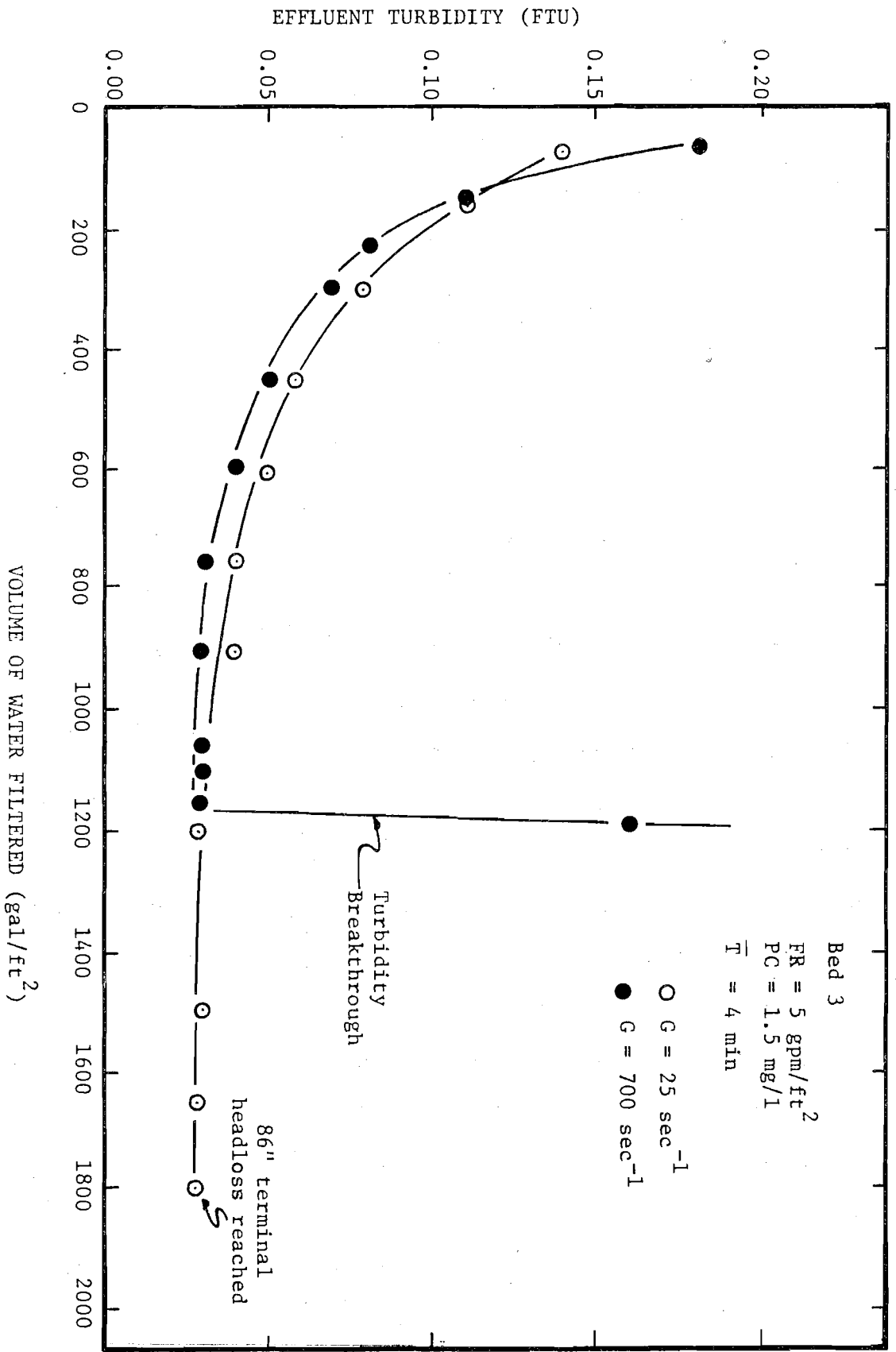


Figure 12. Effluent Turbidity versus Volume of Water Filtered With and Without Turbidity Breakthrough

layer (the size distribution of which was the same in all experiments) and the high filtration efficiency achieved in this range of polymer concentrations.

Figure 13a shows the mean effluent turbidity obtained for the three filter beds at 337 gal/ft<sup>2</sup> filtered plotted versus the polymer concentration. The range of turbidity values at each polymer concentration was within  $\pm 0.01$  FTU. This is within the repeatability range of the instrument used for turbidity measurements. Note that polymer concentrations between about 1.5 and 5 mg/l essentially minimized the effluent turbidity at 337 gal/ft<sup>2</sup> filtered. Figure 13b shows that this range of polymer concentrations corresponds to particle zeta potentials in the range -5 to + 12 mv. In the preliminary filtration studies, when Cat-Floc T was used for the direct filtration of natural suspensions from Lake Michigan, particle zeta potentials in the range from -4 to 13 mv corresponded to an interval of minimum effluent turbidity (see Figure 7). The results of the preliminary and laboratory studies are in agreement.

The effect the polymer concentration has on the effluent turbidity results from two factors, the floc formation which occurs in the prefiltration flocculation reactor and the floc to filter grain (or deposit) collision efficiency. The rate of flocculation in the prefiltration reactor is a maximum at a zero particle zeta potential (16). According to Yao, et al., (17), the filtration efficiency increases as the particle size increases above approximately 1  $\mu$ m. Therefore, an increased

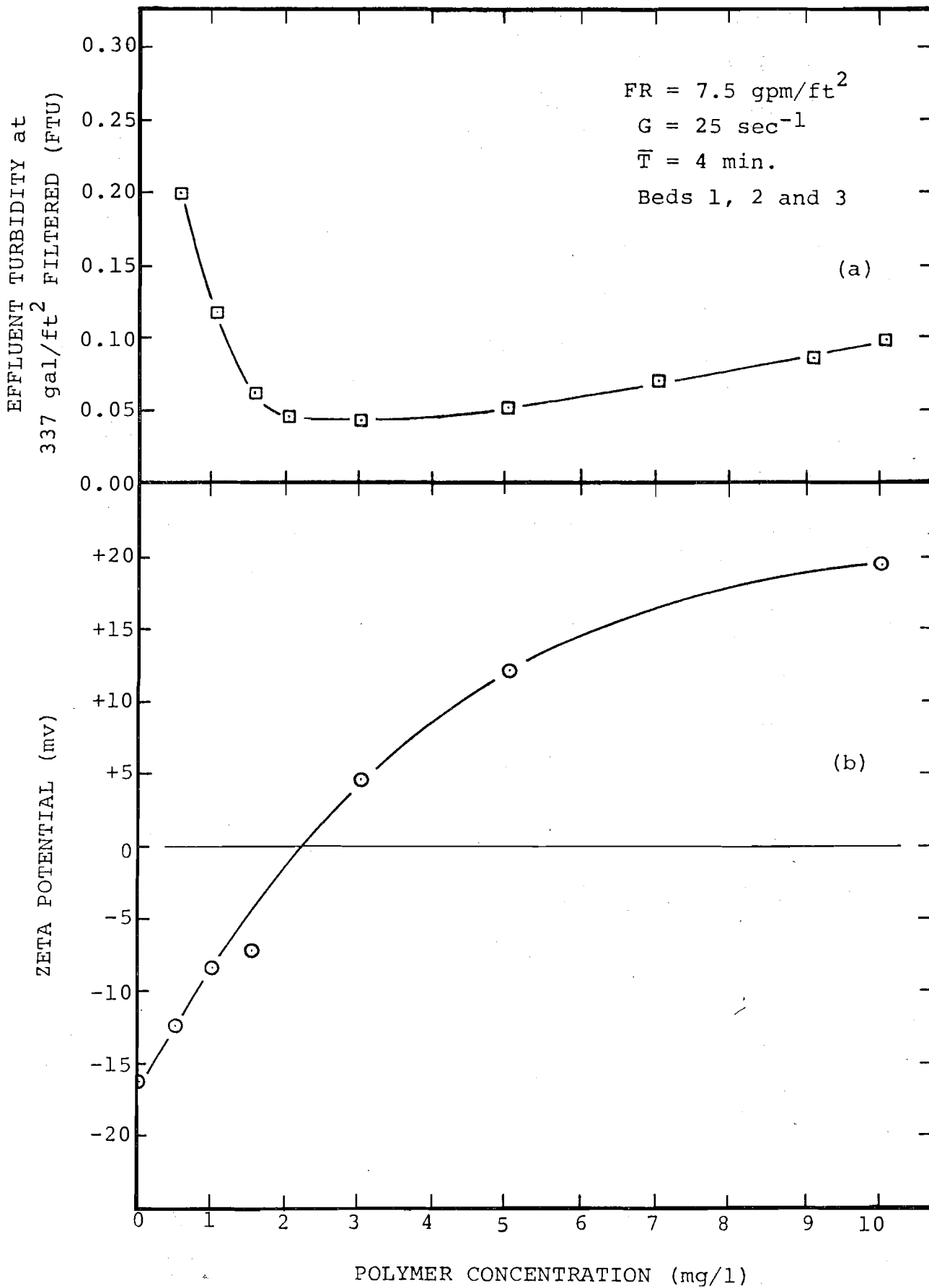


Figure 13. Effluent Turbidity at 337 gal/ft<sup>2</sup> and Particle Zeta Potential versus Polymer Concentration.

rate of flocculation might result in the formation of a greater mass of flocs larger than  $1\ \mu\text{m}$  and consequently a higher filtration efficiency and lower effluent turbidity.

According to Habibian (9), during the initial portion of the filter run when the media grains are clean, the collision efficiency between a polymer treated particle and a filter media grain is a maximum when the particle surface charge (and the particle zeta potential) is somewhat positive, a condition which is compatible with the negative surface charge of the sand grains. The broad interval of effective polymer concentrations and zeta potentials suggests that both the floc to filter grain collision efficiency and the extent of floc formation before filtration are significant factors. However, the insensitivity of the effluent turbidity to the other pretreatment and filter operating variables which effect the floc size and in general the fluid to grain transport step indicates that the floc to filter grain collision efficiency is probably the more significant factor.

Figure 14 is a plot of the headloss across the entire filter bed versus the volume per unit area filtered for the two experiments used for Figure 13. These curves are typical of the results observed throughout the study. In each experiment the relationship between the overall headloss and the volume filtered was approximately linear until significant deposition began to take place in the region where the sand and coal intermixed. At this point, as shown in Figure 14, the curves begin to turn upward.

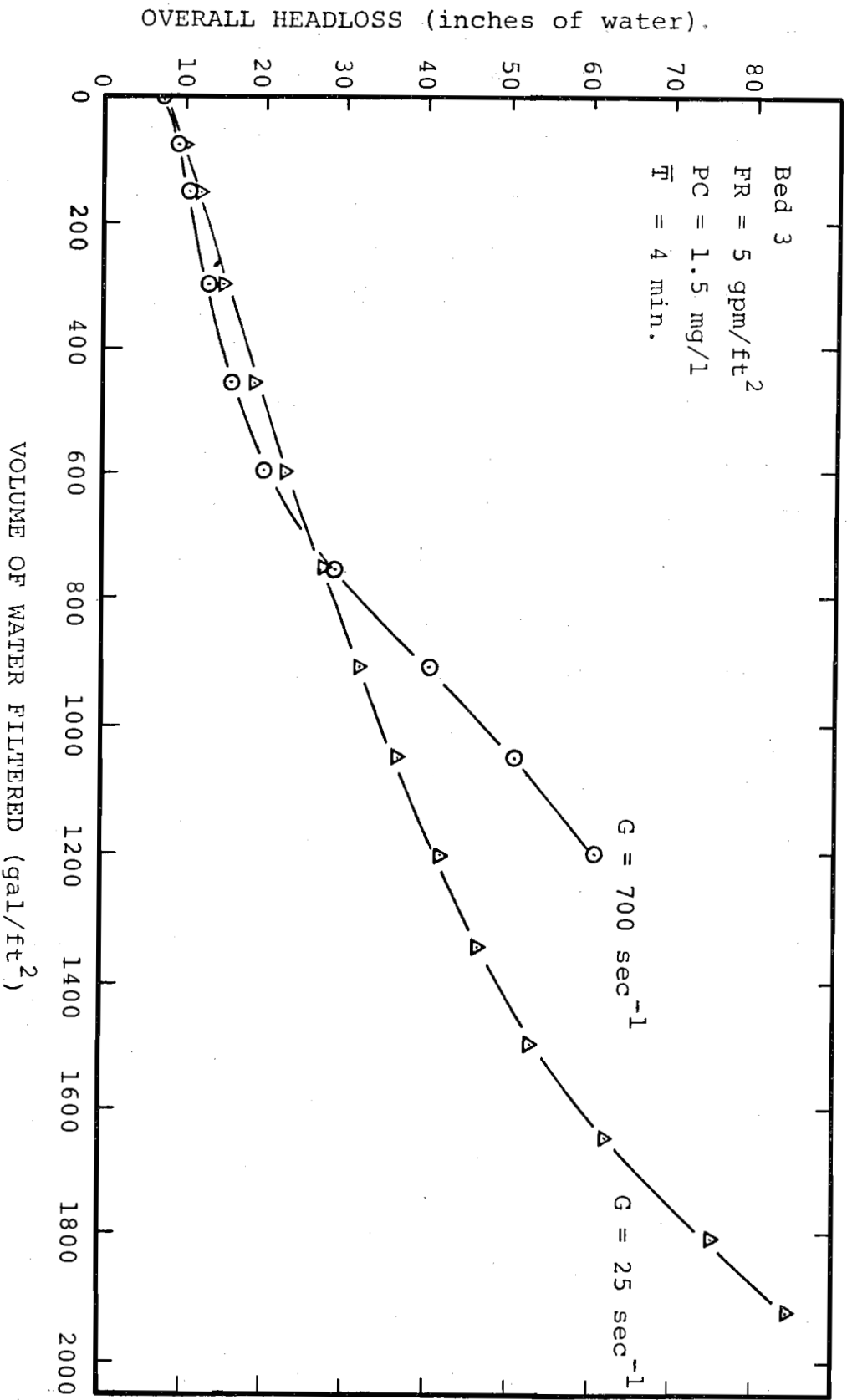


Figure 14. Overall Headloss versus Volume of Water Filtered

Figures 15 and 16 are plots of the headloss across the individual layers of the filter bed versus the volume filtered per unit area of bed. These curves illustrate the "clogging front" described by Adin and Rebhun (8). The upturn in each headloss curve indicates the point at which the leading edge of the clogging front entered the layer. Figure 15 and 16 also illustrate the significance of the rate of clogging front advancement through the bed. For example, in the case of  $G = 25 \text{ sec}^{-1}$ , the upturn in layer 5 occurs at approximately  $1200 \text{ gal/ft}^2$ . In the case of  $G = 700 \text{ sec}^{-1}$  the upturn occurs at approximately  $500 \text{ gal/ft}^2$  and, in addition, as shown in Figure 15 the clogging front enters layer 6, the bottom section of the sand layer. As shown in Figure 15, the  $G = 700 \text{ sec}^{-1}$  run was terminated at  $1200 \text{ gal/ft}^2$  because of turbidity breakthrough. In every experiment in which turbidity breakthrough occurred it was observed that the clogging front had advanced rapidly through the bed and that breakthrough was preceded by a rapid increase in headloss in layer 6. During the laboratory filtration study it was determined that the rate of the clogging front advancement could be increased or decreased using the pretreatment and filter operating variables. For example, the rate of the clogging front advancement could be increased by:

1. increasing or decreasing the polymer concentration above or below approximately 3 mg/l,
2. increasing the filtration rate,
3. increasing the prefiltration mixing intensity above approximately  $G = 25 \text{ sec}^{-1}$  and
4. increasing the effective size of the anthracite media.



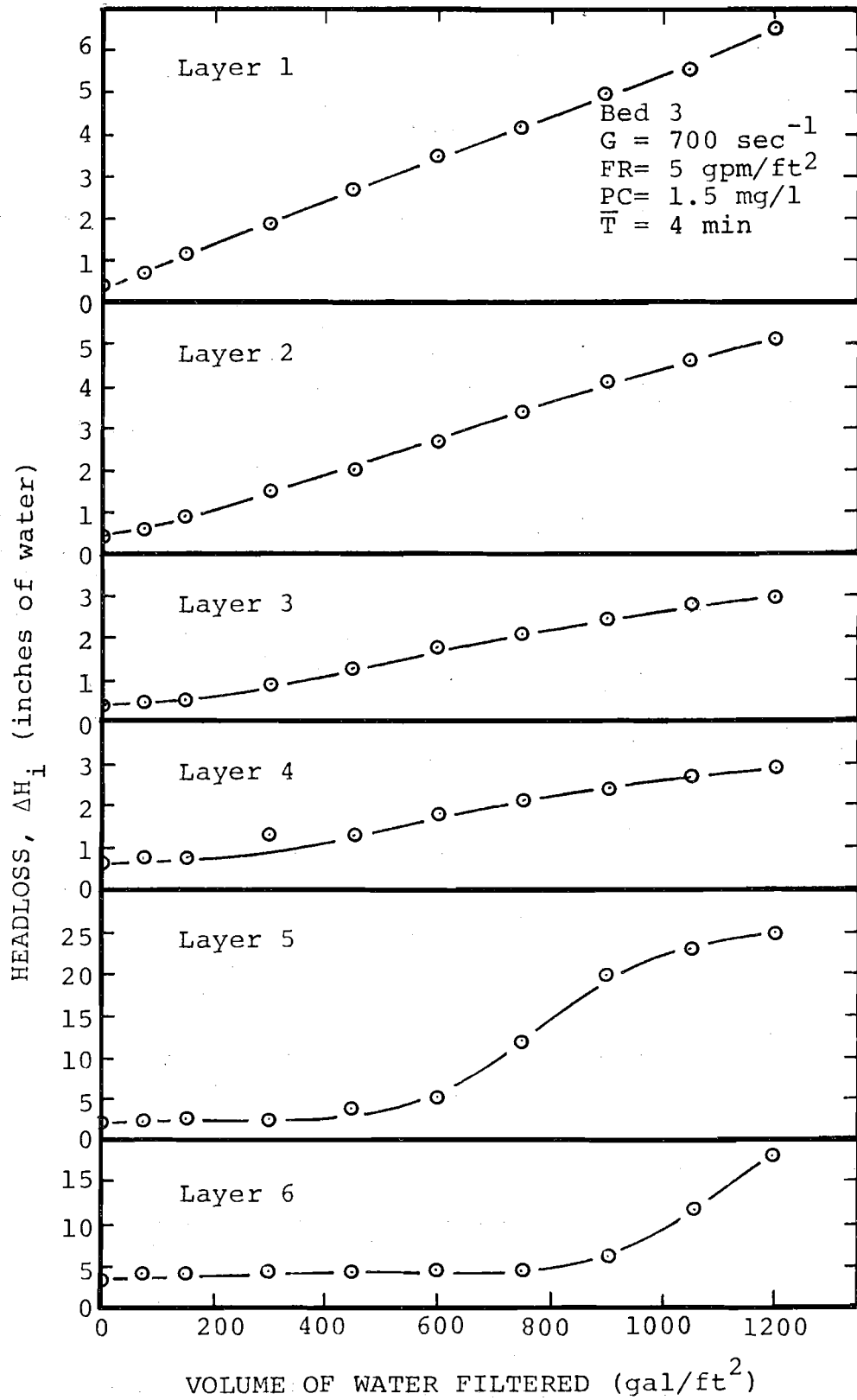


Figure 15. Headloss versus Volume of Water Filtered for Each Layer of the Filter Bed,  $G = 700 \text{ sec}^{-1}$

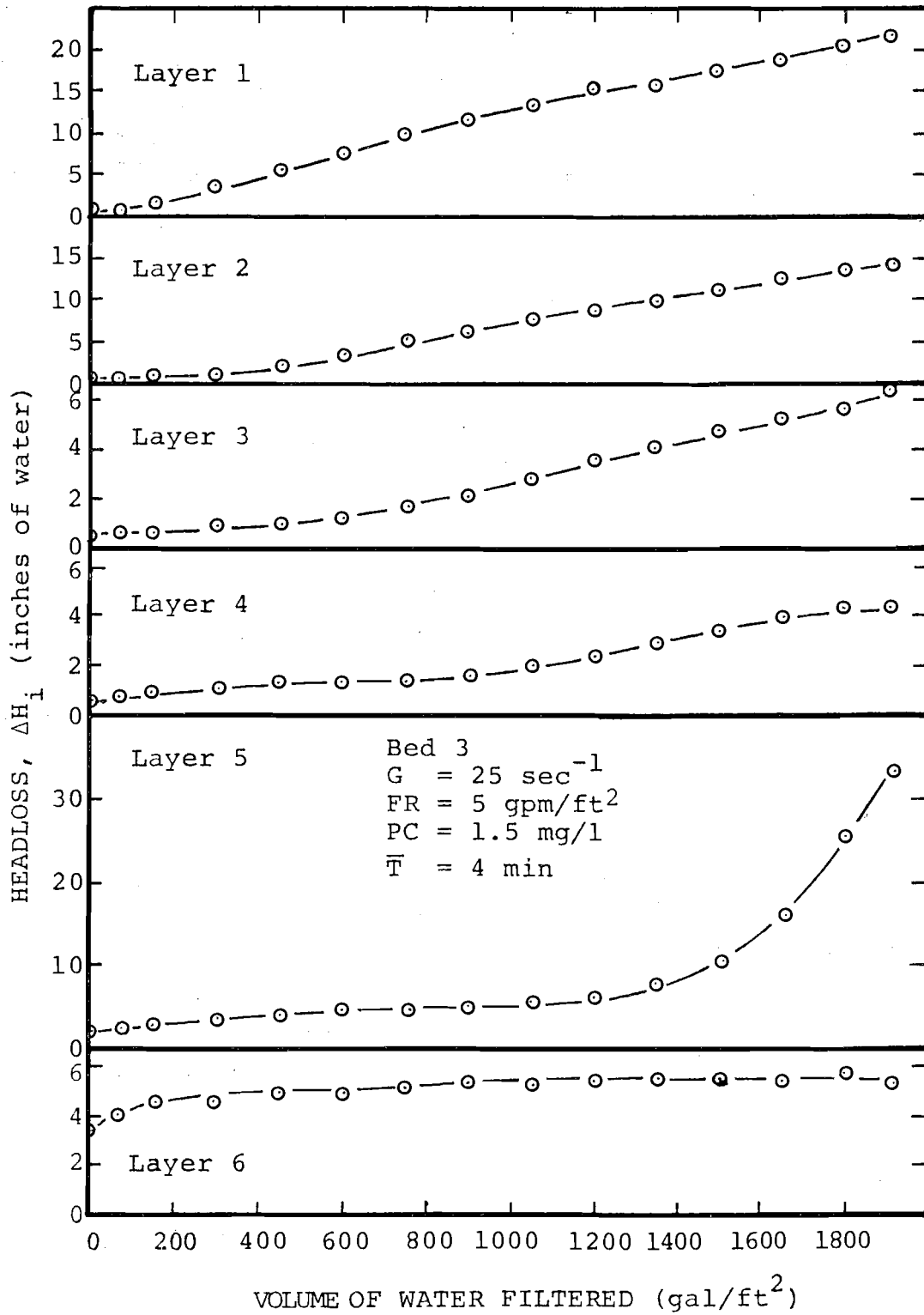


Figure 16. Headloss versus Volume of Water Filtered for each Layer of the Filter Bed,  $G = 25 \text{ sec}^{-1}$ .

In each case the rate of the clogging front advancement could be increased by one or a combination of the above adjustments until turbidity breakthrough occurred before the terminal headloss was reached. And as noted previously, breakthrough was preceded in each case by an increase in the headloss in layer 6. This observation is important in that it suggests that the monitoring of headloss layer by layer is an effective and practical way of protecting against breakthrough, particularly when polymer coagulants are used. In this case the clogging front is relatively defined, i.e., the headloss upturn in each layer is relatively abrupt. The significance of controlling the rate of the clogging front advancement will be discussed again in Section III-D.

Backwashing was accomplished using an average flowrate of approximately 25 gpm/ft<sup>2</sup> for a period of about 10 minutes. Air agitation of the top layer of the anthracite was necessary in practically every case to break-up large coal-floc agglomerates which formed during the initial stages of the backwash as the media began to fluidize. It was also necessary to tap the sides of the filter during bed fluidization to prevent the media from rising as a plug. A larger diameter filter column would probably have prevented this problem. Backwashing deposited materials from the lower layers of the filter bed was not a problem. Details concerning the backwash procedure and the intermixing of the media can be found in DiDomenico's thesis (18).

C. Optimum Specific Deposit Distribution Concept: The optimum specific deposit distribution concept was developed during

this study to enable the calculation of the maximum possible water production per filter run, given the granular filter media design, filtration rate, influent turbidity or suspended solids concentration and terminal (total available) headloss. The concept enables the comparison of alternative filter designs and operational strategies and the assessment of the advantages of effective pretreatment control.

The basic premise of the optimum specific deposit distribution concept is given by the following. If a granular bed filter is divided conceptually into  $n$  equal depth layers there is, for any given total headloss across the filter bed, a distribution of the total specific deposit (volume of deposit per volume of bed) among these  $n$  layers which corresponds to maximum water production per filter run. This can be illustrated using an expression for a mass balance across the filter bed,

$$\begin{array}{l} \text{mass of solids} \\ \text{removed from the} \\ \text{fluid per unit} \\ \text{area of bed during} \\ \text{the run} \end{array} = \begin{array}{l} \text{mass deposited in} \\ \text{the bed per unit} \\ \text{area of bed during} \\ \text{the run} \end{array}$$

or

$$\int_{t=0}^{t=T} Q(C_o - C_e) dt \cong \rho D \frac{\sum_{i=1}^n \sigma_i}{n} \quad (1)$$

where  $T$  is the length of the filter run,  $Q$  is the filtration rate,  $C_o$  and  $C_e$  are the influent and effluent suspended solids concentrations,  $\rho$  is the mass density of the deposit,  $D$  is the depth of the filter bed and  $(\sum_{i=1}^n \sigma_i)/n$  is the average specific deposit in the entire bed. If  $C_e \ll C_o$  and the filtration rate

is constant during the filter run then Eq. (1) can be simplified to the following expression,

$$C_o WP \approx \rho D \frac{\sum_{i=1}^n \sigma_i}{n} \quad (2)$$

where WP is the water production per unit area of bed. Note that  $WP = QT$ . It is apparent from Eq. (2) (and the assumption that  $\rho$  is not a function of time) that the water production is a linear function of the sum of the average specific deposit in each layer,  $\sum_{i=1}^n \sigma_i$ . The determination of the maximum possible water production per filter run is therefore a matter of determining how the total specific deposit should be allocated among the  $n$  layers of the bed such that  $\sum_{i=1}^n \sigma_i$  is maximized and the constraint that the sum of the headlosses across the individual layers of the bed is equal to the terminal headloss is obeyed. In other words the problem is to maximize  $\sum_{i=1}^n \sigma_i$  subject to  $\sum_{i=1}^n \Delta H_i = \Delta H$  where  $\Delta H_i \geq \Delta H_{oi}$ , the clean bed headloss in layer  $i$ . To solve this problem it is necessary to have a mathematical expression or experimental data which relate  $\Delta H_i$ , the headloss in layer  $i$  to,  $\sigma_i$ , the average specific deposit in layer  $i$ .

Herzig, et al. (19) and Sakthivadivel, et al. (20) have described and critiqued many of the numerous empirical mathematical expressions which have been developed to relate  $\Delta H_i$  to  $\sigma_i$ . All of these expressions are based on the Kozeny-Carman equation and have the general form

$$\frac{\Delta H_i}{\Delta H_{oi}} = f(\sigma_i, \theta_i, \text{coefficients})$$

where  $\theta_i$  is the porosity of layer  $i$ . Examples of this relationship

are Mohanka's eq. (20),

$$\frac{\Delta H_i}{\Delta H_{oi}} = \left(1 + p \frac{\sigma_i}{\theta_i}\right)^2 \left(1 - \frac{\sigma_i}{\theta_i}\right)^{-1} \quad (3)$$

and Sakthivadivel's eq. ( )

$$\frac{\Delta H_i}{\Delta H_{oi}} = \frac{(1 - \theta_i + \sigma_i)^2}{(\theta_i - \sigma_i)^3} \frac{\theta_i^3}{(1 - \theta_i)_2} \frac{1}{\xi^2} \quad (4)$$

where  $p$  is a coefficient which is a function of the specific surface area of the filter media and  $\frac{1}{\xi^2}$  is usually assumed to be equal to one. These equations are plotted in Figure 17 for  $\theta_i = 0.45$  and a media grain size of 1.2 mm.

The optimum specific deposit distribution and the corresponding layer by layer headloss distribution can be determined using an expression such as Eq. (3) or (4) and the optimization technique, dynamic programming. The procedure is time consuming if attempted without the aid of a digital computer. Table 5 contains layer by layer terminal headlosses determined using experimental values of the bed 2 clean bed headlosses at a filtration rate of 2.5 gpm/ft<sup>2</sup> and overall terminal headlosses of 86 and 30 inches of water. Sakthivadivel's equation was used to relate  $\Delta H_i$  and  $\sigma_i$ . This expression was chosen because it was developed using data obtained from filtration experiments in which non-colloidal particles were filtered (20). This is similar to conditions in this study. The effect of particle size on headloss development has been noted by O'Melia (21). The sums of the headlosses listed in Table 5 do not equal exactly the overall terminal headlosses of 86 and 30 inches

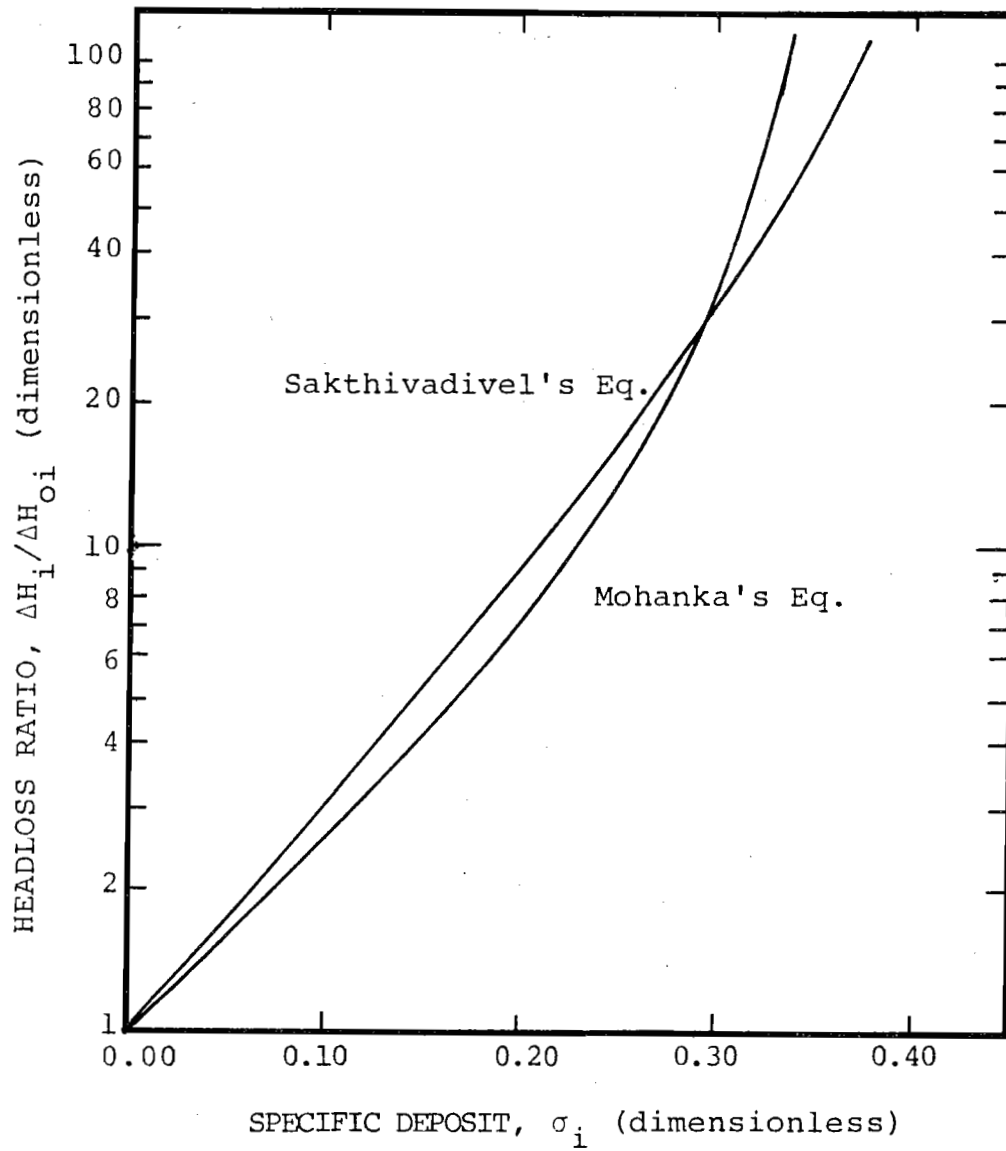


Figure 17. Graphs of Mohanka's (20) and Sakthivadivel's (20) Equations.

because of approximations in the iterative method used to obtain the solution by dynamic programming (22).

Also listed in Table 5 are terminal headloss values calculated using a simplified and more practical procedure which does not involve the dynamic programming technique. This procedure is based on the assumption that the relationship between  $\Delta H_i$  and  $\sigma_i$  can be approximated by the expression

$$\sigma_i \approx K \log \frac{\Delta H_i}{\Delta H_{oi}} \quad (5)$$

where K is a constant. As indicated by the nearly straight line portions of the curves in Figure 17, this expression is a close approximation of both Mohanka's and Sakthivadivel's empirical equations for  $\sigma_i$  less than approximately 0.25. Using Eq. 5, the sum of the average specific deposit in each layer is given by

$$\sum_{i=1}^n \sigma_i \approx \sum_{i=1}^n K \log \frac{\Delta H_i}{\Delta H_{oi}} \quad (6)$$

Using this expression it is a trivial problem to determine that  $\sum_{i=1}^n \sigma_i$  and, according to Eq. 2, the water production per filter run, WP, are maximized and the constraints are met when

$$\Delta H_1 = \Delta H_2 = \dots = \Delta H_n = \frac{\Delta H}{n} \quad (7)$$

i.e., the headlosses across the layers at run termination are equal. In equation form,

$$WP = K' \sum_{i=1}^n \log \frac{\Delta H_i}{\Delta H_{oi}} \quad (8)$$

and

$$WP_{\Delta H}^* = K' \sum_{i=1}^n \log \frac{\Delta H}{n\Delta H_{oi}} \quad (9)$$



Table 5. Calculated Optimum Terminal Headloss Distributions.

Layer	Overall terminal headloss, $\Delta H=86''$		Overall terminal headloss, $\Delta H=30''$	
	$\Delta H_i^*$	$\Delta H_i^{**}$	$\Delta H_i^*$	$\Delta H_i^{**}$
1	11.9	14.3	4.9	5.0
2	11.9	14.3	4.9	5.0
3	15.1	14.3	4.6	5.0
4	14.9	14.3	4.9	5.0
5	15.0	14.3	4.6	5.0
6	14.7	14.3	4.7	5.0
	<u>83.5</u>	<u>86.0</u>	<u>28.6</u>	<u>30.0</u>

\*Calculated using Sakthivadivels eq. and dynamic programming.

\*\*Calculated using Eq. 7.

where  $WP_{\Delta H}^*$  is the maximum water production per filter run for an overall terminal headloss,  $\Delta H$ . The layer by layer headlosses corresponding to the optimum specific deposit distribution calculated by this simplified procedure are included in Table 5. These values are not significantly different from those calculated by the first method.

Figure 18 compares an observed terminal headloss distribution and the specific deposit distribution calculated using the observed clean bed and terminal headlosses and Eq. 5 with the optimum distributions calculated using the same procedure. Note that in this example the observed headloss distribution is skewed toward the top of the filter and that the  $\Sigma \log \frac{\Delta H_i}{\Delta H_{oi}}$  parameter is significantly less than that obtained using the optimum headloss distribution. This indicates that in this case  $WP_{86}$  should be significantly less than  $WP_{86}^*$ .

Figure 19 is a plot of  $\Sigma \log \frac{\Delta H_i}{\Delta H_{oi}}$  versus the water production,  $WP$  in gal/ft<sup>2</sup> for four complete filter runs. According to Eq. 8 these plots should be straight lines with slopes equal to  $1/K'$ . The shape of these lines, especially the initial curvature may be the result of changes in the way the deposit builds within the interstices of the bed as the run proceeds. Comparison of Eq. 5 with the general form of the relationship between  $\Delta H_i$  and  $\sigma_i$  obtained using the Kozeny-Carman equation (see Herzig, et al. (19)) suggests that  $K$  in Eq. 5 and consequently  $K'$  in Eq. 8 are inversely proportional to a deposit packing constant,  $\beta$ , which is defined by,

FILTER BED LAYER

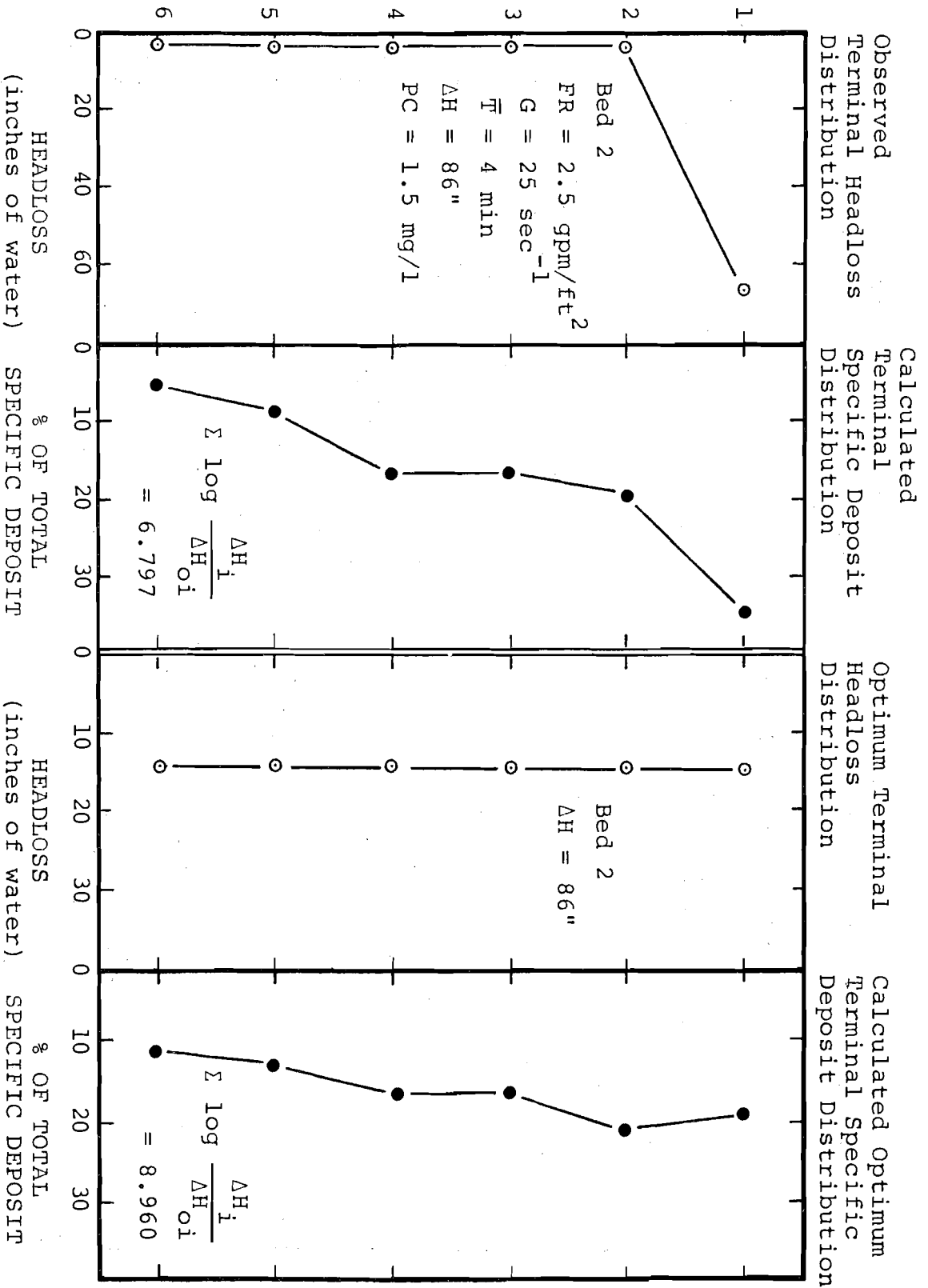


Figure 18. Terminal Headloss and Specific Deposit Distributions

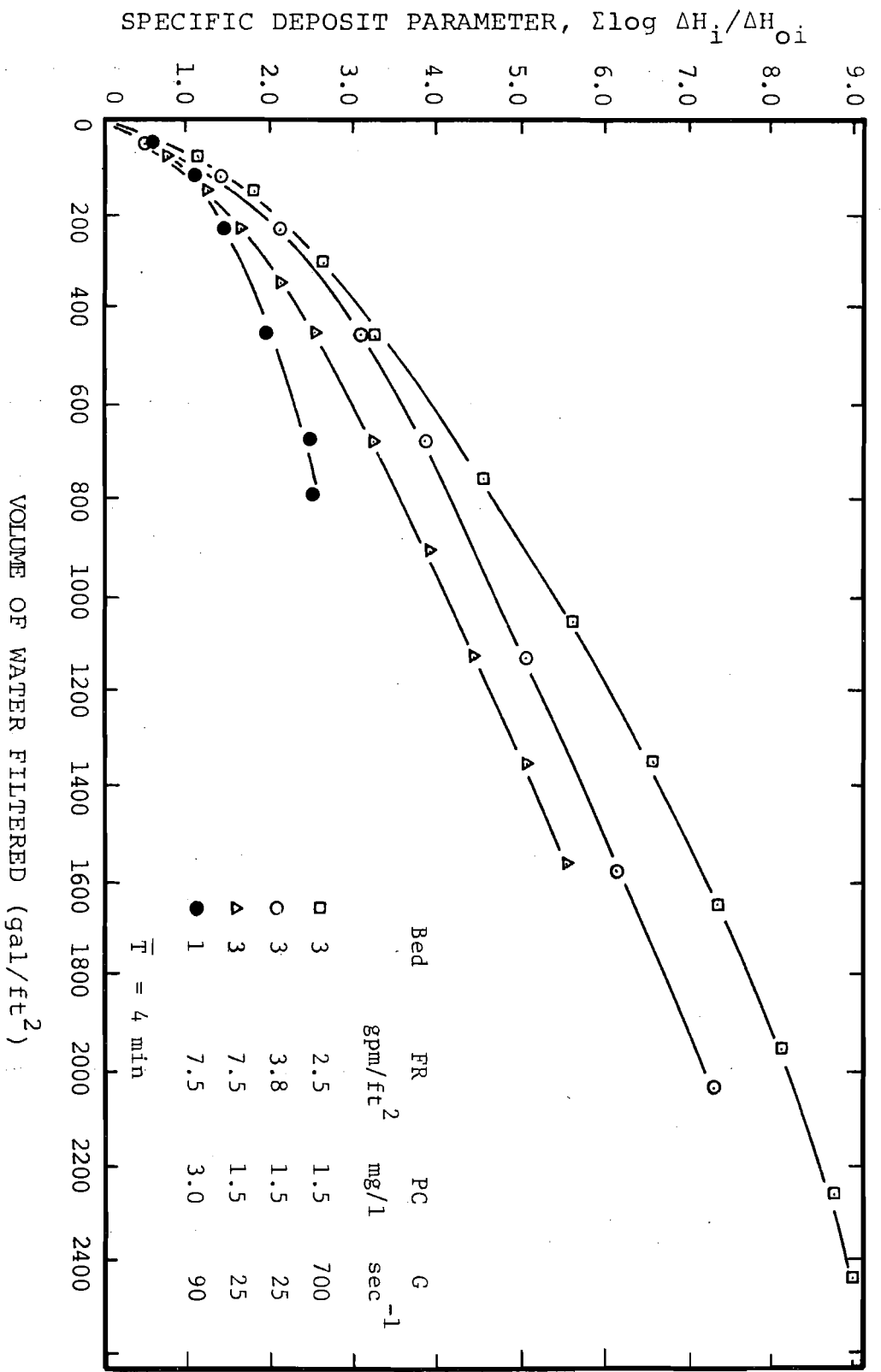


Figure 19. Specific Deposit Parameter versus Volume of Water Filtered for Four Filter Runs

$$\beta = \frac{\text{volume of void space effectively filled}}{\text{volume of deposit}} .$$

An example of the application of  $\beta$  is the following expression for the interstitial fluid velocity  $v'$ ,

$$v' = \frac{v}{\theta - \beta\sigma} ,$$

where  $v$  is the superficial velocity and  $\theta$  is the porosity.

It is possible that in the early stages of deposit formation the deposit builds in an irregular manner rather as a uniform coating on the media grains. This might occur, for example, as a result of preferential attachment of particles to previously deposited material rather than clean filter grains. As the run proceeds and the grains eventually became completely coated, the build-up would become more regular. An irregular build-up of deposit might correspond to a higher value of  $\beta$  which would be in agreement with the higher initial slopes of the curves in Figure 19. As deposition continued and  $\beta$  decreased the curvature would become less and the plots would tend to straighten.

Figures 20 and 21 are graphs of  $\Sigma \log \frac{\Delta H_i}{\Delta H_{oi}}$  versus the water production per filter run for overall terminal headlosses of 30 and 86 inches of water. The plotted data points represent over 40 randomly selected filter runs in which the entire range of pretreatment and filter operating conditions and all three filter beds were used. The plotting of  $\Sigma \log \frac{\Delta H_i}{\Delta H_{oi}}$  versus water production for a particular overall headloss apparently minimizes the effect of the variable packing coefficient. As shown in Figures 20 and 21 the relationship is essentially linear as predicted by Eq. 8. Note, however, that the slope of the

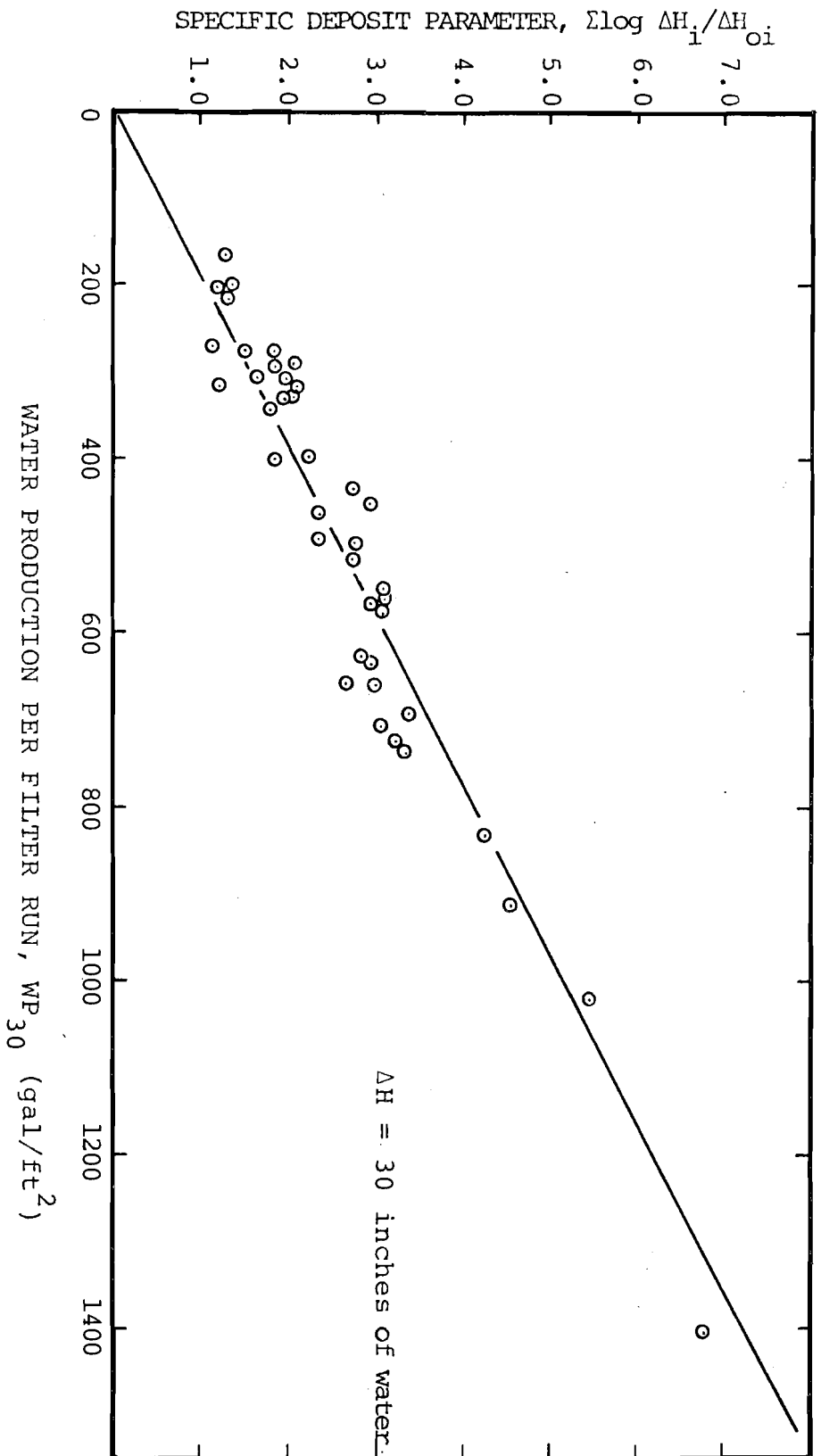


Figure 20. Specific Deposit Parameter versus Water Production per Filter Run,  $\Delta H = 30$ "

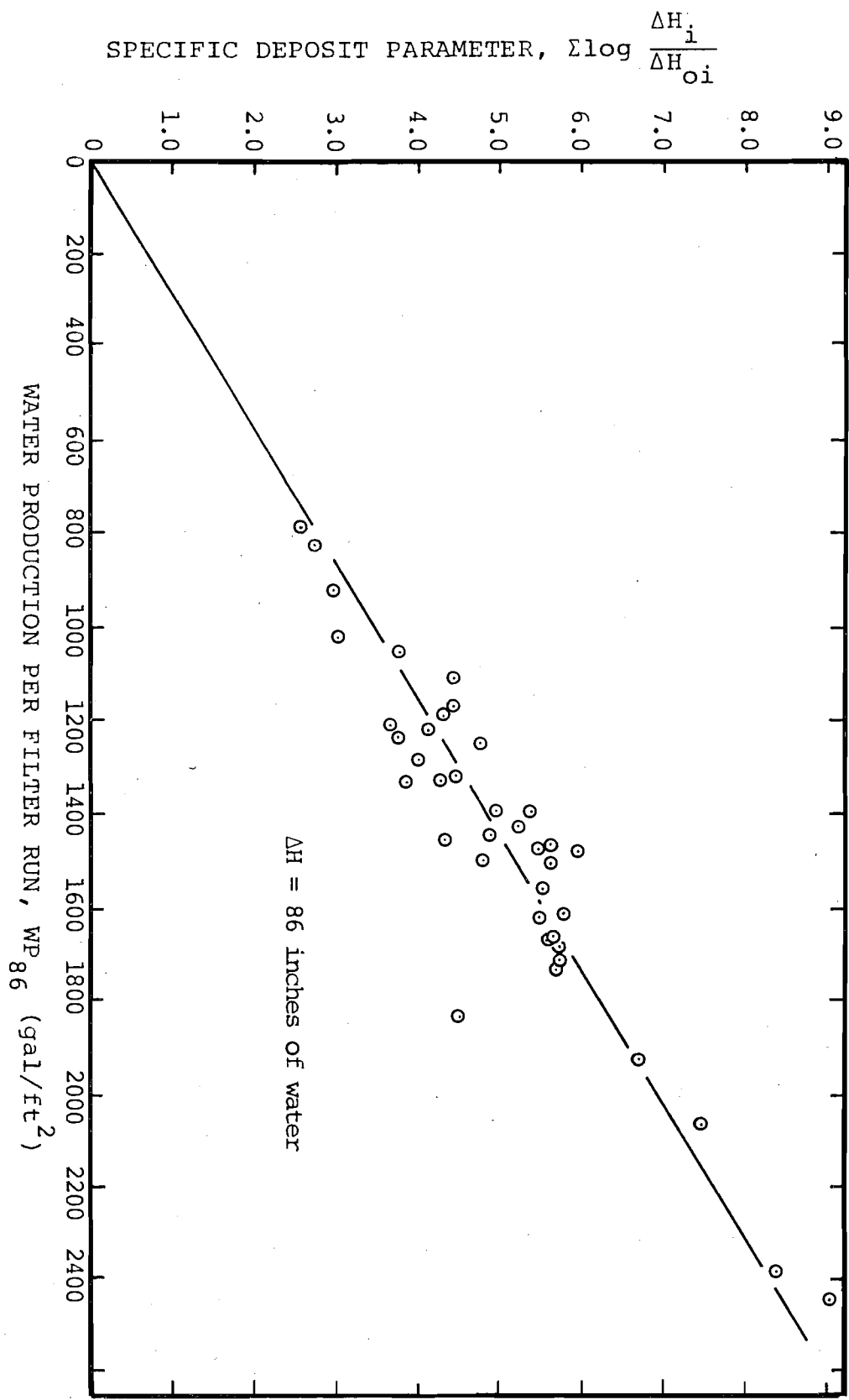


Figure 21. Specific Deposit Parameter versus Water Production per Filter Run,  $\Delta H = 86"$ .

line in Figure 21 is less than that in Figure 20. This is apparently a result of the same phenomenon which determined the shape of the curves in Figure 19. Much of the scatter of the points in Figures 20 and 21 is a result of the sensitivity of the  $\Sigma \log \frac{\Delta H_i}{\Delta H_{oi}}$  parameter to the clean bed headlosses,  $\Delta H_{oi}$ , which were difficult to measure accurately and reproducibly at low filtration rates.

An important application of Figures 20 and 21 is in the determination of, in conjunction with Eq. 9, the maximum water production values  $WP_{30}^*$  and  $WP_{86}^*$ . Using the slopes of the lines in Figures 20 and 21 and Eq. 9,

$$WP_{30}^* \text{ (gal/ft}^2\text{)} = 194 \Sigma \log \frac{30}{6 \cdot \Delta H_{oi}} \quad (10)$$

and

$$WP_{86}^* \text{ (gal/ft}^2\text{)} = 290 \Sigma \log \frac{86}{6 \cdot \Delta H_{oi}} \quad (11)$$

Figure 22 is a plot of  $WP_{30}^*$  and  $WP_{86}^*$  versus the filtration rate for the three filter beds. The clean bed headlosses,  $\Delta H_{oi}$ , which were used with Eqs. 10 and 11 to calculate the plotted values of  $WP_{\Delta H}^*$  were obtained in the following manner. The clean bed headlosses obtained during the study for each filtration rate and each layer of each bed were averaged and plotted versus the filtration rate. In each case the points followed a straight line, the relationship expected for laminar flow. The slopes are listed in Table 6. Using Table 6 the  $\Delta H_{oi}$  for a particular bed, layer and filtration rate was calculated using

$$\Delta H_{oi} = k Q \quad (12)$$

where  $k$  is the slope for that particular layer and bed and  $Q$  is



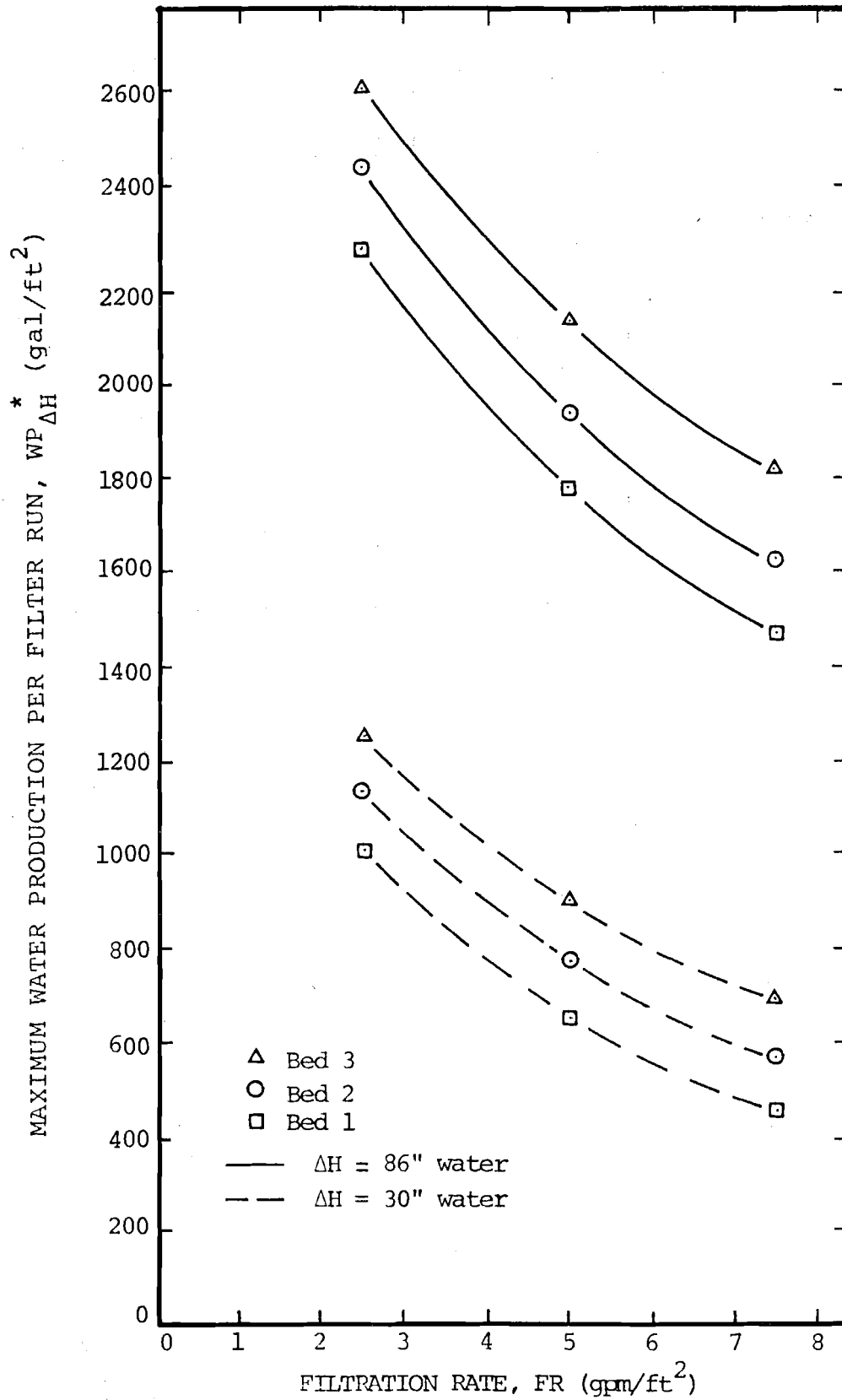


Figure 22. Maximum Water Production per Filter Run versus Filtration Rate

Table 6. Coefficients Used to Calculate Clean Bed Headloss

Layer	k (Eq.12), inches of water per gpm/ft <sup>2</sup>		
	Bed 1	Bed 2	Bed 3
1	0.21	0.12	0.08
2	0.15	0.12	0.08
3	0.15	0.11	0.09
4	0.17	0.15	0.13
5	0.65	0.56	0.44
6	0.77	0.72	0.72

the filtration rate in  $\text{gpm}/\text{ft}^2$ .

Figure 22 illustrates an important point. If the optimum deposit distribution (equal headloss in each layer) is achieved at the same time the overall terminal headloss is reached then the greatest water production per filter run will be obtained when the lowest filtration rate, highest terminal headloss and largest anthracite media grain size are used.

Figure 22 also illustrates indirectly the potential advantages of variable declining-rate filtration, a method of operation described by Cleasby (23). If the filtration rate during the filter run cycle declines uniformly from, for example, 7.5 to 2.5  $\text{gpm}/\text{ft}^2$  then the total filter area required for a particular design flow rate would be based on a filtration rate of approximately 5  $\text{gpm}/\text{ft}^2$ . However, the maximum possible water production,  $WP_{\Delta H}^*$ , would be related to the filtration rate at run termination, 2.5  $\text{gpm}/\text{ft}^2$ , which according to Figure 22 is greater than the  $WP_{\Delta H}^*$  at 5  $\text{gpm}/\text{ft}^2$ , the filtration rate corresponding to the constant-rate design. For the  $WP_{\Delta H}^*$  to be achieved, however, the variable declining-rate method would have to be amenable to achieving the optimum deposit distribution at the point the terminal headloss is reached. This should be possible using proper pretreatment control. Pretreatment control for constant-rate filtration will be discussed in the next section.

Figure 23 shows experimental WP values obtained using the three filter beds, several filtration rates and terminal headlosses of 86 and 30 inches of water. The prefiltration mixing intensity as the G value was 25  $\text{sec}^{-1}$  and the polymer concentration was 1.5 mg/l. These pretreatment conditions tended to result in a

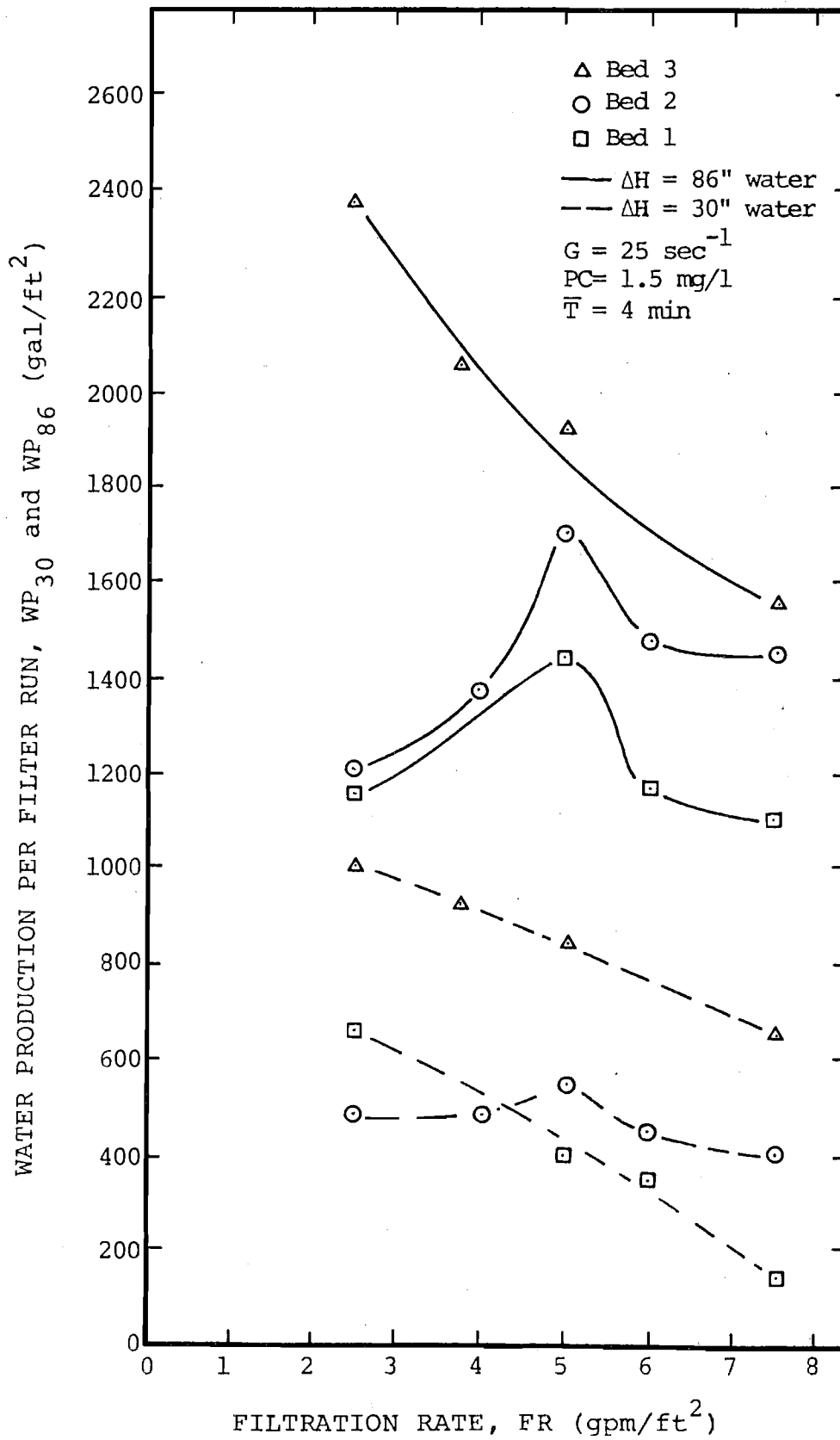


Figure 23. Observed Water Production per Filter Run versus Filtration Rate,  $G = 25 \text{ sec}$ ,  $PC = 1.5 \text{ mg/l}$  and  $\bar{T} = 4 \text{ min}$ .

high filtration efficiency, i.e., efficient particle removal in the upper layers of the filter bed, especially at low filtration rates. For this reason the deposit distributions at run termination for Beds 1 and 2 (the low effective size coal beds) and a filtration rate of  $2.5 \text{ gpm/ft}^2$  were skewed toward the top layer of the anthracite and the water production per filter run was significantly below the maximum. Under these pretreatment conditions more favorable deposit distributions were obtained at higher filtration rates and with the larger effective size coal bed. A detailed discussion of the effect of the pretreatment and filter operating conditions on  $WP_{\Delta H}$  is given in the next section.

D. Pretreatment Studies: The purpose of this portion of the study was to determine how the pretreatment variables including the polymer concentration and the mixing intensity and mean detention time in the prefiltration reactor could be used to maximize the water production per filter run and avoid turbidity breakthrough. The results are summarized in Figures 24, 25 and 26. In these graphs water production per filter run is expressed as a percent of the maximum water production per filter run,  $WP_{\Delta H}^*$ , which was obtained from Figure 22. Several of the values plotted exceed 100 percent apparently because of the method used to estimate  $WP_{\Delta H}^*$  (using Figures 20 and 21 and Eq. (9)) and the experimental error in each value of the water production per filter run.

In Figure 24a water production is plotted versus the prefiltration mixing intensity (as the G value) for terminal headlosses of 86 and 30 inches of water. For  $\Delta H = 86$ " the water production is a maximum at  $G = 60 \text{ sec}^{-1}$ . For  $\Delta H = 30$ " the water production increases as the G value increases from 0 to  $60 \text{ sec}^{-1}$  and from 100 to  $300 \text{ sec}^{-1}$ . In general, the G values which maximized the water production were higher for the lower, 30-inch, terminal headloss. The experimental conditions used in the experiments summarized in Figure 24a were Bed 3, a polymer concentration of 5 mg/l, a filtration rate of  $7.5 \text{ gpm/ft}^2$  and mean detention time of 4 min.

Figure 24b is a plot of water production versus the PMR G value for filtration rates of 2.5 and  $7.5 \text{ gpm/ft}^2$ . As the G value increases from 25 to  $700 \text{ sec}^{-1}$  the water production decreases from 79 to 68 percent of  $WP_{86}^*$  for  $7.5 \text{ gpm/ft}^2$  and

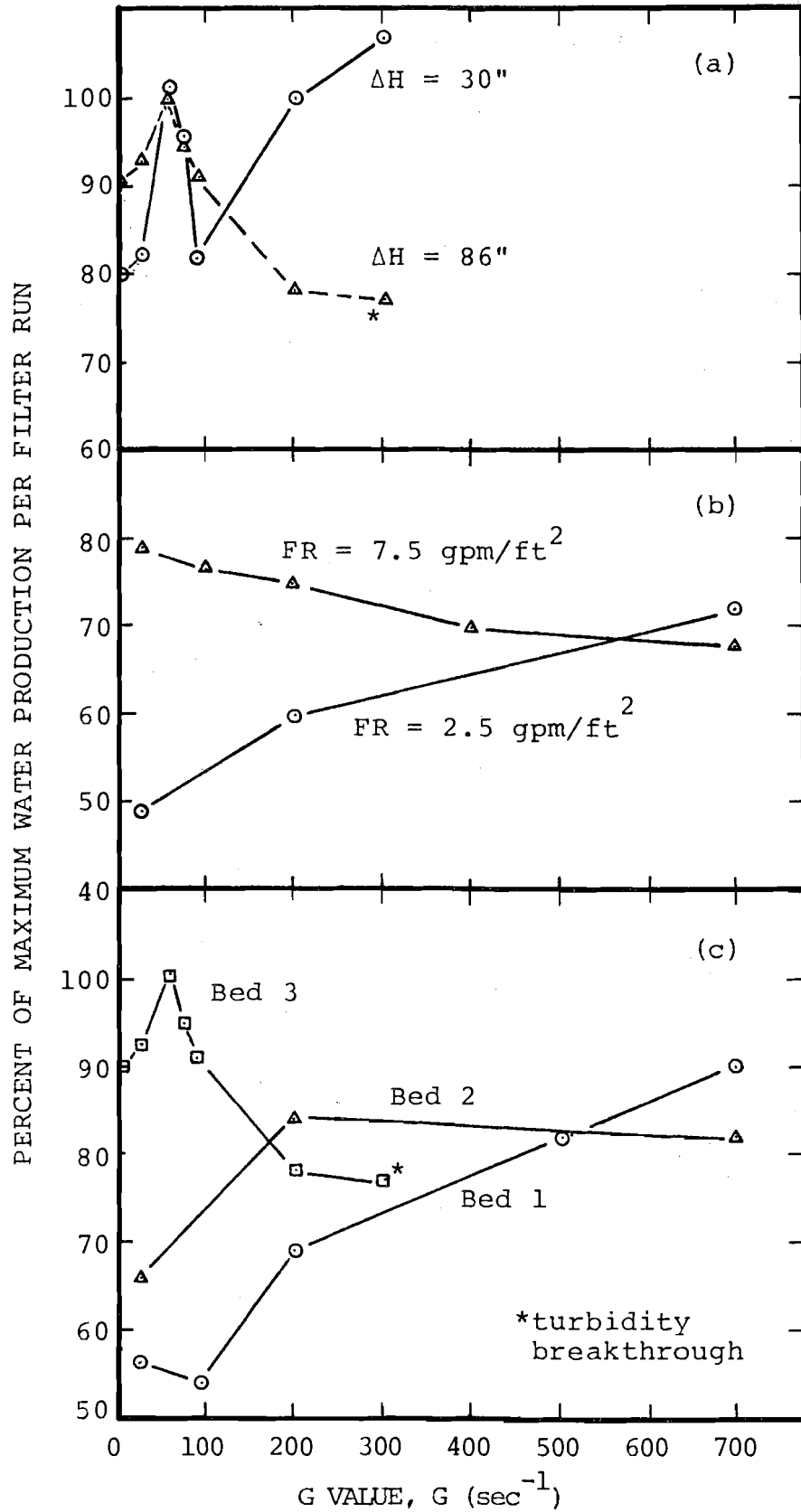


Figure 24. Percent of Maximum Water Production per Filter Run versus  $G$  value

increases from 49 to 72 percent of  $WP_{86}^*$  for 2.5 gpm/ft<sup>2</sup>. Note that Bed 2, a polymer concentration of 1.5 mg/l, a terminal headloss of 86" and a mean detention time of 4 min. were used in these experiments.

Figure 24c is a plot similar to Figure 24a and 24b in which Beds 1, 2 and 3 are compared. For Bed 3, the bed with the coarsest anthracite layer (e.s. = 1.71 mm), the water production is a maximum at  $G = 60 \text{ sec}^{-1}$ . For Beds 2 (e.s. = 1.20 mm) and 1 (e.s. = 0.94 mm) the  $G$  values which maximize the water production are approximately  $200 \text{ sec}^{-1}$  and  $700 \text{ sec}^{-1}$  respectively. The data plotted in Figure 24c were determined using a polymer concentration of 5.0 mg/l with Bed 3 and 3.0 mg/l with Beds 1 and 2. The terminal headloss was 86 inches,  $\bar{T}$  was 4 minutes and the filtration rate was 7.5 gpm/ft<sup>2</sup>.

Figure 25 illustrates the effect of the polymer concentration on water production. Figure 25a is a plot of water production versus the polymer concentration for Beds 1, 2 and 3. The water production is a minimum at a polymer concentration of 3.0 mg/l for Beds 1 and 2. For Bed 3 the water production increases continuously as the polymer concentration is increased from 1.0 to 7.0 mg/l. A  $G$  value of  $25 \text{ sec}^{-1}$ , a  $\bar{T}$  of 4.0 min, a filtration rate of 7.5 gpm/ft<sup>2</sup> and a terminal headloss of 86 inches were used in these experiments.

Figure 25b is plot of water production versus the polymer concentration for terminal headlosses of 86 and 30 inches of water. The experimental conditions include a  $G$  value of  $25 \text{ sec}^{-1}$ , Bed 3 and  $\bar{T} = 4 \text{ min}$ . The water production is a minimum at a polymer concentration of 3.0 mg/l when the terminal



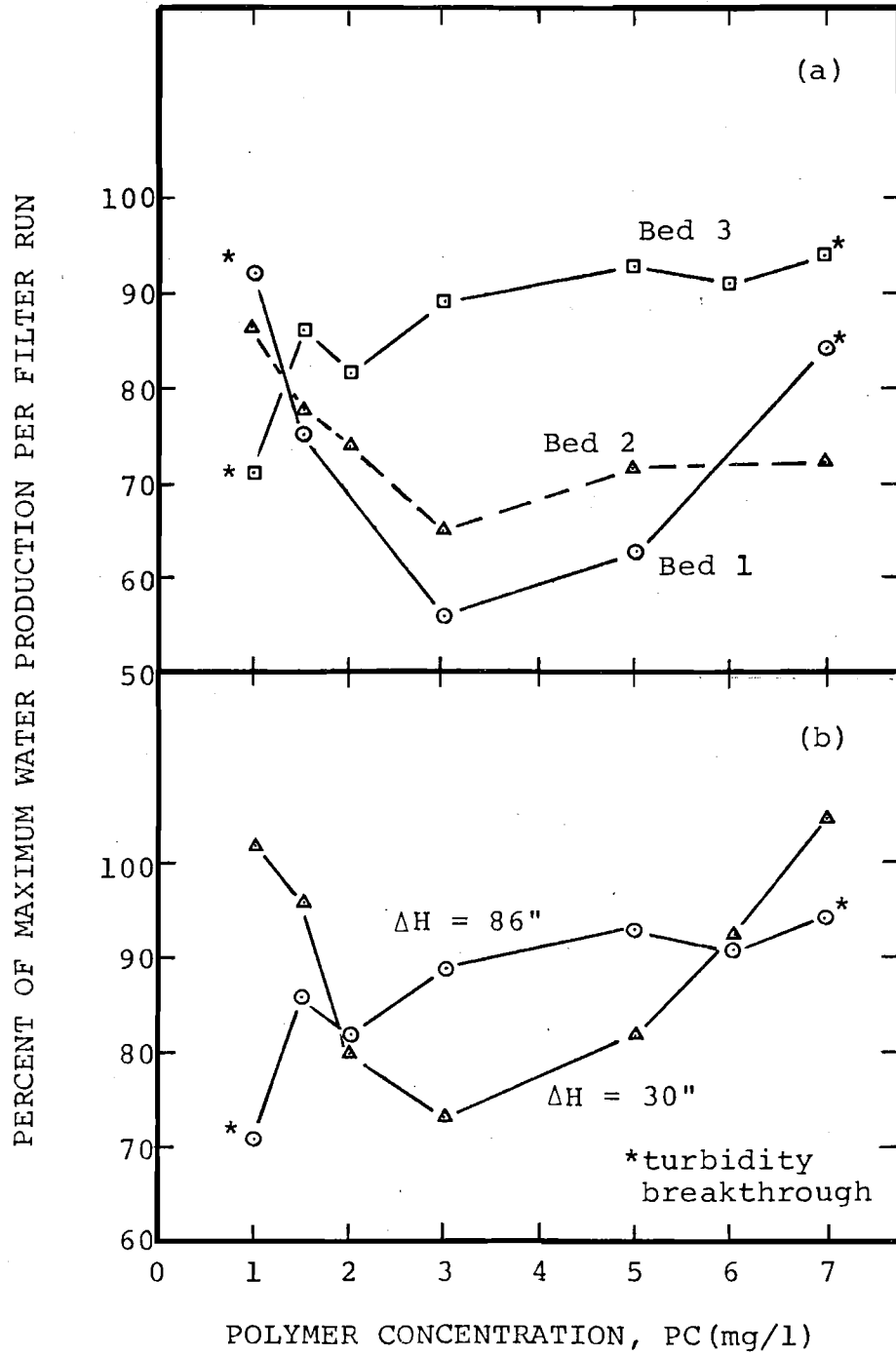


Figure 25. Percent of Maximum Water Production versus Polymer Concentration

headloss is 30 inches, however, as noted in the discussion of Figure 25a, when a terminal headloss of 86 inches is used the water production increases continuously as the polymer concentration increases from 1.0 to 7.0 mg/l.

Figure 26 illustrates the effect of the prefiltration reactor mean detention time,  $\bar{T}$ , on the water production per filter run. The data was determined using Bed 1, a polymer concentration of 1.5 mg/l, terminal headlosses of 75 and 30 inches of water and the G values listed with the figure. It was necessary to use a terminal headloss of 75 inches because hydraulic losses in the water supply system reduced the total available head to 75 inches when the flow rate was increased to produce a  $\bar{T}$  of 2.0 min. The optimum G values listed with the figure are the G values which maximized the water production for  $\Delta H = 75"$ . For example, in Figure 24 c, Bed 3, the optimum G value is  $60 \text{ sec}^{-1}$ . For the conditions used in Figure 26 the G value which maximized  $WP_{75}$  decreased from  $400 \text{ sec}^{-1}$  at  $\bar{T} = 2.0 \text{ min}$  to  $100 \text{ sec}^{-1}$  at  $\bar{T} = 9.2 \text{ min}$ . The relationship between the optimum G value and  $\bar{T}$  is a function of the polymer concentration. At a polymer concentration of 1.0 mg/l and  $\bar{T} = 9.2 \text{ min}$ , the optimum G value was  $275 \text{ sec}^{-1}$ . In general, the results plotted and tabularized in Figure 26, indicate that the water production increases as  $\bar{T}$  increases from 2.0 to 9.2 minutes. This trend is also the case when the optimum G value corresponding to each  $\bar{T}$  is used.

The results obtained in the pretreatment studies can be interpreted by considering the relationships between the pretreatment and filter operating conditions and the rate of

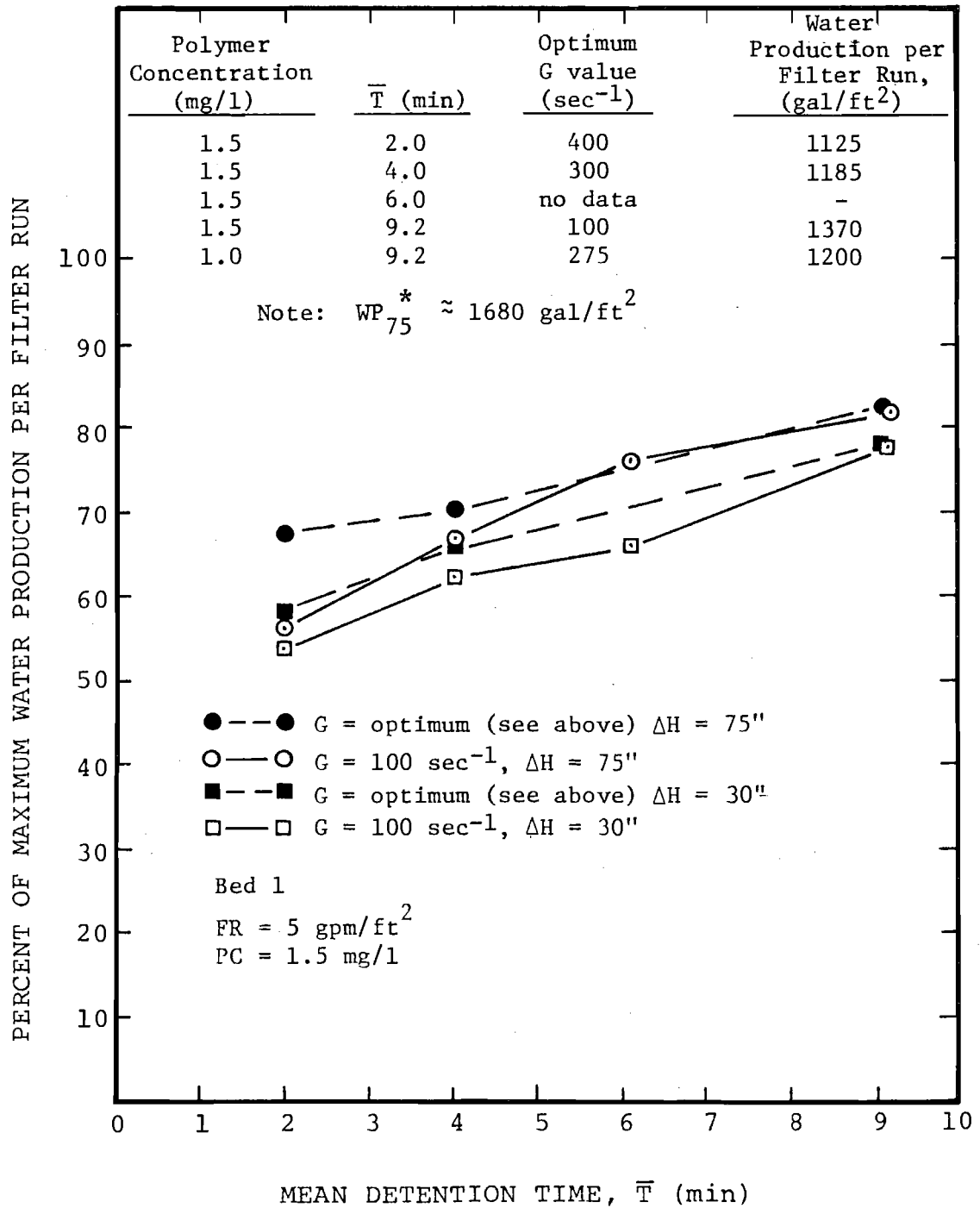


Figure 26. Percent of Maximum Water Production per Filter Run versus Mean Detention Time

advancement of the clogging front down through the filter media. The rate of advancement of the clogging front determines the distribution of specific deposit at run termination and whether or not turbidity breakthrough occurs before the terminal headloss is reached. The terminal specific deposit distribution, as discussed in the previous section, is related to the water production per filter run.

The rate of advancement of the clogging front is an inverse function of the particle removal efficiency within the filter. The more efficiently particles are removed at any location in the filter the slower the rate of advancement of the clogging front. A conceptual filtration model by O'Melia (21) and Yao, et al. (17), although it is no longer state-of-the-art, can be used to estimate the effect of various factors on the particle removal efficiency. The model predicts that the particle removal efficiency of a clean granular filter will increase as:

1. the particle diameter increases above or decreases below approximately 1 to 10  $\mu$ ,
2. the filter media grain diameter decreases,
3. the filtration rate decreases,
4. the degree of particle destabilization increases and
5. the density of the particles increases.

O'Melia's (21) model provides a useful qualitative relationship between most of the variables studied in this investigation and the rate of advancement of the clogging front. However, the relationship between the prefiltration reactor mixing intensity and the rate of advancement of the clogging

front is not obvious. The supplementary study described in Section II-C was conducted to determine the effect of the prefiltration mixing intensity on the size distribution and density of the flocs that are applied to the filter. A polymer concentration of 1.5 mg/l and a 4 min. period of mixing were used in these batch-type experiments.

Figure 27 is a plot of the relative mass concentration of floc versus the floc diameter for G values of 25, 200 and  $700 \text{ sec}^{-1}$ . The bimodal distribution for  $G = 25 \text{ sec}^{-1}$  suggests that under these conditions a significant population of primary particles exists after the 4 min. flocculation period. For  $G = 200 \text{ sec}^{-1}$  the primary particle peak has disappeared and the floc distribution is centered at a floc diameter of approximately  $200 \mu\text{m}$ . For  $G = 700 \text{ sec}^{-1}$  the floc distribution has narrowed somewhat and primary size particles or flocs are apparent.

Floc density was determined as a function of floc diameter using the method described in Section II-C. The final results are plotted in Figure 28. Floc density decreases with floc diameter in two stages. Between floc diameters of 10 and  $80 \mu\text{m}$  the density decreases from 2.6 to  $1.05 \text{ gm/cm}^3$ . Above a floc diameter of approximately  $100 \mu\text{m}$  the dependence of floc density on size is significantly less. The results suggest that floc growth occurs in two stages. Michaels and Bolger (24) have noted that floc growth may occur by the agglomeration of primary particles followed by a second stage in which the flocs join to form loose aggregates.

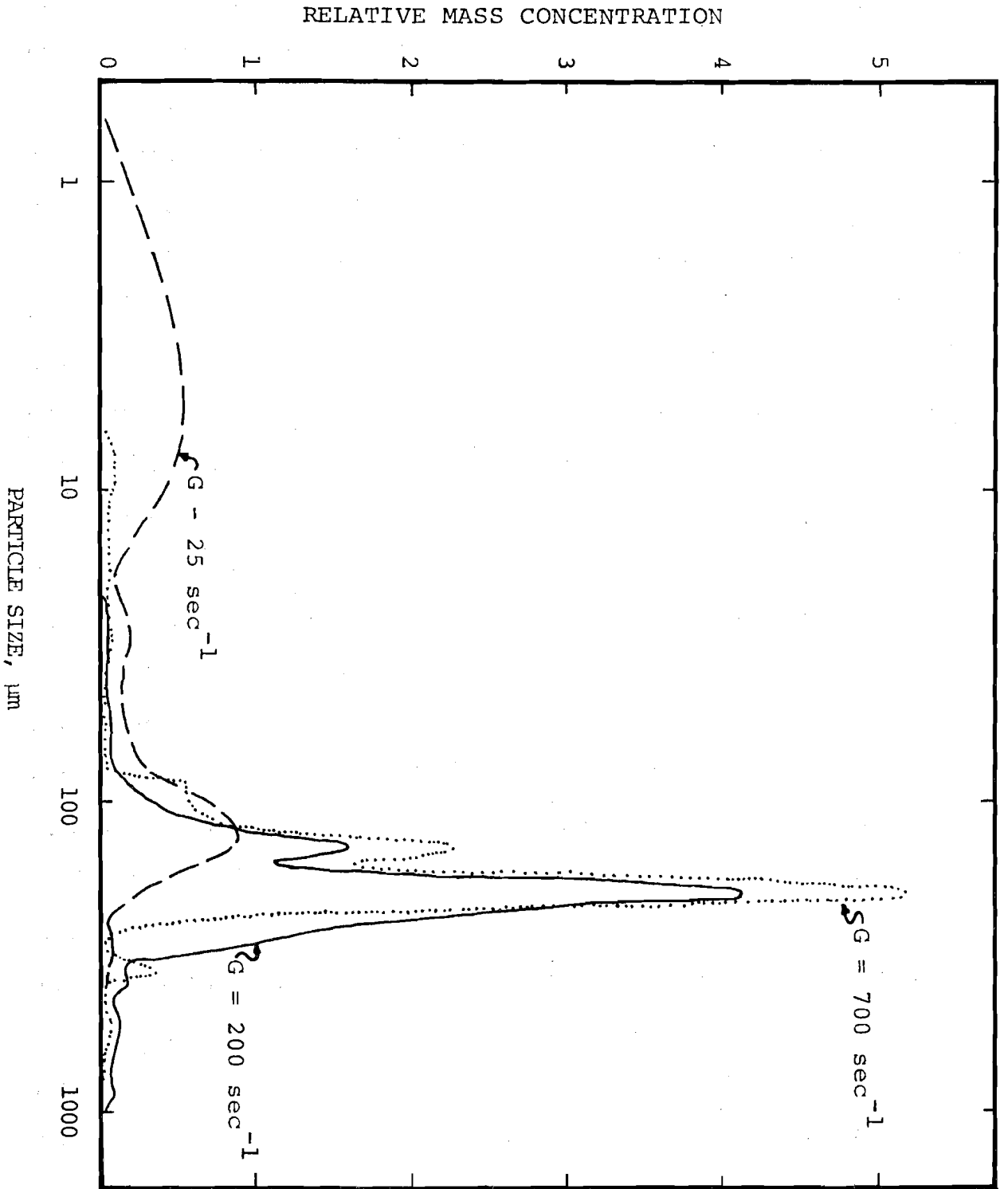


Figure 27. Floc Size Distributions

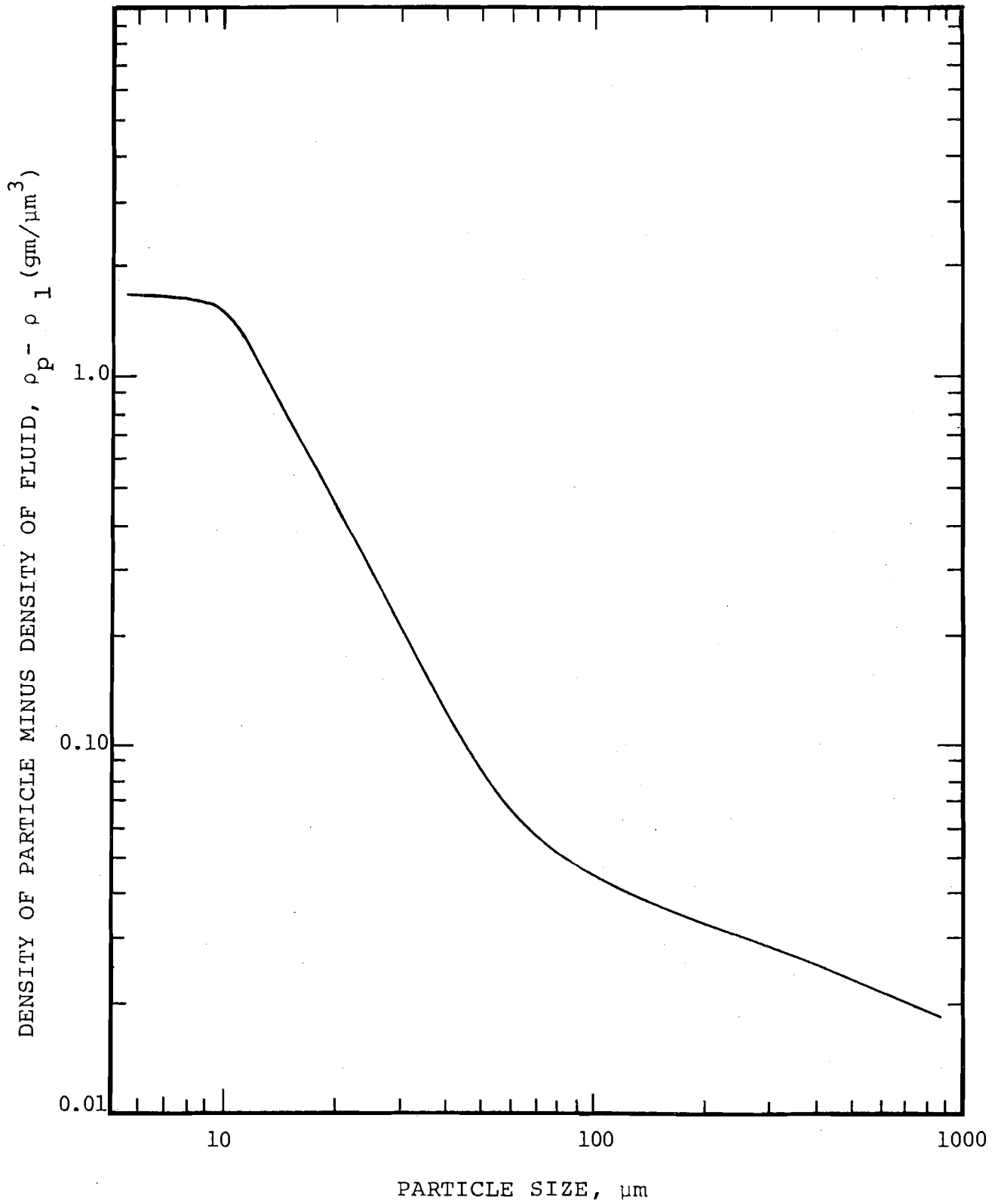


Figure 28. Relationship Between Floc Size and Density

It is apparent from these supplementary experiments that the prefiltration mixing intensity has a significant effect on the size distribution and density of the flocs that are applied to the filter. According to the filtration model of Yao, et al., (17) the prefiltration mixing intensity should therefore be related to the filtration efficiency and consequently to the rate of advancement of the clogging front. A complete interpretation of the effect of the prefiltration mixing intensity on the clogging front advancement and terminal specific deposit distribution is made difficult by the fact that the particle size and density factors are counteracting, i.e., the particle density decreases as the particle size increases. In Figure 24b the water production for the  $7.5 \text{ gpm/ft}^2$  filtration rate decreases continuously from  $G = 25 \text{ sec}^{-1}$  to  $G = 700 \text{ sec}^{-1}$  because of an increasing amount of buildup in the sand layer. Apparently the primary particles remaining after the flocculation step at  $G = 25 \text{ sec}^{-1}$  either flocculate while moving between the PMR and the filter or they are efficiently removed because of their size. It is also possible, based on a review of jar test results (25), that the primary particles formed in the PMR by the erosion or break-up of flocs are inefficiently removed in the upper, deposit-containing layers of the bed. The number of primary particles formed by the erosion or break-up mechanism would increase as the G value is increased.

The effect of the G value on headloss and specific deposit distributions at run termination is illustrated in Figures 29 and 30. The data plotted were obtained from the experiments used to develop the  $\Delta H = 86$  inches curve in Figure 24a. Note



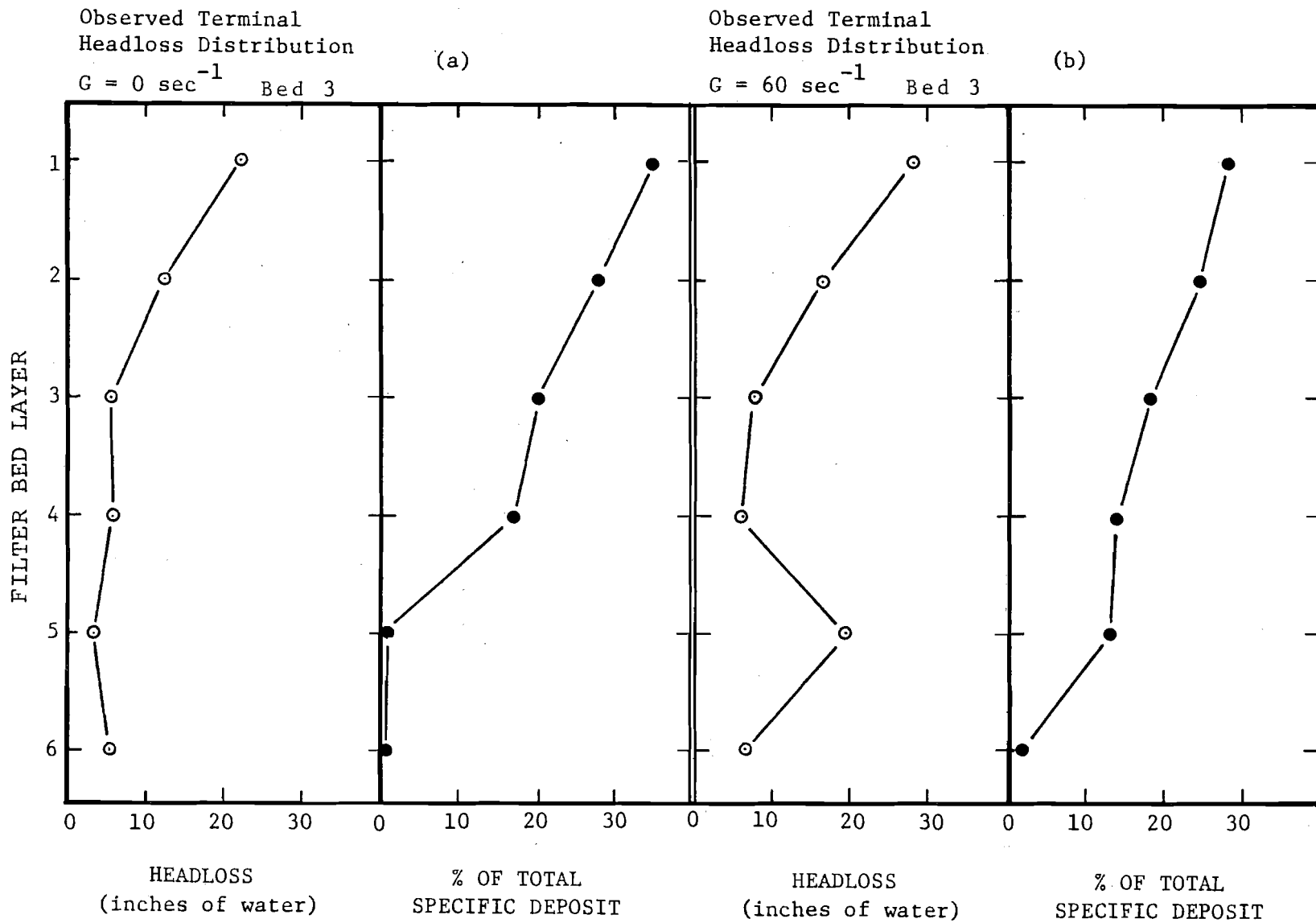


Figure 29. Terminal Headloss and Specific Deposit Distributions

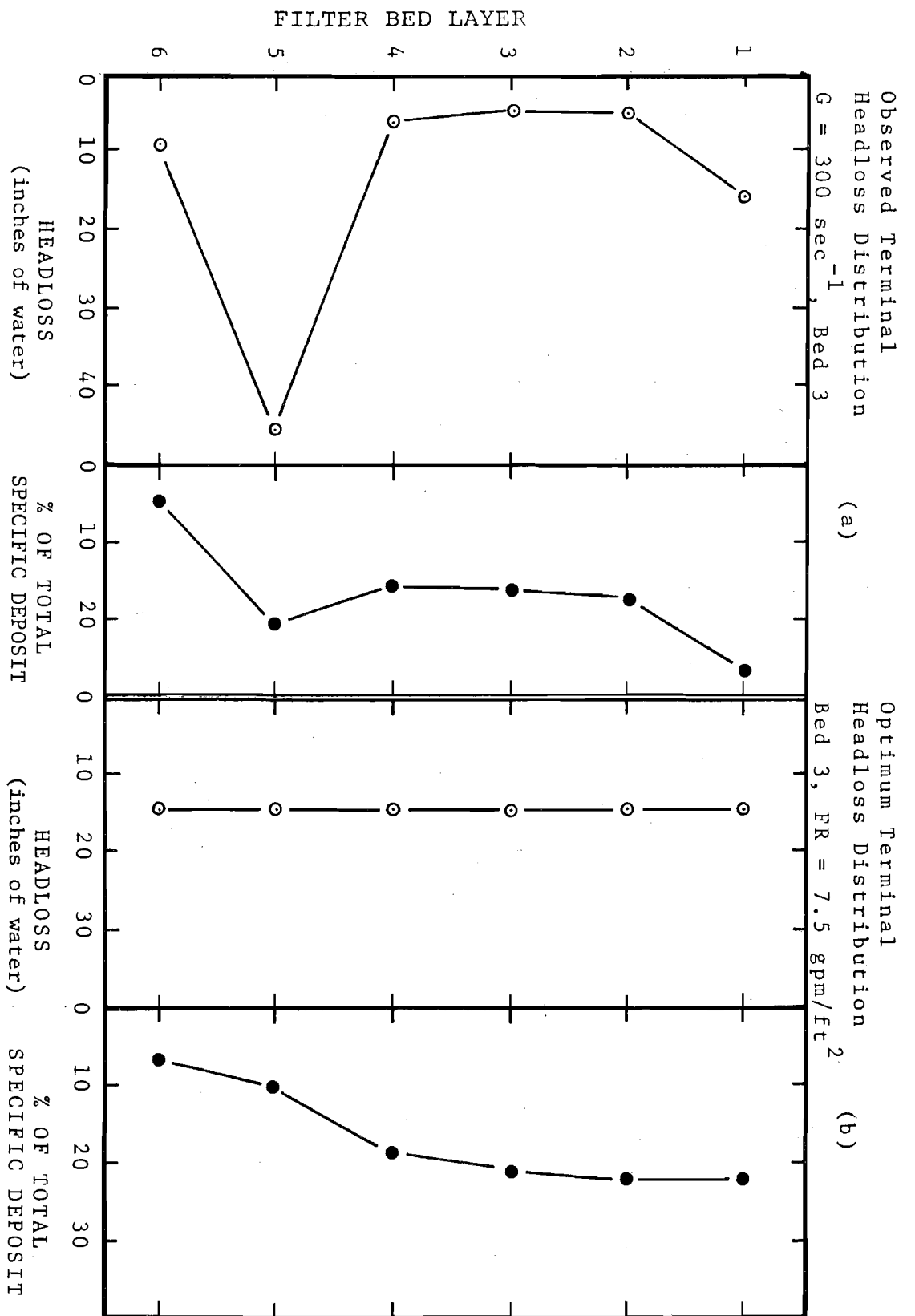





Figure 30. Terminal Headloss and Specific Deposit Distributions

that a G value of  $60 \text{ sec}^{-1}$  produced the terminal distributions closest to the optimum distributions plotted in Figure 30b. The distributions for  $G = 0 \text{ sec}^{-1}$  are skewed toward the upper layers of the bed and for  $G = 300 \text{ sec}^{-1}$  they are skewed toward the lower layers. The headloss build-up in layer 6 at  $G = 300 \text{ sec}^{-1}$  indicates that turbidity breakthrough was imminent. The rate of advancement of the clogging front under these conditions was increased by increasing the G value from 0 to  $300 \text{ sec}^{-1}$ .

Table 7 illustrates the general relationship between the combined pretreatment and filter operating conditions and the rate of advancement of the clogging front, the terminal specific deposit distribution for  $\Delta H = 86''$  and the tendency for turbidity breakthrough. The lowest rate of advancement of the clogging front was observed when the combination of conditions listed in column 1 was used and the highest rate was observed when the combination listed in column 3 was used. When the conditions of column 2 or a combination from all three columns was used the rate was intermediate.

The rate of advancement of the clogging front which will result in the optimum specific deposit distribution at run termination depends on the terminal headloss. The lower the terminal headloss the higher the acceptable rate. For example, when the terminal headloss was 86 inches, the conditions in column 2 or any other combination which resulted in an intermediate rate of advancement tended to produce the maximum water production. As shown in Figure 24a, when the

Table 7. Effect of Pretreatment and Filter Operating Conditions on the Rate of Clogging Front Advancement

	Column 1	Column 2	Column 3
Polymer Concentration, (mg/l)	3.0	1.5 or 5.0	1.0 or 7.0
Anthracite Media size distribution, e.s., (mm)/u.c.	0.94/1.65 (Bed 1)	1.20/1.60 (Bed 2)	1.71/1.16 (Bed 3)
Prefiltration mixing intensity, G value (sec <sup>-1</sup> )	0-25	100	700
Filtration rate (gpm/ft <sup>2</sup> )	2.5	5.0	7.5
Mean detention time (min)	2.0	4.0	9.2
Rate of advancement of the clogging front	very slow		very rapid
Terminal specific deposit distribution, ΔH = 86"	skewed toward the top of the bed		skewed toward the bottom of the bed
Tendency for turbidity breakthrough to occur	very low		very high

terminal headloss was 30 inches a combination of conditions with all or several tending toward the values in column 3 was more acceptable.

Within the range of magnitudes used in this study the effect of certain conditions on the rate of advancement of the clogging front was more significant than others. The system was very sensitive to the polymer concentration and much less so to the mean detention time. For example, when a polymer concentration of 3 mg/l was used with Beds 1 and 2 it was not possible (Figure 24c) to increase the water production above 90 percent of  $WP_{86}^*$  by increasing the G value. Apparently the degree of particle destabilization at a polymer concentration of 3.0 mg/l creates a tendency for particle removal in the upper layers of the bed which is difficult to counteract.

E. Field Study: The field study was conducted using the laboratory filtration apparatus and raw water drawn directly from the offshore intake at Chicago's Central District Filtration Plant on Lake Michigan. The filtration apparatus was operated intermittently during part of the months of May and June, 1975. Unfortunately during this period the raw water turbidity never increased above 1.5 FTU for a significant period of time. Plankton densities were also relatively low during this period ranging from 380 to 800/ml. The water temperature ranged from 10 to 14°C.

The field study was preceded by a statistical analysis of average daily values of the turbidity and the density of plankton organisms in the water drawn from the offshore intake.

The data was obtained from the log at the Central District Filtration Plant. Figure 31 is graph of the percent of the time the offshore water turbidity equalled or exceeded the plotted values. This graph was plotted using data from the years 1971 to 1973. Note that 50 percent of the time the offshore water turbidity was less than approximately 3 FTU.

Figure 32 is a graph similar to Figure 31 for the average number of plankton organisms per ml. One year of record was used for this plot. Fifty percent of the time the plankton density was less than approximately 1200/ml.

The original purpose of the field study was to verify the results of the laboratory experiments, i.e., to focus on the use of the pretreatment step to maximize water production per filter run. However, the low offshore water turbidity levels during the limited period available for the field study experiments made this type of experiment very time consuming and the results essentially moot. Attention was directed instead toward the effluent turbidity and the so-called ripening period. In order to study the effluent turbidity problem under critical filter operating conditions Bed 3, the bed with the coarsest anthracite layer, and a filtration rate of 7.5 gpm/ft<sup>2</sup> were used in most of these experiments.

Figure 33 is a plot of effluent turbidity and overall headloss versus the volume of water filtered. A polymer concentration of 0.5 mg/l (Cat-Floc T), a G value of 25 sec<sup>-1</sup> and a mean detention time of 4 min were used in this experiment. A preliminary study in which the polymer concentration

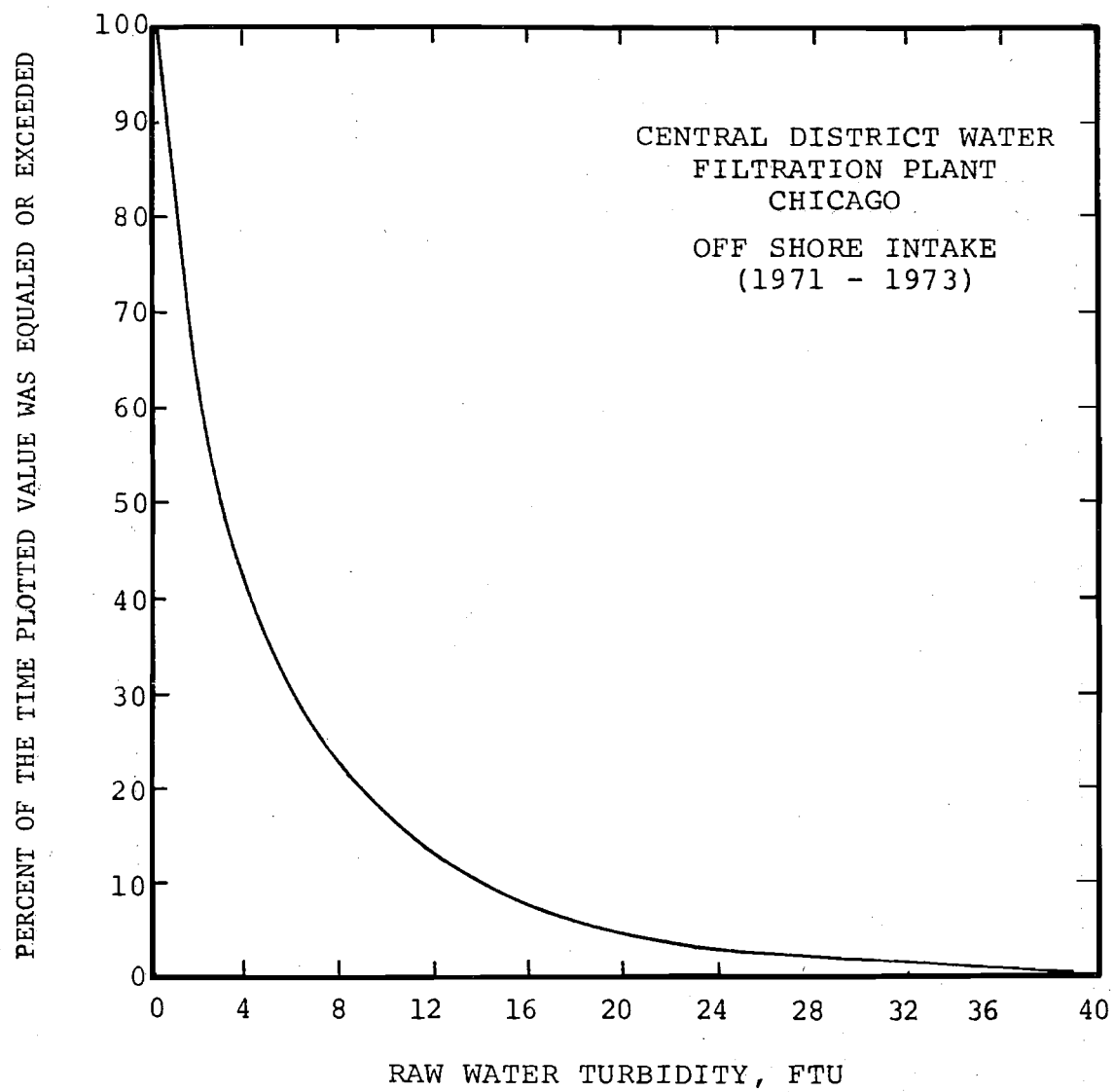


Figure 31. Statistical Distribution of Lake Michigan Water Turbidity

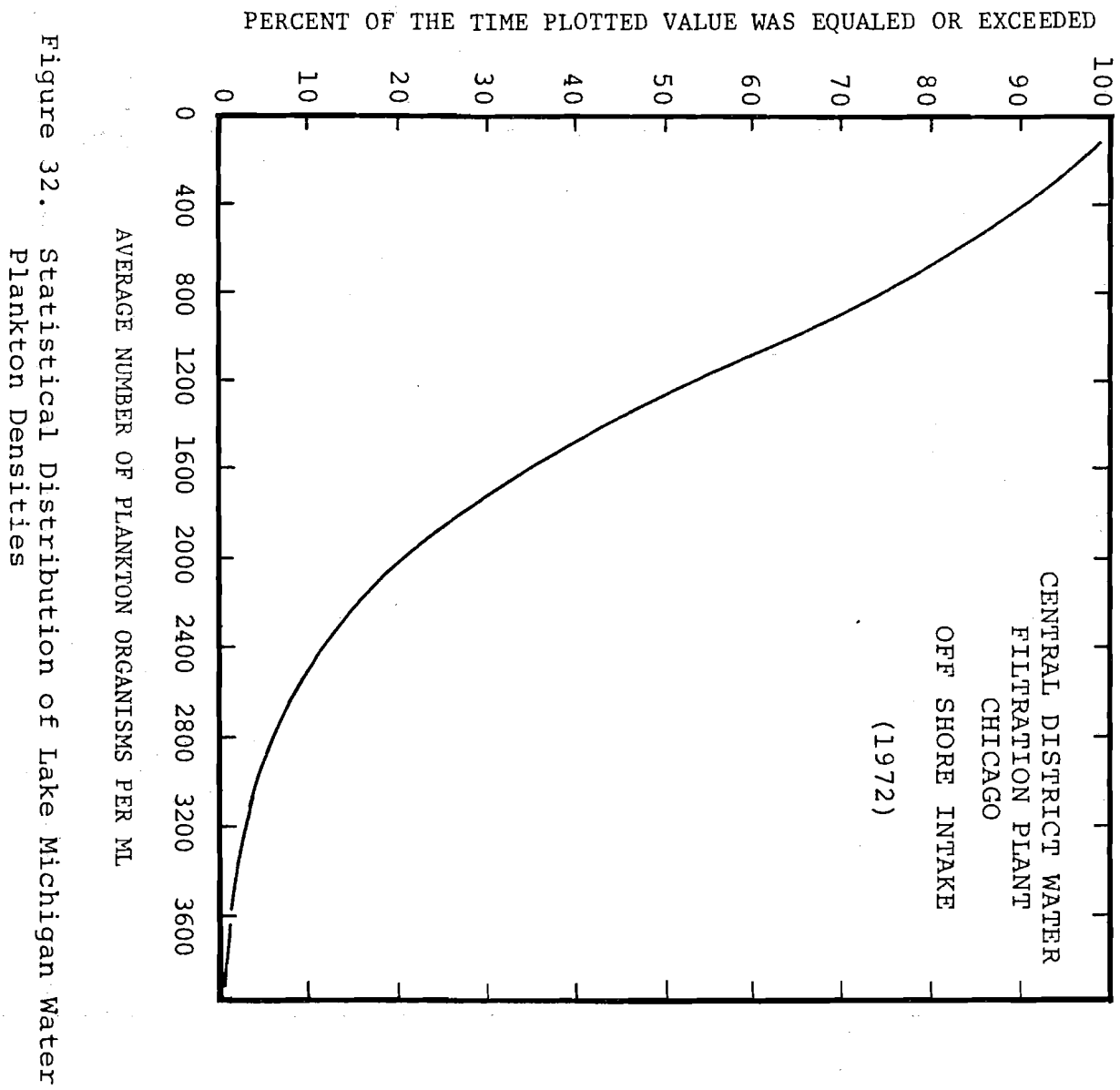


Figure 32. Statistical Distribution of Lake Michigan Water Plankton Densities



was varied from 0.1 to 1.0 mg/l in a series of runs indicated that a 0.5 mg/l concentration minimized the effluent turbidity. Particle zeta potentials were not measured during the field study.

It is apparent from Figure 33 that turbidity removal under low influent turbidity conditions is poor compared to the removals obtained in the laboratory study when the 32 FTU kaolin/bentonite suspension was used (See Figure 12). In the laboratory study effluent turbidities less than 0.1 FTU were obtained consistently with these filter operating conditions. In the preliminary study (Section III-A) effluent turbidities less than 0.1 FTU were obtained with the 0.67 mm effective size sand filter, however, high rates of headloss build-up were also observed (Figure 7).

Several short filter runs were conducted during the field study when the influent turbidity increased to about 3.2 FTU. The turbidity removal efficiency at 200 gal/ft<sup>2</sup> filtered increased from approximately 30 percent when the influent was 0.72 FTU to approximately 80 percent when the influent was 3.2 FTU. A 0.1 FTU effluent, however, was not obtained.

A series of filter runs were conducted when the influent turbidity was 1.4 FTU to determine the effect of the filtration rate on the turbidity removal efficiency at 200 gal/ft<sup>2</sup> filtered. The removal increased from 45 percent at 7.5 gpm/ft<sup>2</sup> to 55 percent at 2.5 gpm/ft<sup>2</sup>. It did not appear, however, that effluent turbidity levels on the order of 0.1 FTU could be obtained by decreasing the filtration rate.

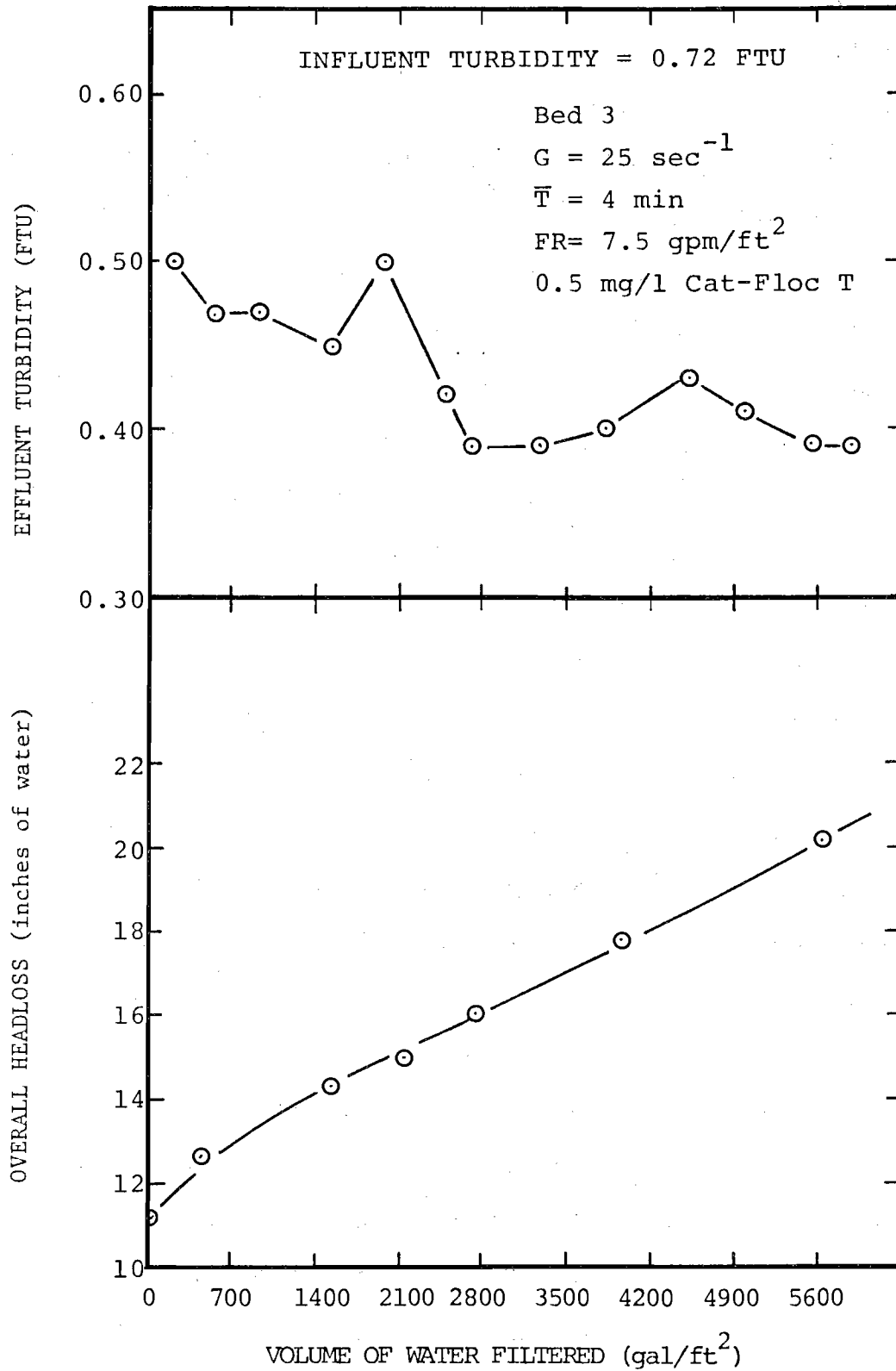


Figure 33. Effluent Turbidity and Overall Headloss vs. Volume of Water Filtered - Field Study

An experiment was conducted to determine if the effluent turbidity could be improved by increasing the rate at which the filter was "ripened", i.e., the rate at which a coating of deposit was formed on the filter media. Bed 3, a G value of  $25 \text{ sec}^{-1}$  and a filtration rate of  $7.5 \text{ gpm/ft}^2$  were used in this experiment. A concentrated suspension of bentonite clay was pumped to the constant head tank of the filter apparatus. The bentonite concentration in the water flowing to the filter was  $30 \text{ mg/l}$ . A polymer concentration of  $3.0 \text{ mg/l}$  was used. (No effort was made to determine the optimum polymer concentration.) The bentonite addition was continued until the effluent turbidity appeared to have reached a minimum. At this point the bentonite feed was terminated and the polymer concentration was reduced to  $0.5 \text{ mg/l}$ .

The results of this experiment are plotted in Figure 34. Note that the effluent turbidity decreased to a level lower than obtained without the bentonite and that this minimum was reached by approximately  $800 \text{ gal/ft}^2$ . However, the overall headloss increased at a much greater rate than the case without bentonite shown in Figure 33. Without bentonite the volume filtered at a 20 inch headloss was  $5500 \text{ gal/ft}^2$  and with the bentonite the volume filtered was  $200 \text{ gal/ft}^2$ .

After the bentonite addition was terminated the effluent turbidity increased to levels comparable to those expected if no bentonite had ever been added. This suggests that the higher effluent turbidities obtained with low influent turbidities are not the result of a slow ripening of the filter media but a result of insufficient flocculation in the PMR.

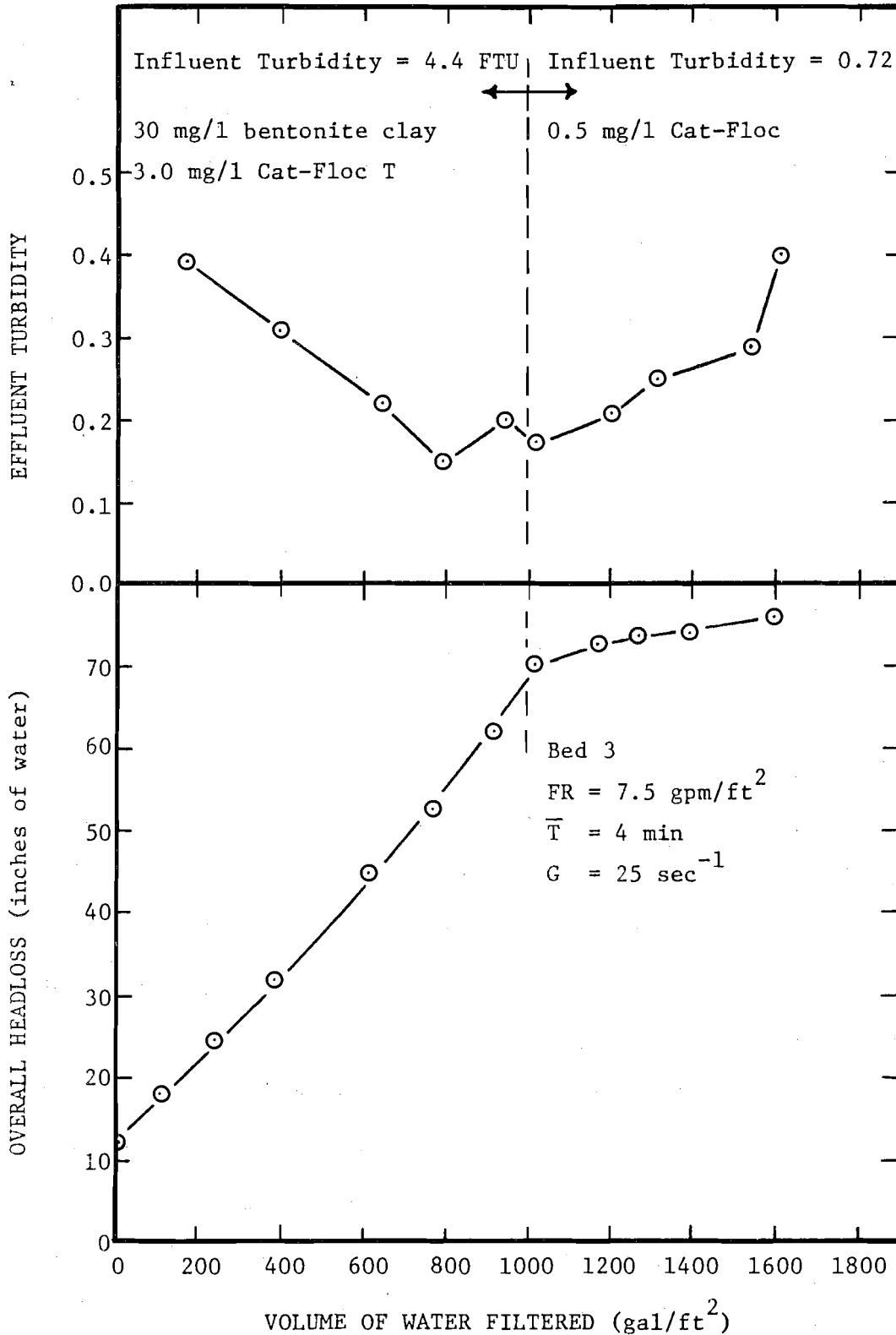


Figure 34. Effluent Turbidity and Overall Headloss versus Volume of Water Filtered - Field Study

The difficulties involved in the flocculation of dilute suspensions using cationic polyelectrolytes prior to removal by sedimentation are well known (11).

In one short filter run the G value was increased to  $200 \text{ sec}^{-1}$  and a mean detention time of 9.2 minutes was used to provide a greater opportunity for floc formation in the PMR. A filtration rate of  $5 \text{ gpm/ft}^2$  was used. No improvement in the effluent turbidity over the experiments in which  $\bar{T} = 4 \text{ min}$ ,  $G = 25 \text{ sec}$  and  $FR = 7.5 \text{ gpm/ft}^2$  were used was observed.

A common practice in treating low turbidity water with dual media filters is the use of a hydrolyzing salt coagulant such as aluminum sulfate in addition to a polymer coagulant. Shea, et al. (7) found that the ripening period, which was excessive when a coarse (2.5 mm effective size) anthracite layer was used, could be reduced substantially by the addition of alum along with a cationic polyelectrolyte. The polyelectrolyte, it was found, was necessary to "strengthen" the floc to prevent it from penetrating the bed.

Figure 35 is a graph of effluent turbidity and overall headloss versus volume of water filtered when the influent turbidity was 0.8 FTU and 10 mg/l of  $\text{Al}_2(\text{SO}_4)_3 \cdot 18 \text{ H}_2\text{O}$  plus 0.5 mg/l of Cat-Floc T were used. Experiments were not conducted to optimize the polymer concentration. It is expected, based on the results of Shea, et al. (7), that effluent turbidities less than 0.1 FTU and an acceptable ripening period could have been achieved by a better choice of the polymer concentration.

The absence of a ripening period in Figure 35 is apparent. The effluent turbidity is essentially constant at 0.22 FTU. Note that the rate of headloss build-up is, as expected,

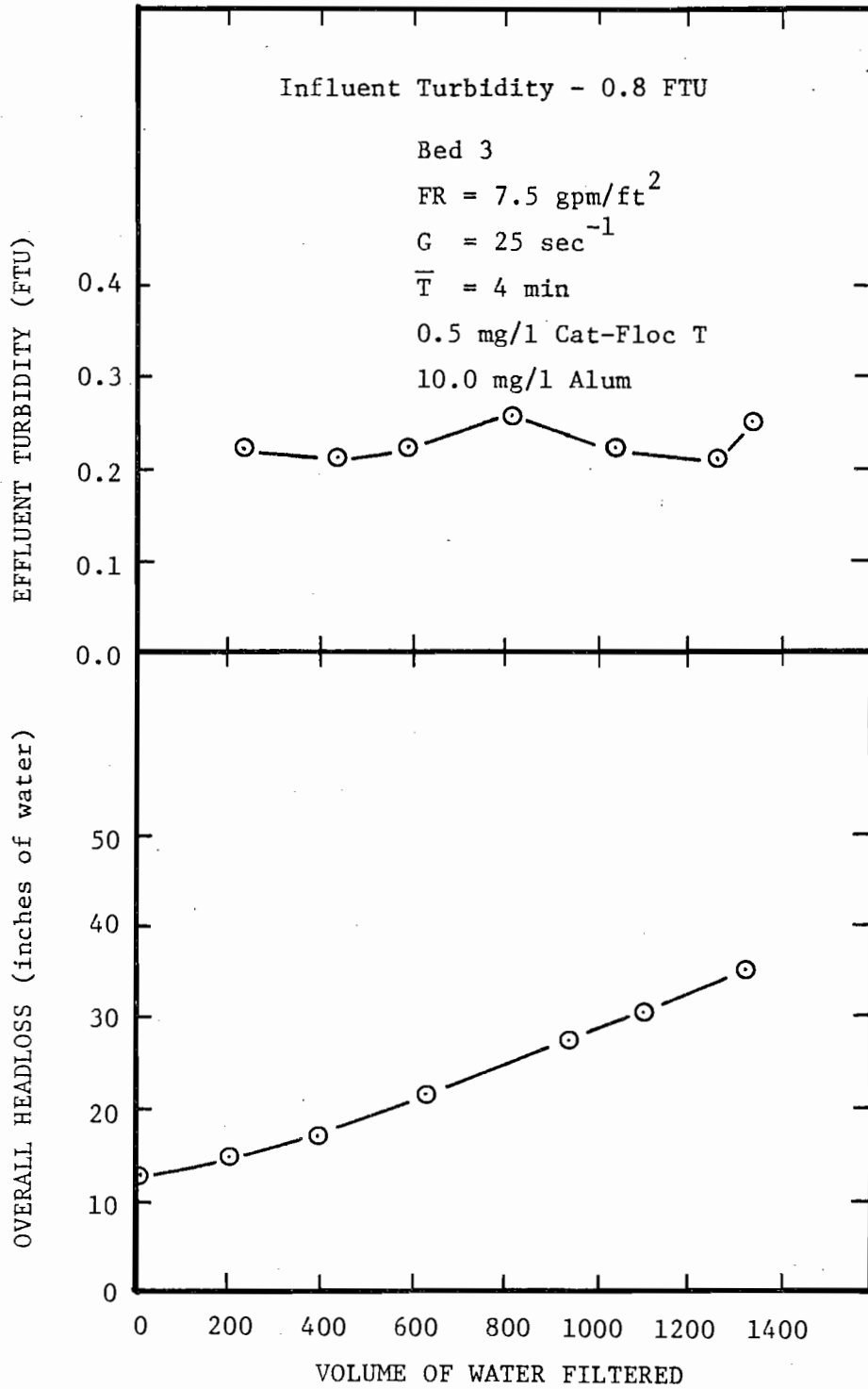


Figure 35. Effluent Turbidity and Overall Headloss versus Volume of Water Filtered - Field Study

significantly greater than when the Cat-Floc T was the sole coagulant. The volume of water filtered at an overall head-loss of 20 inches is 600 gal/ft<sup>2</sup> versus 5500 gal/ft<sup>2</sup> when the polymer was used alone.

In summary, the results of the field study suggest that under low (<5 FTU) influent turbidity conditions the media size distribution and the filter operating conditions, in particular the filtration rate, may be governed by consideration of the effluent turbidity and not just the water production per filter run criteria. However, the selection of specific operating conditions, a filter design and coagulant types and concentrations will have to be based in part on economic considerations.

#### IV SUMMARY AND CONCLUSIONS

The purpose of this investigation was to determine the effectiveness of the direct filtration process in treating water of the quality generally obtained from Lake Michigan and to use data obtained during the study to aid the derivation of and to substantiate mathematical relationships which can be used in process design and optimization. Emphasis was placed on evaluating the influence of pretreatment conditions such as the pretreatment mixing intensity and duration and the coagulant concentration on effluent quality and headloss across the filter bed using selected filter operating and design conditions. Filter operating and design conditions studied include the filtration rate, the terminal headloss and the filter media grain size distribution. The study focused on the use of dual media (anthracite coal over sand) filters and cationic polyelectrolytes as the sole coagulants. Both laboratory and field studies were conducted using a 1 gpm constant rate direct filtration pilot plant system which included an 8.5 liter pretreatment reactor. In the laboratory study the suspension used consisted of kaolin and bentonite clays in Chicago tap water. In the field study the raw water was drawn directly from Lake Michigan.

In general the results of this study show that direct filtration using cationic polyelectrolytes and dual media filters can be used to effectively treat water obtained from Lake Michigan and that effective operation can be maintained under varying influent turbidity and filter operating conditions



by pretreatment control. The results are summarized by the following specific conclusions.

1. The operation of a dual media filter using a cationic polyelectrolyte as the sole coagulant is characterized by the formation of a distinct working layer or clogging front which moves down through the bed at a rate which is a function of the filter media size distribution and the pretreatment and filter operating conditions. The rate of clogging front advancement is increased by
  - a) increasing or decreasing the polymer concentration above or below a concentration corresponding to a zeta potential of approximately +5 mv,
  - b) increasing the filtration rate,
  - c) increasing the prefiltration mixing intensity above approximately  $G = 25 \text{ sec}^{-1}$  and
  - d) increasing the effective size of the anthracite media.
2. If a granular bed filter is divided into n equal depth layers, there is, for any given terminal headloss, media size distribution and filtration rate a distribution of the deposit (and the total headloss) among these n layers which corresponds to the maximum.

possible water production per filter run.

The optimum headloss distribution as determined by an optimization technique is approximately equal headloss across every layer.

3. The maximum possible water production per filter run is increased by decreasing the filtration rate and by increasing the terminal headloss and the size of the filter media.
4. A pretreatment step consisting of cationic polyelectrolyte addition followed by a short period of flocculation (2 to 10 min) can be used to obtain a rate of clogging front advancement which results in, at least approximately, the optimum specific deposit distribution at run termination and hence a water production which approaches the maximum possible for the media size distribution, filtration rate and terminal headloss being used. The pretreatment step can also be used to avoid turbidity breakthrough which occurs when the rate of clogging front advancement is too fast. The rate of clogging front advancement which results in the deposit distribution which gives the maximum water production per filter run decreases as the terminal headloss is increased.

5. The zeta potential determination is an effective method for cationic polyelectrolyte coagulant control in the direct filtration of water from Lake Michigan. The polymers studied exhibited a concentration range which maximized the turbidity removal and minimized the filter ripening period and the rate of clogging front advancement in the filter bed. The concentrations which maximized turbidity removal corresponded to particle zeta potentials in the range +5 to +14 mv. In this concentration range the effluent turbidity was essentially independent of the influent turbidity and the other pretreatment and filter operating conditions.
6. The amount of polymer needed to achieve a given particle zeta potential increased slightly as the influent Lake Michigan water turbidity increased from 0.6 to 35 FTU.
7. When the pretreatment and filter operating conditions are held constant the rate of headloss buildup depends to a significant extent on the cationic polyelectrolyte used.
8. The optimum specific deposit distribution concept can be used in conjunction with a pilot plant filter of arbitrary design to estimate the maximum possible water production per filter run for any particular media design and filtration rate. This concept is based on the assumption

that the specific deposit in layer  $i$  of the filter bed,  $\sigma_i$ , is related to the headloss  $\Delta H_i$ , and clean bed headloss across the layer,  $\Delta H_{oi}$ , by the equation  $\sigma_i = K \log \Delta H_i / \Delta H_{oi}$ .

9. When the influent turbidity is less than approximately 5 FTU and the anthracite layer is coarse (effective size  $>1.7$  mm) the pre-treatment step (with a cationic polyelectrolyte as the sole coagulant) becomes ineffective in maintaining an effluent turbidity less than 0.1 FTU. Under these conditions it may be necessary to use a supplementary coagulant such as aluminum sulfate or to use deeper beds or an anthracite layer with an effective grain size on the order of 1 mm.

## V RESEARCH APPLICATIONS

The interim drinking water standards recently issued by the U.S. Environmental Protection Agency contain a treated water turbidity standard of 1 FTU, a value significantly less than the 5 FTU value of the 1962 Public Health Service standards. The enforcement of these new standards will force many communities which today do no more than chlorinate to build treatment facilities capable of turbidity removal. Direct filtration should prove to be an economical alternative for many of these communities and other communities which need to expand existing conventional facilities. The results obtained in this study indicate that the use of cationic polyelectrolyte coagulants in conjunction with dual-media filters and a controlled pre-treatment step is an effective method of direct filtration. The use of cationic polyelectrolytes as sole coagulants produces significantly less sludge than the more conventional hydrolyzing salt coagulants. Sludge disposal is a major problem in conventional water treatment plant operation.

The optimum specific deposit distribution concept developed as part of this study provides a new approach to granular filter design and optimization. Using this concept limited pilot plant tests conducted using a filter of arbitrary design can be used to estimate water production per filter run values for all proposed filter media designs and filter operating conditions. This should prove to be an important tool in conducting economic analyses of design alternatives.

## APPENDIX A

## LIST OF EXPERIMENTAL CONDITIONS

Run	Pretreatment Conditions			Filtration Rate (gpm/ft <sup>2</sup> )	Filter Bed No.
	G value (sec <sup>-1</sup> )	Polymer Conc., (mg/l)	$\bar{T}$ (min.)		
1	200	1.5	4	7.5	2
2	100	1.5	4	7.5	2
3	25	1.5	4	7.5	2
4	700	1.5	4	7.5	2
5	25	1.5	2	7.5	2
6	400	1.5	2	7.5	2
7	200	1.5	2	7.5	2
8	400	1.5	4	7.5	2
9	700	1.5	2	7.5	2
10	400	1.5	4	5	2
11	200	1.5	4	5	2
12	25	1.5	4	5	2
13	200	1.5	4	5	2
14	700	1.5	4	5	2
15	250	1.5	4	5	2
16	200	1.5	4	2.5	2
17	700	1.5	4	2.5	2
18	25	1.5	4	2.5	2
19	25	1.5	4	4	2
20	700	1.5	4	4	2
21	700	1.5	4	6	2
22	25	3.0	4	6	2
23	25	3.0	4	6	2
24	25	3.0	4	5	2
25	25	3.0	4	6	2
26	25	3.0	4	6	2
27	25	3.0	4	6	2
28	25	3.0	4	6	2
29	25	3.0	4	6	2
30	25	3.0	4	7.5	2
31	700	3.0	4	7.5	2
32	200	3.0	4	7.5	2
33	25	3.0	4	6	2
34	200	3.0	4	2.5	2
35	25	3.0	4	2.5	2
36	700	3.0	4	6	2
37	25	3.0	4	6	2
38	700	3.0	4	6	2
39	200	3.0	4	5	2
40	25	3.0	4	6	2
41	25	3.0	4	6	2
42	25	3.0	4	6	2
43	25	3.0	4	6	2
44	25	3.0	4	7.5	2
45	25	5.0	4	7.5	2

## LIST OF EXPERIMENTAL CONDITIONS (continued)

Run	Pretreatment Conditions			Filtration Rate (gpm/ft <sup>2</sup> )	Filter Bed No.
	G value (sec <sup>-1</sup> )	Polymer Conc., (mg/l)	$\bar{T}$ (min.)		
46	25	10.0	4	7.5	2
47	25	1.0	4	7.5	2
48	25	1.0	4	7.5	2
49	25	3.0	4	7.5	2
50	25	2.0	4	7.5	2
51	25	0.5	4	7.5	2
52	25	1.5	4	7.5	2
53	25	1.5	4	7.5	2
54	700	1.5	4	7.5	2
55	25	7.0	4	7.5	2
56	25	1.5	4	6	2
57	25	1.5	4	6	2
58	25	1.5	4	6	2
59	700	1.5	4	6	2
60	700	1.5	4	5	2
61	700	1.5	4	4	2
62	700	1.5	4	2.5	2
63	200	1.5	4	6	2
64	200	1.5	4	4	2
65	700	10.0*	9.2	5	2
66	25	1.5	4	7.5	1
67	25	1.5	4	5	1
68	25	1.5	4	2.5	1
69	25	1.5	4	7.5	1
70	25	0.5	4	7.5	1
71	25	3.0	4	7.5	1
72	25	5.0	4	7.5	1
73	25	7.0	4	7.5	1
74	25	9.0	4	7.5	1
75	90	3.0	4	7.5	1
76	200	3.0	4	7.5	1
77	500	3.0	4	7.5	1
78	700	3.0	4	7.5	1
79	700	1.5	4	7.5	1
80	700	1.5	4	7.5	1
81	700	1.5	4	5	1
82	700	1.5	4	2.5	1
83	25	1.5	4	6	1
84	25	1.5	4	6	1
85	25	1.5	4	7.5	1
86	25	1.5	4	6	1
87	25	1.5	4	5	1

\* Nalco 607

## LIST OF EXPERIMENTAL CONDITIONS (continued)

Run	Pretreatment Conditions			Filtration Rate (gpm/ft <sup>2</sup> )	Filter Bed No.
	G value (sec <sup>-1</sup> )	Polymer Conc., (mg/l)	$\bar{T}$ (min.)		
88	25	1.5	4	6	1
89	25	1.5	4	6	1
90	25	1.5	4	7.5	1
91	0	1.5	9.2	5.0	1
92	25	1.5	9.2	5.0	1
93	90	1.5	9.2	5.0	1
94	275	1.5	9.2	5.0	1
95	400	1.5	9.2	5.0	1
96	700	1.5	9.2	5.0	1
97	25	1.0	9.2	5.0	1
98	100	1.0	9.2	5.0	1
99	275	1.0	9.2	5.0	1
100	400	1.0	9.2	5.0	1
101	700	1.0	9.2	5.0	1
102	100	1.5	6.1	5.0	1
103	100	1.5	4.0	5.0	1
104	100	1.5	2.0	5.0	1
105	275	1.5	2.0	5.0	1
106	400	1.5	2.0	5.0	1
107	700	1.5	2.0	5.0	1
108	90	2.5	9.2	5.0	1
109	400	2.5	9.2	5.0	1
110	170	10.0*	9.2	5.0	1
111	375	10.0*	9.2	5.0	1
112	700	10.0*	9.2	5.0	1
113	90	1.5	6.1	2.5	1
114	90	1.5	6.1	7.5	1
115	200	1.5	4.0	5.0	1
116	300	1.5	4.0	5.0	1
117	600	1.5	4.0	5.0	1
118**	90	1.3	9.2	5.0	1
119	275	1.5	9.2	5.0	1
120	700	1.5	4	7.5	3
121	25	1.5	4	7.5	3
122	700	1.5	4	7.5	3
123	25	1.5	4	5	3
124	25	1.5	4	2.5	3
125	700	1.5	4	2.5	3
126	25	3.0	4	7.5	3
127	25	1.0	4	7.5	3
128	25	2.0	4	7.5	3

\*Nalco 607

\*\*Influent suspended solids reduced by one-half.



## LIST OF EXPERIMENTAL CONDITIONS (continued)

Run	Pretreatment Conditions			Filtration Rate (gpm/ft <sup>2</sup> )	Filter Bed No.
	G value (sec <sup>-1</sup> )	Polymer Conc., (mg/l)	$\bar{T}$ (min.)		
129	25	5.0	4	7.5	3
130	25	7.0	4	7.5	3
131	200	5.0	4	7.5	3
132	25	4.0	4	7.5	3
133	25	6.0	4	7.5	3
134	90	5.0	4	7.5	3
135	60	5.0	4	7.5	3
136	0	5.0	4	7.5	3
137	25	5.0	4	7.5	3
138	25	5.0	4	7.5	3
139	60	5.0	4	7.5	3
140	25	5.0	4	7.5	3
141	60	5.0	4	7.5	3
142	90	5.0	4	7.5	3
143	200	5.0	4	7.5	3
144	75	5.0	4	7.5	3
145	300	5.0	4	7.5	3
146	25	6.0	4	7.5	3
147	25	1.5	4	3.75	3

## APPENDIX B

## LIST OF SYMBOLS AND ABBREVIATIONS

$C_o$	influent suspended solids concentration
$C_e$	effluent suspended solids concentration
D	total depth of the filter bed
FR	filtration rate
FTU	formazin turbidity units
g	acceleration of gravity
G	rms velocity gradient or G value
$\Delta H$	terminal headloss
$\Delta H_i$	headloss across layer i of the filter bed
$\Delta H_{oi}$	clean bed headloss across layer i of the filter bed
k, K, K'	constants
$\Sigma \log \Delta H_i / \Delta H_{oi}$	specific deposit parameter
n	number of equal depth layers in the filter bed
N	shaft rotational speed
p	coefficient in Mohanka's equation
PC	polymer concentration
PMR	prefiltration mixing reactor
Q	filtration rate
$\bar{T}$	mean residence time
T	net torque and length of filter run
$\forall$	volume of fluid in reactor
v	superficial fluid velocity
v'	interstitial fluid velocity
WP	water production per unit area of filter bed or volume of water filtered at any time during the filter run.

$WP_{\Delta H}$	water production per unit area of filter bed at a terminal headloss of $\Delta H$
$WP_{\Delta H}^*$	maximum possible water production per unit area of filter bed at a terminal headloss of $\Delta H$
$zP$	zeta potential
$\beta$	deposit packing constant
$\xi$	coefficient in Sakthivadivel's equation
$\theta$	porosity
$\theta_i$	porosity of layer $i$ of the filter bed
$\mu$	absolute viscosity
$\rho$	mass density of the deposit
$\rho_p$	floc mass density
$\rho_l$	fluid mass density
$\sigma_i$	specific deposit in layer $i$ of the filter bed
$\sigma$	specific deposit

## VII REFERENCES

1. Hutcheson, W. and Foley, P.D., "Operational and Experimental Results of Direct Filtration," Jour. AWWA, 66:2:79, (Feb., 1974).
2. Tredgett, R.G., "Direct Filtration Studies for Metropolitan Toronto," Jour. AWWA 66:2:103, (Feb., 1974).
3. Sweeney, G. and Prendiville, P.W., "Direct Filtration: An Economic Answer to a City's Water Needs," Jour. AWWA, 66:2:65, (Feb., 1974).
4. Spink, C.M. and Monscvitz, J.T., "Design and Operation of a 200-mgd Direct Filtration Facility," Jour. AWWA, 66:2:127, (Feb., 1974).
5. Hay, W.A. and Prendiville, P.W., "Prospect Water Treatment Works for Sydney, Australia - World's Largest Direct Filtration Facility," paper presented at the annual conference, AWWA, Boston, Mass., 1974.
6. Camp, J.R. and Kreske, W.J., "Speed-Up Water Plants," Water and Waste Engineering, (Jan., 1974).
7. Shea, T.G., Gates, W.E. and Argaman, Y.A., "Experimental Evaluation of Operating Variables in Contact Flocculation," Jour. AWWA, 63:1:41, (Jan., 1971).
8. Adin, A. and Rebhun, M., "High-Rate Contact Flocculation-Filtration with Cationic Polyelectrolytes," Jour. AWWA 66:2:109, (Feb., 1974).
9. Habibian, M., "The Role of Polyelectrolytes in Water Filtration," Doctoral Dissertation, University of North Carolina at Chapel Hill, 1971.
10. Wnek W., "Electrokinetic and Chemical Aspects of Water Filtration," Filtration and Separation, May/June, 1974.
11. Kleber, J.P., "Municipal Water Treatment with Polyelectrolytes," Public Works, (Oct., 1973).
12. Craft, T.F., "Comparison of Sand and Anthracite for Rapid Filtration," Jour. AWWA, (Jan., 1971).
13. Unpublished report by personnel at the Central Water Filtration Plant, Chicago, Illinois (1973).
14. Tanner, R.D., "Direct Filtration of Lake Michigan Water," M.S. thesis, Illinois Institute of Technology, Chicago, (1974).
15. Kulprapha, P., "Computer Simulation of a Granular Media

Filter, M.S. thesis, Illinois Institute of Technology, Chicago, (1975).

16. Black, A.P., Birkner, F.B. and Morgan, J.J., "The Effect of Polymer Adsorption on the Electrokinetic Stability of Dilute Clay Suspensions," Jour. of Colloid and Interface Science, 21, 626, 1966.
17. Yao, K.M., Habibian, M.T. and O'Melia, C.R., "Water and Wastewater Filtration: Concepts and Applications," Environmental Science and Technology, Vol. 5, 1105-1112, (1971).
18. DiDomenico, E.J., "Effect of Media Size Distribution on Pretreatment for Direct Filtration," M.S. thesis, Illinois Institute of Technology, Chicago, (1975).
19. Herzig, J.P., LeClerc, D.M. and LeGoff, P., "Flow of Suspensions Through Porous Media - Application to Deep Filtration," Ind. and Eng. Chem. 62:5:8, (1970).
20. Sakthivadivel, R., Thanikachalam, V., Seetharaman, S., "Headloss Theories in Filtration," Jour. AWWA, 62:4: 233, (1972).
21. O'Melia, C.R., "The Role of Polyelectrolytes in Filtration Processes," National Environmental Research Center Report PB-233271, April, (1974).
22. Burgarino, A.E., "Mathematical Determination of Optimum Specific Deposit Distribution in a Granular Filter," paper presented at the annual Illinois section meeting of the American Water Works Assoc., Peoria, March, (1975).
23. Cleasby, J.L. and Baumann, E.R., "Wastewater Filtration: Design Considerations," U.S. EPA Technology Transfer Seminar Publication, July, (1974).
24. Michaels, A.S. and Bolger, J.C., "The Plastic Flow Behavior of Flocculated Kaolin Suspensions," I & E.C. Fundamentals, 1:153 (1962).
25. Sama, R.R., "Influence of Initial Mixing on Direct Filtration," M.S. thesis, Illinois Institute of Technology, Chicago, (1974).

## VIII LIST OF PUBLICATIONS

- 1974 Sama, R.R., "Influence of Initial Mixing on Direct Filtration," M.S. thesis, Illinois Institute of Technology, Chicago.
- 1974 Tanner, R.D., "Direct Filtration of Lake Michigan Water," M.S. thesis, Illinois Institute of Technology, Chicago.
- 1974 Letterman, R.D. and Tanner, R.D., "Zeta Potential Measurements for Polymer Coagulant Dose Control in Direct Filtration," Water and Sewage Works, 121:8:62, August.
- 1975 DiDomenico, E.J., "Effect of Media Size Distribution on Pretreatment for Direct Filtration," M.S. thesis, Illinois Institute of Technology, Chicago.
- 1975 DiDomenico, E.J. and Sama, R.R., "Pretreatment for Direct Filtration," paper to be published in the Proceedings of the Annual Conference of the American Water Works Association, Minneapolis.
- 1975 Kulprapha, P., "Computer Simulation of a Granular Media Filter," M.S. thesis, Illinois Institute of Technology, Chicago.